The Role of SUMOylation in the Auxin Response Pathway

CHARLOTTE KIRSTEN WALSH

The Role of SUMOylation in the Auxin Response Pathway

Thesis submitted for the degree of Doctor of Philosophy

Charlotte K Walsh

School of Biological and Biomedical Sciences

Durham University

September 2016

Contents

List of Figures

List of Tables

Acknowledgements

A big thank you...

To my principal supervisor Professor Ari Sadanandom, without whom this work would not have completed; I would like to thank him for his time, his knowledge and his endless patience. Professor Malcolm Bennett for his invaluable insight and guidance. Ms. Nicola Leftley for her patient instruction regarding the phenotyping of *Arabidopsis thaliana*. And to Dr Teva Vernoux for providing me with several valuable constructs throughout the course of my PhD.

To the lab members: Dr. Cunjin Zhang for all his help and advice throughout; Dr Beatriz Orosa, Dr Anjil Srivastava, Dr Vivek Verma and Dr Mark Bailey for encouraging me to think outside the box. Dr Stuart Nelis for his camaraderie, invaluable advice regarding western blotting and for introducing me to the wonder that is Geo Guessr. Dr Jack Lee, Linda Millyard, Helen Riordan and Alberto Campinaro for their friendship and willingness to join me in the pub. And Gary Yates for his hilarious, if infuriating, company.

To my parents for their love, support and encouragement.

And finally, to Andrew Hoare, who still wonders exactly what it is that I do all day.

Declaration

This thesis is submitted to Durham University in support of my application for the degree of Doctor of Philosophy. This document has been composed by the author and has not been submitted in any previous application for any degree. The work detailed herein was generated by the author unless otherwise explicitly specified.

The research detailed within was funded by the BBSRC DTP Scheme and Tozer Seeds, Ltd.

- Charlotte Walsh

Summary

The Small Ubiquitin-like Modifier 1 (SUMO1) protein is a stress-inducible posttranslational modification present in all eukaryotic organisms. Conjugation of this modifier to a target protein results in the alteration of target protein function. The subsequent de-conjugation of SUMO from target proteins is conducted by a class of enzymes termed SUMO proteases.

Previous research regarding the SUMO E3 ligases SIZ1 and HPY2 has inferred a connection between protein SUMOylation and auxin signalling (Huang, et al., 2009). Here, that connection has been strengthened through phenotypic analysis of *Arabidopsis thaliana* double knock-out mutant line for the SUMO proteases OVERLY TOLERANT TO SALT 1 and -2 (OTS1 and -2), *ots1 ots2,* and through the confirmation of the SUMOylation of several auxin cascade proteins.

Loss of OTS1 and -2 was shown to result in an increase in auxin response in *Arabidopsis thaliana* seedlings exposed to exogenous auxin stimulus, indicating that an increase in global SUMOylation levels alter auxin homeostasis. Further investigation regarding components of the auxin signalling cascade revealed that the auxin receptor, TIR1, and two of the auxin-regulated transcription factors, ARF7 and ARF19, undergo SUMOylation under transient assay conditions. Mutations in TIR1 inducing lysine to arginine substitution of the SUMO-binding residues at each predicted SUMO site eliminated SUMO1 binding under transient assay conditions, further confirming that WT TIR1 is SUMOylated and that the predicted locations were correct. These non-SUMOylatable TIR1 mutant clones were then transformed into the auxin signalling *Arabidopsis* mutant line *tir1/afb2/afb3* to further elucidate the role SUMOylation plays in auxin signalling *in planta.*

Nomenclature

2,4-D	2,4-Dichlorophenoxyacetic acid
ABA	Abscisic acid
AFB	Auxin F-box
ARF	AUXIN RESPONSE FACTOR
ASK1	ARABIDOPSIS SKP1-LIKE PROTIEN 1
ATP	Adenosine triphosphate
AUX1	tryptophan-2-monooxygenase
AUX2	indole-3-acetamide hydrolase
AUX/LAX	AUXIN1/LIKE AUXIN1
AuxRE	Auxin Response Element
BLAST	Basic Local Alignment Search Tool
BR	Brassinosteroid
cDNA	Complementary DNA
COI1	CORONATINE-INSENSITIVE PROTEIN 1
Col-0	Columbia-0
COP1	CONSTITUTIVE PHOTOMORPHOGENESIS PROTEIN 1
CUL1	CULLIN
DMSO	Dimethylsulfoxide
DNA	Deoxyribonucleic acid
EAR	Ethylene Response Factor
EDTA	Ethylenediaminetetraacetic acid
ESD4	EARLY IN SHORT DAY 4
Fig.	Figure
GA	Gibberellic acid
GAI	GIBBERELLIC ACID-INSENSITIVE MUTANT PROTEIN
gDNA	Genomic DNA
GFP	Green Fluorescent Protein
GG	di-glycine
HA	Hemaglutinin of Influenza Virus
HECT	HOMOLOGOUS TO THE E6-AP CARBOXYL TERMINUS
HPY2	HIGH PLOIDY 2
HRP	Horseradish Peroxidase
IAA	Indole-3-acetic acid
IAD	Indole-3-acetaldehyde
IAM	Indole-3-acetemide
IAOX	Indole-3-acetaldoxime

InsP6	Inositol hexakisphosphate
IPA	Indole-3-pyruvic acid
JA	Jasmonic Acid
KO	Knock Out
LB	Luria Broth medium
LR	Lateral Root
LRP	Lateral Root Primordia
LRR	Leucine Rich Repeat
MS	Murashige and Skoog medium
NAA	1-Naphthaleneacetic acid
NCBI	National Centre for Biotechnology Information
OD	Optical Density
OTS1 and -2	OVERLY TOLERANT TO SALT 1 and -2
PAGE	Polyacrylamide Gel Electrophoresis
PAT	Polar Auxin Transport
PCR	Polymerase Chain Reaction
PHY B	PHYTOCHROME B
PIF	PHYTOCHROME INTERACTING FACTOR
PIN	PIN-FORMED
QC	Quiescent Centre
qPCR	Quantitative PCR
RAM	Root Apical Meristem
RBX	RING-BOX
RGA	REPRESSOR ON THE GA1-3 MUTANT
Ri	Root-inducing
RING	REALLY INTERESTING NEW GENE
RNA	Ribonucleic acid
rpm	Revolutions per minute
RT	Room Temperature
SA	Salicylic acid
SAE1 and -2	SUMO-ACTIVATING ENZYME 1
SAM	Shoot Apical Meristem
SAR	Structure-Activity Relationship
SCE1	SUMO-CONJUGATING ENZYME 1
SCF	SKP1-CULLIN-F-box
SDS	Sodium dodecyl sulphate
SIM	SUMO-interacting Motif
SIZ1	SAP and MIZ1
SUMO	SMALL UBIQUITIN-LIKE MODIFIER
TAA1	TRYPTOPHAN AMINOTRANSFERASE OF ARABIDOPSIS 1
TAIR	The Arabidopsis Information Resource
TAM	Tryptamine
TDC	TRYPTOPHAN DECARBOXYLASE
TEMED	N,N.N'N'-tetramethylethane-1,2-diamine
TIBA	2,3,5-triiodobenzoic acid
TIR1	TRANSPORT INHIBITOR RESPONSE 1
TPL	TOPLESS
TRP	Tryptophan
Ub	Ubiquitin
UBL	Ubiquitin-like
ULP1	UBIQUITIN-LIKE PROTIEN-SPECIFIC PROTEASE 1
UPS	Ubiquitin-Proteasome System

v/v	Volume per volume
WT	Wild Type
w/v	Weight per volume
XPP	Xylem Pole Pericycle
YFP	Yellow Fluorescent Protein
YUCCA	PROBABLE INDOLE-3-PYRUVATE MONOOXYGENASE

1. Introduction

1.1 Auxin

1.1.1 Overview

Plant hormones, known as phytohormones, are a group of chemicals that regulate growth and development. Unlike mammalian hormones, which are often large and complex, phytohormones are simple chemical compounds able to be produced by every cell. These compounds are synthesised in response to both internal and external stimuli, allowing the plant maintain the large amount of phenotypic plasticity required for life as a sessile organism.

There are five major classes of phytohormones, with members of each class defined by their structural similarities or their effects upon plant physiology. These are auxins, cytokinins, gibberellins, abscisic acid, and ethylene. There are many other plant hormones, including brassinosteriods and jasmonates, however these are not as easily categorised.

Of these phytohormones, auxin is widely considered to be the first ever discovered. It is a crucial morphogen and plays an important role in the growth and development of all plant species.

A Brief History of Auxin

The effects of auxin upon plants have been known for millennia. Indeed, one of the earliest depictions of the phototropic response, in which auxin plays a major role, is in the epic narrative poem *Metamorphoses* by Ovid. In this poem (iv. 204, 234-256), the phototropic response is alluded to through the story of the water nymph Clytie, who was transformed by Venus into a Heliotrope (also known as Turnsole: a rocky, sun-loving plant), becoming destined to forever follow the movements of her beloved sun god across the sky (Ovid, et al., 1998).

From this tale, it is clear that the concept of phototropism has been known about for a long time. However, whilst the phototropic effects of auxin have been recognised for millennia (Whippo & Hangarter, 2004), it wasn't until the 1800s that the first mechanism of action for this phenomenon was proposed.

The first auxin experiments were conducted in 1881 by Charles Darwin and his son Francis (Darwin and Darwin, 1881). In these experiments, they discovered that plant coleoptiles were able to sense and bend towards a unidirectional light stimulus. Through the addition of light impermeable coverings on various parts of the coleoptile and hypocotyl, they were able to determine that light is perceived in the coleoptile tip but that the light-responsive bending occurs in the hypocotyl. They therefore proposed the idea of a 'moving messenger', allowing the plant to sense light in one structure, yet respond in another.

The Darwins' work was later continued by Peter Boysen-Jensen (1913), who showed that the signal was indeed mobile (Pennazio, 2002). He demonstrated signal motility through the use of permeable and impermeable barriers, which he placed between the coleoptile tip and the hypocotyl.

However, the definitive proof of the existence of the messenger came from a series of experiments conducted by Frits Went. He demonstrated that this messenger could be captured from plants exposed to phototropic stimulus and used to incite a response those that had not

been exposed (Tivendale & Cohen, 2015). This messenger was later identified as the auxin Indole-3-Acetic Acid (IAA), the first phytohormone to be discovered.

The Roles of Auxin within Plant Growth and Development

Auxins have a great many roles within the plant, participating in every stage of development from the cellular level up to the plant as a whole.

At a cellular level, auxin is primarily responsible for cell expansion and, in concert with the phytohormone cytokinin, cell division (Perrot-Rechenmann, 2010). Auxin mediates cell expansion through the acidification of the cell wall via induction of a plasma membrane-bound ATPase proton pump (Philippar, et al., 2004). The acidification of the cell wall activates proteins known as expansins, which are thought to disrupt the non-covalent bonds formed between the cellulose and hemicellulose polymers that form the cell wall, allowing expansion and therefore growth of the cell to occur (Sampedro & Cosgrove, 2005). Alongside cell growth, experiments involving the auxin starvation of cells in tissue culture also show that lack of auxin causes division arrest (Takatsuka & Umeda, 2014), and conversely, that addition of auxin to arrested cells stimulates division.

On a wider scale, auxin is responsible for the morphological changes induced by the various plant tropsims, such as phototropism, hydrotropism and gravitropism (Muday, 2001). It also plays an important role in the growth and development of many plant organs, such as the roots (Overvoorde, et al., 2010), fruit growth and development (Pattison, et al., 2014), and floral development (Krizek, 2011).

1.1.2 Auxin Biosynthesis

To date, over 200 compounds with auxinic activity have been discovered (Calderon-Villalobos, et al., 2010). Though these compounds vary wildly in molecular structure, they all contain two conserved features: a planar aromatic ring and a side chain containing a carboxyl group. The most prevalent and well-studied of these auxinic compounds is indole-3-acetic acid (IAA). IAA was the first plant hormone ever identified and is a key regulator of many essential plant growth and developmental processes, such as cell division, apical dominance and flowering (Spiess, et al., 2014).

Unlike the auxin signalling pathways, *de novo* auxin biosynthesis remains very poorly understood. IAA synthesis in plants is a complex process, with the contribution of many different pathways proposed to be involved, some of which may be species specific. To date, two forms of IAA biosynthesis have been proposed: tryptophan-independent and tryptophan-dependent (Gray, et al., 2001). Very little is known about tryptophan (trp)-independent auxin biosynthesis.

Tryptophan-Dependent IAA Biosynthesis

In comparison to trp-independent auxin biosynthesis, far more is known about trp-dependent biosynthesis. To date, there are four hypothesised trp-dependent pathways: i. the indole-3-acetemide (IAM) pathway, ii. the indole-3-pyruvic acid (IPA) pathway, iii. the tryptamine (TAM) pathway, and iv. the indole-3-acetaldoxime (IAOX) pathway (reviewed in Mano & Nemoto (2012). It is currently unclear if all stated pathways are present in all plant species; current research indicates this is unlikely.

Tryptophan-Dependent Biosynthesis: IAM Pathway

Originally, the IAM auxin biosynthesis pathway was thought to be bacteria specific. Hairy root disease, caused by the pathogen *Agrobacterium rhizogenes*, is an infection that exploits the plant's auxin system. The pathogen contains an Ri plasmid with two auxin synthesis genes, *aux1*

and *aux2*, which upon infection become integrated within the host DNA (Nemoto, et al., 2009). The activation of these genes by the host results in synthesis of IAA, thereby disturbing the distribution and concentration of endogenous auxin within the plant, resulting in the proliferation of root tissue, giving rise to hairy root disease. In this pathway, tryptophan is converted to IAM by tryptophan-2-monooxygenase (*aux1*) (Gaudin, et al., 1993; Camilleri & Jouanin, 1991). IAM is then converted to IAA by indole-3-acetamide hydrolase (*aux2*) (Thomashow, et al., 1984; Offringa, et al., 1986).

Later research showed that the IAM synthesis pathway was not just bacteria specific, but was also present in higher plants. The presence of IAM has been detected in the extracts of many plant species, such as Japanese cherry (Saotome, et al., 1993), tobacco (Lemcke, et al., 2000), *Arabidopsis* (Pollmann, et al., 2002), maize and rice (Sugawara, et al., 2009), indicating that IAM is a native compound and almost certainly an intermediate in IAA biosynthesis in both monocots and dicots.

To date, relatively little is known about the enzymes involved in the synthesis of IAM *in planta*. Cell-free extracts from several plant species are able to mimic the pathway identified in hairy root disease, converting tryptophan to IAM and on to IAA (Pollmann, et al., 2009). However, no candidates for enzymes homologous to the *aux1* and *aux2* genes have been identified. This could be due to a large divergence in sequence between the bacterial and plant homologues, rendering current bioinformatic techniques inadequate for the task (Mano, et al., 2010). Or, the limited success in suitable enzyme candidate identification could be down to a case of convergent evolution, the synthesis of IAM (and subsequent conversion to IAA) achieved through a different pathway.

Tryptophan-Dependent Biosynthesis: IPA Pathway

The identification of the IPA pathway originally occurred through experiments used to characterise *Arabidopsis* mutants defective in both shade response (Tao, et al., 2008) and ethylene response (Stepanova, et al., 2008). The two groups who conducted these experiments isolated an aminotransferase enzyme, Tryptophan Aminotransferase of *Arabidopsis* 1 (TAA1), able

to convert tryptophan to the auxin biosynthesis intermediate IPA. Further experiments showed an increase of intercellular IAA concentration upon exposure to shade and a dramatic reduction in free IAA concentration in *Arabidopsis* mutants lacking TAA1, indicating the importance of this pathway in IAA biosynthesis in response to shade (Tao, et al., 2008).

Like the IAM pathway, the IPA pathway is also exploited by bacteria. This pathway is predominantly used by growth-promoting rhizobacteria, such as *Azospirillium brasilense* and *Pseudomonas putida* (Somers, et al., 2005). As before, this pathway is better characterised in bacteria, with experiments indicating that the conversion of tryptophan to the IAA precursor indole-3-acetaldehyde (IAD) occurs via IPA (Hilbert, et al., 2012). To date, it is unclear whether plants also produce the auxin intermediate IAD as part of this pathway.

Tryptophan-Dependent Biosynthesis: TAM Pathway

TAM is a protoalkaloid involved in the terpenoid indole alkaloid biosynthetic pathway (Di Fiore, et al., 2002). Tryptophan is converted to TAM by tryptophan decarboxylase (TDC). Experiments involving the overexpression of TDC in transgenic tobacco show that though a dramatic increase in TAM concentration occurs, the levels of IAA remain unaffected. This suggests that despite TAM being considered an IAA biosynthesis intermediate, TDC itself plays virtually no role in IAA biosynthesis (Songstad, et al., 1990).

In *Arabidopsis thaliana*, TAM is thought to be an intermediate in IAA biosynthesis. As part of this pathway, the oxidization of TAM to N-hydroxytryptamine by a flavin monooxygenase-like enzyme called YUCCA is thought to occur (Zhao, et al., 2001). Orthologues of this gene have been identified in both monocots and dicots, suggesting that this pathway is widespread amongst higher plants (Yamamoto, et al., 2007; Expósito-Rodríguez, et al., 2011). Experiments involving the overexpression of OsYUCCA1 in transgenic rice (Yamamoto, et al., 2007) have shown the involvement of this enzyme in the IAA biosynthetic pathway, as increased levels of IAA and typical excess-auxin phenotypes were observed. However, the TAM pathway metabolite N-hydroxytryptamine has not yet been identified in plant extracts, suggesting that TAM may not be the true YUCCA substrate (Mano & Nemoto, 2012).

Recent data, however, has suggested a role in IAA biosynthesis for the YUC protein family through the previously mentioned IPA pathway (Mashiguchi, et al., 2011). Experiments involving the inhibition of TAA1 in transgenic *Arabidopsis* plants overexpressing the YUC1 gene showed a drastic reduction in the high auxin phenotypes observed for these mutants (Stepanova, et al., 2011). Further experiments involving the *Arabidopsis* YUC family triple knock-out mutant, *yuc1 yuc2 yuc6*, showed that these plants contain a far higher level of the IAA biosynthesis intermediate IPA in comparison to wild type (Won, et al., 2011). Taken together, these findings indicate a pivotal role for the YUC gene family in the IPA auxin biosynthesis pathway.

Tryptophan-Dependent Biosynthesis: IAOX Pathway

The IAOX IAA biosynthesis pathway is thought to be species specific, with the enzymes involved in tryptophan conversion as yet only identified in *Arabidopsis thaliana* and *Brassica* (Ludwig-Müller & Hilgenberg, 1988). The IAA intermediate IAOX is converted from tryptophan by two cytochrome P450 enzymes: CYP79B2 and CYP79B3 (Hull & Celenza, 2000; Mikkelsen, et al., 2000). No homologues of these enzymes have been identified in other plant species to date, and the generation of IAOX does not appear to occur in many plant species, such as tomato (Cooney & Nonhebel, 1991), rice or maize (Sugawara, et al., 2009).

Like TAM, IAOX is an intermediate in many other pathways, such as IAN production and the synthesis of the alkaloid camalexin (Mikkelsen, et al., 2009). Recent work in *Arabidopsis* using double knock-out mutants of AtCYP79B2 and AtCYP79B3 show that though the levels of secondary metabolites for which IAOX is an intermediate dramatically decrease, the levels of IAA within the plant do not. Overexpression of AtCYP79B2 also shows little change in IAA levels but large changes in secondary metabolite levels (Zhao, et al., 2002). This data suggests that the IAOX auxin biosynthesis pathway is unlikely to be involved in any major scale production of IAA.

1.1.3 The Importance of Auxin

Auxins are heavily involved in practically every stage of plant growth. They are vital in the development and maintenance of all primordia, holding sway over the body plan of a plant (Casimiro, et al., 2001). Mutants defective in auxin production and signalling often show faults in proper plant body plan establishment, with errors seen in internode elongation, apical dominance and organ formation, such as the establishment of lateral/adventitious roots.

Auxin and Root Tissue Organisation

In order for a plant to thrive in its environment, well-established plant root systems with the ability to respond appropriately to both exogenous and endogenous stimuli are required. Through roots, plants are not only able to take in nutrients and water from the surrounding soil, but also able to provide themselves a strong anchor into the substratum, an essential function for plant survival (Den Herder, et al., 2010). It is via auxin that these essential changes occur.

Plant roots are very complex organs. A single root itself contains a vast array of different cell types and tissues. The development of these cell types as part of the establishment and maintenance of the root primordia is regulated by auxin (Overvoorde, et al., 2010). To date, three areas of auxin concentration maxima have been identified. The first maxima is located at the Root Apical Meristem (RAM), with the auxin gradient generated between the RAM and the quiescent centre (QC) regulating the maintenance of the stem cell niche from which all root tissues are derived (Sabatini, et al., 2003). The second of these maxima is located at the root-shoot junction of the plant, regulating the initiation and development of adventitious roots (Gonzali, et al., 2005). And the third is located in the xylem pole pericycle cells of the basal meristem, where the auxin maxima induces the priming and later initiation of the development of lateral roots (De Smet, et al., 2007).

Auxin has several well-documented effects upon the plant root system. These auxin-associated phenotypes include the bimodal effect of the hormone upon primary root length, the dose-dependent effects upon root hair length and the average number of lateral root primordia, and

the plant's response to gravitational stimuli (Rahman, et al., 2002; Péret, et al., 2009; Dolan, 1998). It is through the establishment of differential auxin gradients within root tissues that these effects can be achieved.

In wild type roots, auxin accumulates strongly within the root tip, columellar cells and progeny, and within cambial tissues (Uggla, et al., 1996). Upon the disruption of auxin flux using genetic and physiological methods (such as phytotropin treatment), the special patterning of the root changes dramatically (Sabatini, et al., 1999). The organisational defects in columellar and vascular tissue observed in auxin transport mutants are highly indicative of a role for auxin in the differentiation of root cell tissue.

Auxin and Lateral Roots

The *Arabidopsis* root system, like many dicots, consists of one large primary root from which lateral roots branch (Osmont, et al., 2007). The formation of these lateral roots in response to environmental (Leyser & Fitter, 1998) and internal cues is one of the ways in which root phenotypic plasticity contributes to a plant's adaptation to an ever-changing environment.

The structure of *Arabidopsis* roots is relatively simple, consisting of four main tissue layers named the epidermis, cortex, endodermis, and pericycle, which surround the inner vascular bundle. The pericycle is composed of a unique layer of cells in a state of G2 cycle arrest (Beeckman, et al., 2001). This layer contains two cell types: differentiated phloem pole cells and meristematic xylem pole pericycle (XPP) cells (Parizot, et al., 2012). It is from triplets of cells adjacent to XPP cells, termed pericycle founder cells, that lateral roots develop (Lucas, et al., 2008).

Lateral roots are formed at regular intervals down the root, emerging in an alternating left-right pattern (De Smet, et al., 2007). The predictable nature of LR patterning is dictated by an 'auxin clock'; XPP cells adjacent to pericycle founder cells are primed for LR formation via a 15 hour auxin-response oscillatory pattern at the basal root meristem (Moreno-Risueno, et al., 2010). This is achieved through PIN-mediated channelling of auxin back to the basal meristem through the

inverse fountain pathway (Adamowski & Friml, 2015). Once these cells have been primed, they are able to undergo LR initiation. During initiation, primed founder cells divide in an anticlinal fashion to produce a small cell file, approximately 10 cells thick, termed the lateral root primordia (Casimiro, et al., 2001). This group of cells then continues to divide in both a periclinal and anticlinal fashion, generating a dome-shaped, vascularised structure that emerges from the primary root to form a new lateral root (Dubrovsky, et al., 2001).

Aside from founder cell priming, auxin also plays a large role in lateral root initiation, tissue patterning and emergence. Experiments involving mutations in the auxin pathway have shed light on the proteins involved (figure 1.1).

Auxin and Arial Tissues

Alongside the regulation of the plant root system, auxin also plays a large role in the development of plant shoot tissue and the establishment of the main apical-basal-axis of growth (Gallavotti, 2013). As with roots, auxin is responsible for the maintenance of the core of pluripotent stem cells located at both the shoot apical meristem (SAM) and axilliary meristems (Weigel & Jürgens, 2002).

The development of the plant shoot is organised into morphological modules named phytomers (Galinat, 1959), each composed of an internode, a node bearing a leaf and one or more auxiliary meristem. Variations in this pattern of phytomers, and thus diversity between plant species, is controlled largely via auxin patterning.

FIGURE 1.1| THE MECHANISM OF LATERAL ROOT PATTERNING IN ARABIDOPSIS

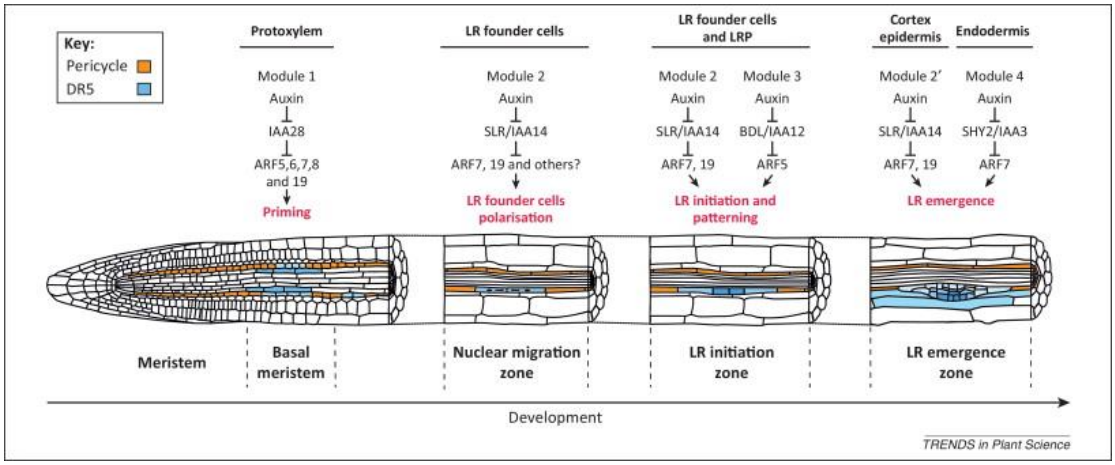

Figure taken from Lavenus, et al. (2013).

Lateral root development is primarily controlled through auxin signalling. There are several pathways involved in this process. Priming of LR founder cells involves the degradation of IAA28, releasing the repression of activating ARFs 5, 6, 7, 8 and 19. Once primed in the basal meristem, the founder cells are able to undergo nuclear migration though the SLR/IAA14 – ARF7/19 signalling module. Initiation and patterning then occurs using the IAA14 module and the BDL/IAA12 – ARF5 module. After initiation and division of the Lateral Root Primordia (LRP), another auxin pathway becomes involved: the SHY2/IAA3 – ARF7 pathway, which promotes the emergence of the lateral root.

1.1.4 Auxin Patterning

Auxin signalling relies on the formation of hormone gradients within plant tissues. These local auxin minima and maxima guide plant growth and development in a spatiotemporal manner, with alterations in auxin flux driving morphological change. This changing spatial distribution of auxin within plant tissues is achieved through a mechanism known as polar auxin transport (PAT).

PAT is achieved through the active transportation of the hormone via auxin influx and efflux carriers (van Berkel, et al., 2013). These transporter proteins assist in the directional cell to cell transport of auxin from the source (the chloroplasts in which auxin is synthesised) to the sink.

Auxin Influx Carrier Proteins

Though protonated auxin is able to easily traverse the plasma membrane without assistance, directional transport of the phytohormone is achieved, in part, through the use of the AUXIN1/LIKEAUX1 (AUX/LAX) family of auxin influx proteins. To date, four AUX/LAX family proteins have been identified in *Arabidopsis thaliana* (AUX1 and LAX1-3), with the presence of homologues reported throughout the multicellular plant kingdom (Swarup & Péret, 2012).

Auxin Efflux Carrier Proteins

Whilst the low pH of the plant cell wall aids in the protonation of auxin, allowing it to move easily into the cell, the much higher pH of the cytosol renders the hormone incapable of moving back across the membrane unassisted (Hasenstein & Rayle, 1984). To ensure the flow of auxin from cell to cell, auxin efflux carriers, called PIN-FORMED proteins (PINs), are used.

The PIN proteins are a family of secondary transporter proteins found in all multicellular plants. All proteins within this family have a broadly similar structure, with N- and C-terminal membrane-spanning domains separated by a central hydrophilic domain (Krecek, et al., 2009). Using the

electrochemical gradient generated by the plasma membrane, these transporters pump the unprotonated form of auxin from the cytosol back into the cell wall and intercellular spaces, allowing it to be taken up by adjacent cells and thus propagating the signal (Zazímalová, et al., 2010).

Directional transport of auxin is achieved through the unique subcellular distribution of these PIN proteins within the cell, which are localised to the basal membrane (Willemsen, et al., 2003). Through this manifestation of cell polarity, auxin can be efficiently transported in a unidirectional manner from source to sink.

1.1.5 The Auxin Signalling Cascade

Perhaps the most well understood auxin signalling pathway is that involving the degradation of the AUX/IAA family of transcriptional repressors. This form of hormone-mediated transcriptional regulation involves three major protein families: the TIR1/AFB family of auxin receptors, the AUX/IAA family of transcriptional repressors and the ARF family of transcription factors (Parry, et al., 2009). Without auxin, the AUX/IAA transcriptional repressor is bound tightly to the ARF transcription factor, preventing transcription of the auxin-response genes. Upon the perception of auxin by the TIR1/AFB protein family, the AUX/IAA protein is tagged for degradation by the UPS, which subsequently releases the ARF, allowing ARF-dependent transcription of the auxin response genes to occur (see figure 1.2).

The AUX/IAA Family

The AUX/IAA proteins are a family of small, short-lived nuclear proteins involved in the auxin response. These proteins are found throughout the entirety of the higher plants, with the *Arabidopsis* genome containing the genes of 29 AUX/IAA family members (Leyser, 2010). Originally discovered in soybean and pea, these proteins are rapidly transcribed in response to auxin and were originally known, along with the SAUR and GH3 gene families, as the 'early induced' auxin genes (Goda, et al., 2004). Later research with semi-dominant AUX/IAA *Arabidopsis* mutants, such as AXR2/IAA7, SHY2/IAA3 and BDL/IAA12 (Overvoorde, et al., 2005), elucidated the role of these genes as the transcriptional repressors of the auxin response pathway.

All AUX/IAA proteins share a similar four-domain structure (Mockaitis & Estelle, 2008). The first of these conserved domains, Domain I, contains an EAR (Ethylene Response Factor (ERF)-associated amphilic repression) motif. This domain has the canonical sequence LxLxL and is used in the formation of the AUX/IAA repressor complex with the transcriptional co-repressor TOPLESS (TPL) (Long, et al., 2006). Through the formation of this complex in the absence of an auxinic signal, the auxin response genes are tightly repressed.

The second of the four domains, Domain II, is the degron domain. This 17 amino acid motif interacts with the auxin receptor protein TIR1/AFB in the presence of auxin (Mockaitis & Estelle, 2008). Upon binding, the rest of the $SCF^{TIR1/AFB}$ E3 ligase complex then proceeds to ubiquitinate the AUX/IAA protein, targeting it for degradation by the 26S Proteasome and thereby releasing the ARF and thus repression of auxin responsive transcription. Mutations within this domain act to vary the degradation rate of the AUX/IAA proteins. Variations in this highly conserved region between AUX/IAA family members lead to vastly different rates of protein turn over. For example, IAA7 has been shown to have a half-life of 5-10 minutes in the presence of auxin (Dreher, et al., 2006). In comparison, IAA28, which has a similar but not identical domain II, has a half-life of 80 minutes in the presence of auxin (Calderon-Villalobos, et al., 2010).

The third and fourth domains, Domain III and IV, confer binding between the AUX/IAA repressor and the ARF family of transcription factors. These domains share a high homology with two similar regions within the ARF proteins, allowing for homo-dimerisation and heterodimerisation (Ulmasov, et al., 1997). Through the heterodimerisation of AUX/IAAs and ARF, transcriptional repression is achieved in the absence of a suitable auxinic signal.

The ARF Family

Like the AUX/IAA family of transcriptional repressors, the size of the ARF family of transcription factors is also large, with 23 of these genes identified in *Arabidopsis*. As with the AUX/IAAs, the ARFs also show a degree of redundancy between family members. They are broadly classified into two groups; those that activate the auxin response genes (i.e. ARF5, ARF6, ARF7, ARF8 and ARF19) and those that repress them (Chandler, 2016).

The ARF family of proteins contain four distinct conserved domains: a DNA binding Domain I, a highly variable Domain II, and dimerisation-conferring Domains III and IV which promote ARF homodimerisation and AUX/IAA binding. The first of these domains, Domain I, is a B3-like DNA binding domain. This domain contains a motif highly conserved amongst the auxin- and abscisic acid-regulated transcription factors (Yamasaki, et al., 2004). This motif forms a structure similar to that of the non-catalytic DNA binding domain of the *Eco*RII restriction enzyme, consisting of a

seven-stranded β-barrel flanked by a single α-helix at each end. It is through this motif that the ARFs are able to recognise and bind the auxin response elements (*Aux*REs) present in the promoter regions of auxin-induced genes (Ulmasov, et al., 1995).

FIGURE 1.2| THE AUXIN SIGNALLING CASCADE

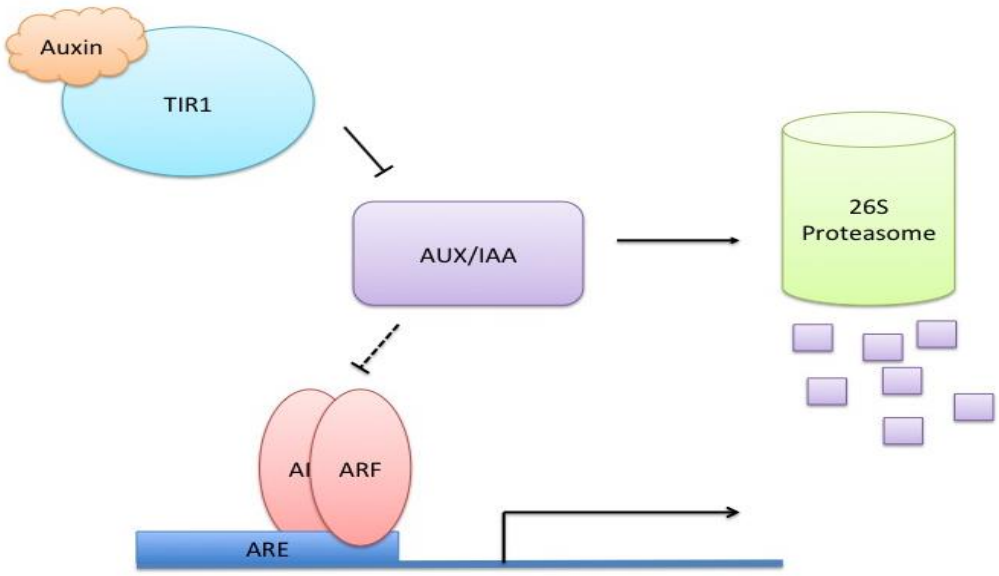

A schematic showing the auxin signalling cascade. The auxin signal is perceived by the auxin receptor SCF^{TIR1} ubiquitin E3 ligase complex (light blue). Upon binding auxin (orange), the SCF^{TIR1} ligase catalyses the ubiquitination and subsequent degradation, by the 26S Proteasome (green), of the auxin repressor proteins, the AUX/IAAs (purple), releasing the ARF transcription factors (red). This then allows auxin-induced transcription of the auxin responsive genes to occur.

1.1.6 The TIR1/AFB Family of Auxin Receptors

The auxin receptor TIR1 is a member of a large family of F-box proteins. This family includes the auxin receptors TIR1, AFBs 1-5 (Parry, et al., 2009), and the jasmonic acid receptor COI1. Through the formation of SCF-type ubiquitin protein ligase (E3) complexes containing these receptors, plants are able to regulate transcription of auxin responsive genes via the UPS-mediated degradation of the AUX/IAA proteins (Maraschin Fdos, et al., 2009).

E3 Ligases and the UPS

The ubiquitin-proteasome system (UPS) is a powerful regulator of cellular processes present in all eukaryotes. It an integral part of plant cellular machinery, with the UPS-mediated degradation of protein an essential aspect of almost every stage of development (Vierstra, 2009).

Through the UPS, targeted protein degradation is achieved via the attachment of the small protein modifier, ubiquitin (Deshaies, 1995). Ubiquitin moieties are conjugated via one of 7 conserved lysine residues to the target protein through the sequential action of three distinct enzymes: the ubiquitin-activating enzyme (E1), the ubiquitin-conjugating enzyme (E2) and the ubiquitin-ligase enzyme (E3) (Hershko & Ciechanover, 1998). Targeted proteins cycle repeatedly through this cascade until a short chain of ubiquitin moieties is formed, with Ub-chain topology determining the fate of the target protein (Walsh & Sadanandom, 2014). Chains linked via the K48 residue typically act as a signal for degradation by the 26S Proteasome as part of the UPS.

Via the ubiquitin-mediated degradation of targeted proteins, plants are able to quickly and efficiently respond to new stimuli. The specificity of target protein selection is determined through the E3 ubiquitin ligase. This large family of enzymes can be separated into three distinct classes: RING-type E3s, HECT-type E3s and SCF-type E3s (Pickart, 2001). In plants, it is the latter of these classes that form the largest group.

SCF E3 ubiquitin-ligase complexes consist of four subunits: ARABIDOPSIS SKP1-LIKE PROTEIN (ASK), CULLIN (CUL), RING BOX1 (RBX1) and the substrate receptor F-box proteins (FBPs) (Cardozo & Pagano, 2004). The FBPs confer substrate specificity; this allows the UPS to efficiently and effectively target a vast array of proteins for degradation through the formation of SCF complexes with varying F-boxes. In the auxin signalling system, the TIR1/AFB family of auxin receptors act as hormone-mediated F-box proteins, targeting the AUX/IAA repressor proteins for degradation (Calderon-Villalobos, et al., 2010).

The TIR1/AFB Family

In *Arabidopsis thaliana*, there are six members of the TIR1/AFB family: TIR1 and AFB1-5. Of these proteins, AFB1 is the most closely related homologue to the main auxin receptor TIR1, with 80% sequence similarity. AFB2 and AFB3 also share a high level of sequence similarity with each other, at over 80%, and are 60% identical to TIR1 and AFB1 (Dharmasiri, et al., 2005). Studies have shown that these four homologues act as auxin receptors and have partially overlapping functions in *Arabidopsis thaliana.*

The final two members of the TIR1/AFB family, AFB4 and AFB5, are both structurally and functionally distinct. Unlike TIR1/AFB1-3, these proteins contain an N-terminal extension with a currently unknown function, and aside from auxin binding, they also demonstrate an affinity for the picloram family of auxinic herbicides (Prigge, et al., 2016).

Phylogenetic analysis of this family, conducted by Parry et al. (2009), has shown that these proteins are highly conserved across land plants. They fall into four distinct clades, with three of these clades (TIR1/AFB2, AFB4 and AFB6) established through gene duplication events that occurred before the division of angiosperms and gymnosperms. Shortly before the division of monocot and eudicot plants, the TIR1/AFB2 clade divided further into the two distinct AFB1 and AFB2 clades. The maintenance of these distinct clades strongly suggests that the members of these subgroups have differing functions. Indeed, studies conducted by Parry et al. (2009) using the *tir1-1* auxin resistant mutant indicate the biochemically distinct nature of these proteins; their

experiments show that AFB1 and AFB2, despite their apparent similarity, are unable to fully rescue auxin signalling even when regulated by the TIR1 promoter.

TIR1/AFB Structure and 'Molecular Glue'

Members of the TIR1/AFB family of auxin receptor proteins are very similar in structure to the jasmonic acid receptor COI1 (Sheard, et al., 2010). The crystal structure of TIR1 in complex with ASK1 (Tan, et al., 2007), shows that the auxin receptor forms an 'umbrella-like' structure, the LRR domain forming the 'canopy' and the ASK1-binding F-box domain forming the 'handle' (see, figure 1.3).

The LRR domain, containing 18 leucine-rich repeat sequences, is folded into a twisted horse shoe shaped solenoid with the auxin and Aux/IAA dual binding pocket located at the top of the structure. Below the LRR domain sits the ~40 residue F-box domain, formed from a three helix bundle. It is through this domain that the four helices of the ASK1 C-terminal bind (Calderon-Villalobos, et al., 2010), forming part of the SCF^{TIR1} complex.

Unlike many other hormone receptors, where the hormone binding site and active site are located at different positions within the protein, the TIR1/AFB family of auxin receptors bind both hormone and substrate at the same site. Auxin binds at the bottom of this pocket with the Aux/IAA protein binding above, sealing the opening and trapping the auxin within the binding site until ubiquitination of the Aux/IAA protein occurs.

Unlike other hormone-receptor interactions, auxin binding does not result in any sort of conformational change within the receptor. Instead, auxin mediates the interaction between Aux/IAA and TIR1 through binding directly to both partners. As well as binding to the TIR1 receptor through a hydrophobic patch located in the lower half of the binding pocket, auxin also binds the highly hydrophobic degron domain (domain II) of the Aux/IAA protein through the GWPPV consensus motif (Tan, et al., 2007). This method of hormone perception, where the auxin

molecule directly regulates a high affinity interaction between Aux/IAA and TIR, known as 'molecular glue', is relatively novel.

Auxin Binding Pocket Promiscuity

As previously stated (see 1.2.3), there are over 200 identified auxinic compounds. Of these compounds, only two common features are conserved: a side chain containing a carboxyl group, and a planar aromatic ring structure (Ortiz-Castro, et al., 2011). Between auxinic compounds, the ring structure and associated side chains can vary significantly. However, not all molecules containing a planar ring and carboxyl side chain are auxinic in nature. This indicates a relative degree of promiscuity when it comes to auxin binding, yet also a fine level of specificity. This apparently oxymoronic state of affairs can be partially explained through the structure of the TIR1 binding pocket.

Crystallographic analysis of TIR1, by Tan et al. (2007), shows that the auxin binding pocket of TIR1 is formed between the inner C-terminal section of the LRR domain and a long, flexible loop that emerges from the second TIR1 LRR. Auxin binds at the bottom of this pocket, the planar ring stacked horizontally, through its conserved carboxyl group. Within the pocket, a series of two phenylalanine residues and the LRR β-sheet backbones form a highly hydrophobic site through which it is able to bind the aromatic ring of the auxinic compound.

Through the comparison of the binding strength of three auxinic compounds (IAA, 2,4-D and 1-NAA) within this pocket, Tan et al. (2007) were able to elucidate the mechanism behind the partial promiscuity of TIR1 auxin binding. Though all three compounds contain the two structures required for auxinic activity, a carboxyl side group and planar ring, the rest of the molecules differ wildly in ring structure. These differences, whilst accommodated by the hydrophobic ring-binding site, result in differing degrees of surface complementation between TIR1 and the auxinic compounds. Additionally, the presence of an amine group unique to IAA may strengthen this binding through hydrogen bonding with a carbonyl group located near the auxin binding site in the TIR1 backbone. A combination of these two factors may account for the differences between the observed binding affinities of the chosen compounds, with IAA, the most potent of the auxinic

compounds, showing a higher binding affinity for TIR1 than 2,4-D and 1-NAA. However, more research regarding the structure-activity relationship (SAR) of auxin is required to fully elucidate the factors behind auxin binding specificity and promiscuity.

TIR1 Co-Factor: Inositol Hexakisphosphate

Along with auxin and the AUX/IAA family of proteins, the binding pocket of TIR1 also interacts with a molecule called inositol hexakisphosphate (InsP6) (Tan, et al. 2007). This molecule sits within the LRR domain of the TIR1 auxin binding pocket, surrounded by 10 highly conserved positively charged amino acid residues. The orientation of InsP6 within the pocket allows it to come into direct contact with the basic residue used to bind the conserved carboxyl group of auxin. This allows InsP6 to form a hydrogen bond and salt-bridge network with the auxin molecule (Calderón Villalobos, et al., 2012). The position of InsP6 seems to indicate a role in organising and supporting the function of the binding pocket itself, suggesting that it may be an important co-factor for TIR1 function.

FIGURE 1.3| THE STRUCTURE OF ATTIR1

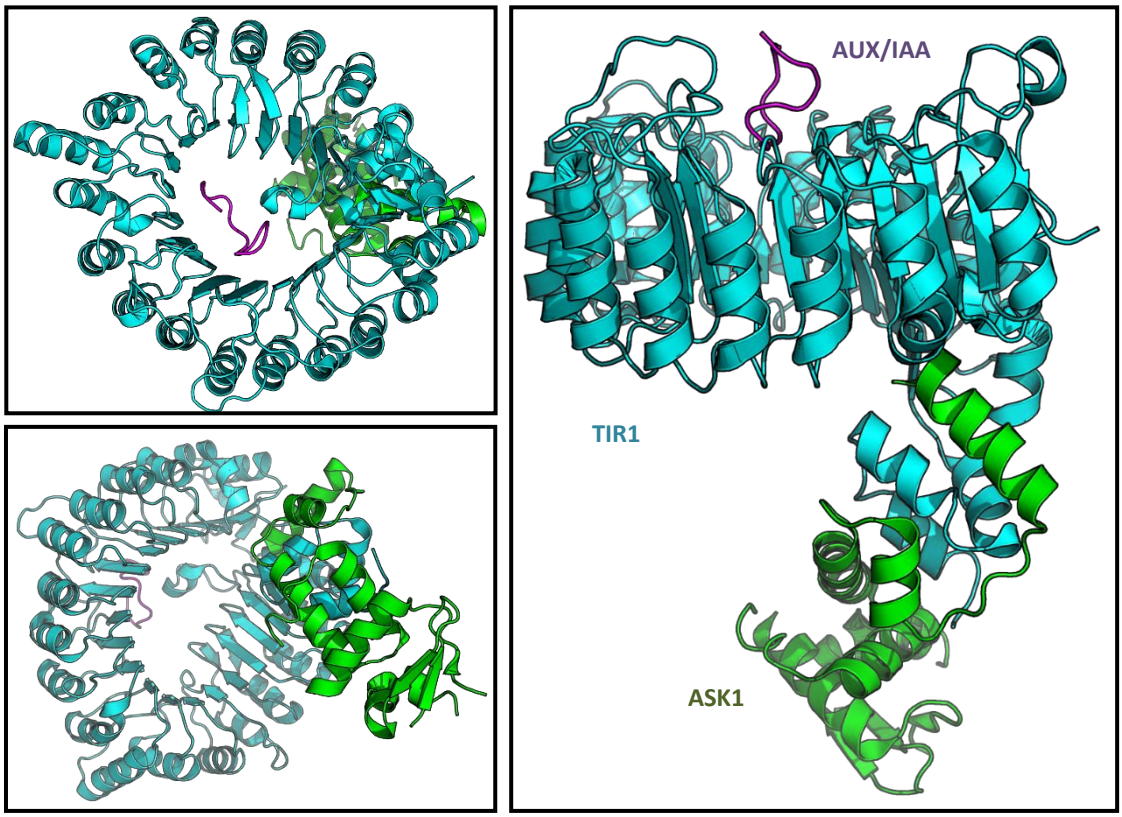

The 3D-structure of the ASK1-TIR1 auxin-receptor complex showing AUX/IAA binding, with each component shown in green, blue and purple, respectively. The Aux/IAA protein binds at the top of the barrel structure of TIR1 through a 'molecular glue' type interaction with auxin, which binds at the bottom of the barrel. Co-ordinates from pdb file 2P1M. (Tan, et al., 2007). Figure generated in PyMOL (Delano, 2002) modelling software, Version 1.8.

1.2 SUMOylation

1.2.1 Overview

The small ubiquitin-like modifier (SUMO) protein family is a subset of ubiquitin-like modifiers present in all eukaryotes. Through addition and removal from a lysine in the target protein, they are able to regulate protein function; these regulatory modifications play a large role in many important aspects of organism growth and development, including signal transduction, cell cycle control and DNA repair (Bossis & Melchior, 2006).

Unlike modifiers, such as acyl or methyl groups, SUMO proteins are more structurally complex than many of their counterparts. Though their sequence similarity to the modifier Ubiquitin is less than 20%, structurally the difference is negligible, with the defining structural feature of both of these proteins being a motif known as the Ub fold (Li & Hochstrasser, 2003). This motif consists of a five-stranded mixed half β-barrel, with β1 and β5 running parallel, and β2, β3 and β4 antiparallel (Bayer, et al., 1998), flanked by two α-helices. The motif itself therefore follows a β-β-α-β-β-α-β strand arrangement (Huang, et al., 2004). Alongside the Ub fold, members of these protein families also share an extreme C-terminal di-glycine (GG) motif through which conjugation to their target proteins occurs.

In *Arabidopsis thaliana,* the SUMO protein family consists of eight genes clustered into five sub-families: SUMO1/2, SUMO3, SUMO5, SUMO4/6, SUMO7/8. Members of these families are highly divergent in nature, unlike their mammalian equivalents, with proteins from one sub-family unable to complement those from another. Members of these sub-families range in sequence similarity from 32% to 86% (Kurepa, et al., 2003) but have several highly conserved residues, as shown in figure 1.4.

Of all the SUMO proteins present in *Arabidopsis*, perhaps the best studied are the SUMO1/2 proteins (Kurepa, et al., 2003). Data obtained by the Vierstra group indicate that these proteins accumulate rapidly in response to environmental stress (Saracco, et al., 2007); this combined with

the lethality observed in SUMO1/2 knock out (KO) mutants (Castaño-Miquel, et al., 2013), indicates their importance in the regulation of plant growth and stress responses.

To date, very little is known about other members of the SUMO protein family. Of the six other family members, only SUMO3 and SUMO5 have undergo any form of study, appearing to accumulate in specific tissues only (Saracco, et al., 2007). SUMO4, SUMO6, SUMO7 and SUMO8 are classed only as putative SUMO proteins, their function unknown.

FIGURE 1.4| ALIGNMENT OF ARABIDOPSIS SUMO PROTEINS

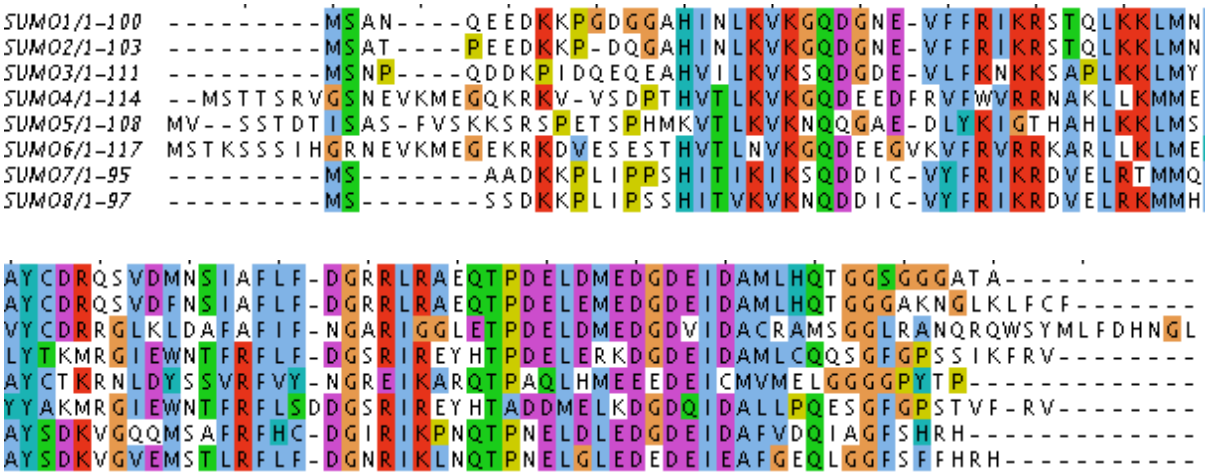

An alignment created with ClustalOmega (Sievers, et al., 2011) *using protein sequences obtained from UniProt records: SUMO1 (P55852), SUMO2 (Q9FLP6), SUMO3 (Q9FLP5), SUMO4 (Q9FKC5), SUMO5 (Q8VZI7), SUMO6 (Q9FKC6), SUMO7 (Q3E8A8), SUMO8 (B3H5R8). The alignment shows some conserved residues across all members of the Arabidopsis SUMO family, such as the C-terminal glycine through which conjugation to target proteins occurs.*

1.2.2 SUMOylation Machinery

As with other posttranslational modifiers, the addition of SUMO to a target protein requires a specialised enzyme set similar to that required for Ubiquitin conjugation (see, fig. 1.5). In order to complete the covalent addition of a SUMO moiety to a target protein, as with ubiquitin, four classes of enzymes are required: a SUMO-activating enzyme (E1), a SUMO-conjugating enzyme (E2), a SUMO ligase (E3) and a SUMO protease.

Before the process of SUMOylation can begin, the newly-synthesised SUMO precursor protein must be processed into its mature form. This processing step is performed by a class of enzymes known as the SUMO proteases; ubiquitin-like (Ulps) and sentrin-specific (SENPs) proteases facilitate the maturation of the SUMO precursor protein through the cleavage of the extreme C-terminus to reveal the di-glycine motif (GG) through which SUMO conjugation occurs (Gareau & Lima, 2010). The members of these families are also involved in the recycling of mature SUMO within the cell; alongside their role in SUMO maturation, the SUMO proteases also cleave the isopeptide linkage generated during SUMO conjugation, releasing SUMO moieties from target proteins. It is through this function that SUMO is able to be recycled quickly and efficiently, with continued cycling between the tagged and un-tagged forms of the target protein playing an important role in the response of the cell to various stimuli (Johnson, 2004). To date, little is known about SUMO proteases in *Arabidopsis thaliana.* Only eight potential SUMO proteases have been identified as of 2016 (figure 1.6), all of which belong to the C48 family of peptidases (Barrett & Rawlings, 2001).

SUMOylation begins with the activation of the SUMO protein. SUMO is activated through the formation of an acyl-anhydride bond between AMP and a carboxyl group located within the di-glycine motif at extreme C-terminus of the SUMO protein. The adenylated SUMO moiety is then attached through a high-energy thioester bond to a conserved cysteine residue within the E1 protein (Capili & Lima, 2007). The SUMO E1 activating enzyme is heterodimeric in *Arabidopsis thaliana*, consisting of one large (SAE2) and one small (SAE1) subunit. SAE2 contains the four essential SUMO activation domains: the Ub fold, the conserved catalytic cysteine, the acetylation domain, and the C-terminal domains (Lois & Lima, 2005). SAE1 completes the acetylation domain by the contribution of Arg21 (Lee & Schindelin, 2008).

Unlike mammalian and yeast species, the small subunit of the E1 enzyme in *Arabidopsis thaliana* is encoded by three paralogous gene sequences, SAE1a, SAE1b1 and SAE1b2. Of these sequences, generated during two independent gene duplication events (Castaño-Miquel, et al., 2013), *Arabidopsis* expresses two functional isoforms of the small subunit, SAE1a and SAE1b (SAE1b1 and SAE1b2 being identical). SUMO conjugation rates differ dependent on the E1 isoform involved in the cascade; an increase in SUMOylation is observed during the formation of an E1 complex containing the SAE1a subunit compared to SAE1b (Budhiraja, et al., 2009). This change in conjugation rate indicates a possible role for the E1 small subunit the downstream regulation of SUMOylation.

Once activated, the SUMO moiety is transferred from the E1 activating enzyme to the E2 conjugating enzyme, once again binding through a highly conserved cysteine reside. Through the E2, the activated SUMO is transferred to the target protein via the formation of an isopeptide bond through the C-terminal di-glycine motif of the SUMO moiety and the ε-amino group of a lysine located within a SUMO binding site in the target protein (Miura, et al., 2007).

The conjugation of SUMO to a specific target protein is achieved through interaction with the final enzyme in the SUMOylation cascade, the E3 SUMO ligase, which acts as a linker. Unlike the previous two enzyme classes described above, the SUMO E3 ligases are not required to simulate the SUMOylation process *in vitro*; the E3 SUMO ligases are involved primarily in determining target specificity rather than direct SUMO transfer (Perdomo, et al., 2012).

To date, three types of SUMO ligases have been identified: PIAS, RanBP2 and PC2. Though structurally unrelated, the PIAS group of E3 ligases do appear to show some structural homology to the RING domain found within E3 ubiquitin ligases (Dohmen, 2004). Currently, only two SUMO ligases have been identified in *Arabidopsis thaliana*, SIZ1 and MMS21/HPY2. Both of these enzymes have been shown to possess the highly conserved SP-RING motif, placing them firmly within the PIAS ligase group (Ishida, et al., 2012). Research has shown that SIZ1 and HPY2 are involved in a diverse number of essential processes, such as copper tolerance (Chen, et al., 2011),

the development and maintenance of the root and shoot meristem (Zhang, et al., 2010), nitrogen assimilation (Park, et al., 2011) and the regulation of the cell cycle (Ishida, et al., 2009).

FIGURE 1.5| THE MECHANISM OF UBIQUITINATION VS. SUMOYLATION IN ARABIDOPSIS

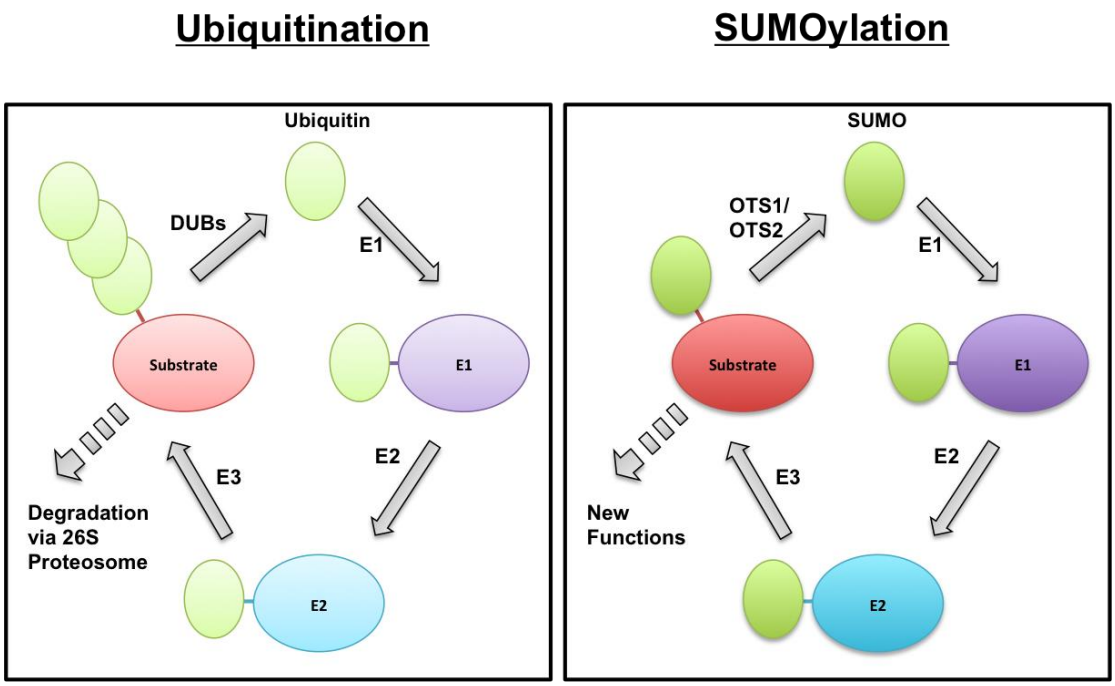

A schematic showing the mechanisms of ubiquitination and SUMOylation in Arabidopsis. Ub/SUMO is activated through the catalysis of ATP by the E1-activating enzyme. It is then transferred to the E2-conjugase before being finally conjugated onto the target protein via the E3-ligase enzyme, whereupon it becomes targeted for degradation, in the case of ubiquitin, or confers new or altered functions to the target protein, in the case of SUMO. The Ub/SUMO moiety is removed via the activation of specialised protease enzymes termed de-ubiquitinating enzymes (DUBs)/SUMO Proteases, such as OTS1 and OTS2, allowing recycling of the Ub/SUMO moieties. It is through this dynamic cycling of posttranslational modification that the cell is able to quickly and efficiently respond to a variety of stimuli.

FIGURE 1.6| SEQUENCE SIMILARITY BETWEEN THE ARABIDOPSIS SUMO PROTEASES

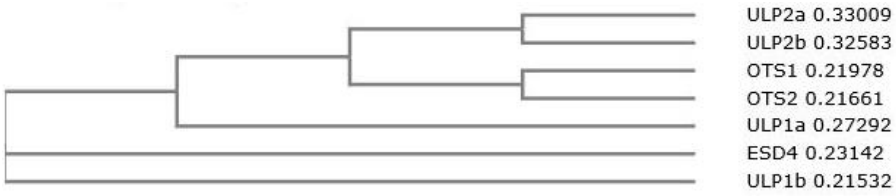

A phylogenetic tree generated from the sequence data of known SUMO proteases from Arabidopsis thaliana. OTS1 and OTS2 can be seen to be closely related, falling into a distinct clade. (Novatchkova, et al., 2012).

1.2.3 The Role of SUMO in Plants

Though research into SUMOylation in plants is still in its infancy, many essential developmental and regulatory pathways have been identified as targets of this process. Plants deficient in SUMO homeostasis, either through disruption of SUMO conjugation or de-conjugation, display defects in organ growth and reproduction, as well as a decreased tolerance to both biotic and abiotic stress (Xu & Yang, 2013). Indeed, mutations in the E1-activating enzyme (SAE1/2), the E2-conjugating enzyme (SCE1) and SUMO1/2 are embryonic lethal (Saracco, et al., 2007), indicating the importance of SUMOylation within plants.

The SUMO E3-Ligases SIZ1 and HPY2

In *Arabidopsis thaliana*, two SUMO E3-ligases have been identified to date: SIZ1 and HPY2 (Yoo, et al., 2006). Though both enzymes are involved the conjugation of SUMO moieties to target proteins, they appear to perform differing functions within the plant (Ishida, et al., 2012), with SIZ1 and HPY2 unable to rescue their respective mutant phenotypes when placed until reciprocal promoter control.

Work conducted by several groups has shown SIZ1 to be integral in the response to many abiotic stresses, such as drought stress (Catala, et al., 2007), phosphate starvation (Miura, et al., 2005) and cold stress (Miura, et al., 2007). SIZ1 has also been implicated in the regulation of plant tissue development with respect to cell proliferation and expansion. In the *Arabidopsis siz1-3* knock-out mutant, the cells of both the mesophyll and epidermis were far smaller than that of the wild type, with 2.3x more cells found per unit area in the mutant plants (Catala, et al., 2007). qPCR data from this mutant line shows the down regulation of several auxin-related genes, such as IAA6, PIN7 and AUX1, suggesting that SIZ1 is involved in at least some aspect of auxin signalling homeostasis.

Research by Ishida, *et al.* (2009) and Huang, *et al.* (2009) has indicated that, alongside SIZ1, HYP2 may also play a role in auxin signalling. The HPY2 E3 ligase has been shown to be essential in the regulation of cell proliferation within the root apical meristem (Huang, et al., 2009). Auxin, in

combination with cytokinin, has long been known as the phytohormone responsible for cell cycle control. It has been suggested that HPY2 acts downstream of this signal as part of the regulation of cell proliferation (Ishida, et al., 2009).

The two E3 ligases also demonstrate differential expression patterns within the plant. Expression of SIZ1 is global, occurring in all cell types throughout the plant (Ishida, et al., 2012), with large amounts of SIZ1 protein accumulating in primary and lateral root tissue. HPY2 expression, however, appears to be tissue specific, with large amounts of HPY2 shown to accumulate in the root apical meristem, but not in the differentiated cells of the more mature root tissue. This data, along with the *siz1-3* qPCR data, phenotyping of *siz1-3* knock-out mutants (Catala, et al., 2007) and the identification of HPY5 as a downstream component of the cell cycle machinery (Ishida, et al., 2009), suggests that SUMOylation plays a significant role in auxin signalling.

The Role of SUMOylation in Photoreception

Recent work by the Sadanandom group has demonstrated that SUMO plays a significant role in the regulation of the *Arabidopsis* photoreception pathway (Sadanandom, et al., 2015). In order to respond appropriately to light, plants employ a wide array of photoreceptors, including cryptochromes and phytochromes (Goyal, et al., 2013). One of these photoreceptors, the phytochrome phy-B, has been shown to be inhibited upon SUMOylation of its C-terminus (Sadanandom, et al., 2015). Once SUMOylated, phy-B is no longer able to interact with its associated negative regulatory factor, PIF5, resulting in the inhibition of photomorphogenesis.

The Role of SUMOylation in Gibberellin Signalling

To date, SUMO has been shown to play a key role in at least one phytohormone signalling pathway, that of gibberellin. Gibberellins (GAs) are plant hormones involved in the regulation of seed germination, flowering and growth (Davière & Achard, 2013). GA stimulates the degradation of the repressor proteins known as DELLAs via the UPS, leading to growth of the plant.

Under stress conditions, these DELLA repressor proteins undergo rapid SUMOylation (Conti, et al., 2014). The addition of a SUMO moiety to the DELLA protein causes an increase in DELLA protein stability, leading to an attenuation of the GA-mediated growth signal. The stabilisation through SUMO of the DELLA proteins is achieved through interaction between SUMOylated DELLAs and the SUMO INTERACTING MOTIF (SIM) site located on the GA-receptor protein GID1. SUMOylated DELLAs are able to sequester the GID1 receptor in a GA-independent manner, leading to the accumulation of non-SUMOylated DELLA proteins and the subsequent suppression of the growth response under stress conditions.

The SUMO Proteases OTS1 and OTS2

The SUMO proteases, OVERLY TOLERANT TO SALT1 (OTS1) and OTS2, have been shown to be involved in the regulation of the salt stress response in *Arabidopsis* (Conti, et al., 2008). These proteases are localized to the nucleus and are responsible to the cleavage of conjugated SUMO1/2 from their target proteins. Experiments by Conti *et al.* have shown that over expression of OTS1 increases salt tolerance in *Arabidopsis*, with seedlings able to germinate and thrive on up to 100mM salt. Similarly, they have shown that double knock out plants, *ots1/ots2,* show a hypersensitive phenotype under salt stress conditions. Perhaps the most interesting aspect of their research was the discovery that *ots1/ots2* plants show a global increase in SUMOylated protein under non-stress conditions, indicating a role for OTS1/2 beyond that of the salt stress response (Conti, et al., 2008).

Recent research by Srivastava, Zhang and Sadanandom (2016) has lead to the identification of an *At*OTS1 homologue in rice, *Os*OTS1. Rice plants with the silenced *Os*OTS1 gene showed an increased susceptibility to salt stress, similar to that seen in *Arabidopsis*, and also demonstrated a significant reduction in germination rate. OsOTS1 knockdown lines showed a reduction in root mass through the reduction of root cell size (Srivastava, et al., 2016). This research indicates the importance of SUMOylation in commercially valuable crop species.

1.3 Study Objectives

In previous work by Conti, et al. (2008), the over expression of the SUMO protease OVERLY TOLERANT to SALT1 (OTS1) has been shown to result in an increased tolerance to salt stress. *Arabidopsis thaliana* double knock-out lines for the *ots1* and close homologue *ots2* genes show a hypersensitivity to salt, resulting in a change in *Arabidopsis* root architecture compared to wild type. Given the well known association between auxin signalling and root growth and development, it was hypothesised that SUMOylation plays a role in auxin signalling through (de-)SUMOylation of integral parts of the auxin signalling machinery, such as TIR1, AUX/IAA and ARF.

The main objectives of this work are as follows:

1. Investigate the role of SUMOylation in the auxin response through phenotypic analysis of the hyper-SUMOylated *Arabidopsis* mutant *ots1/ots2.*
2. Investigate the SUMOylation status of the primary auxin receptor TIR1 and its role within the wider auxin response cascade.
3. Investigate the SUMOylation status of the rest of the auxin signalling cascade machinery, i.e. AUX/IAA and ARF.

2. Methods and Materials

2.1 Plant Growth and Treatment

2.1.1 *Arabidopsis thaliana* Tissue Culture

All *Arabidopsis* seedlings used, ecotype Col-0, were grown on ½ MS medium (Duchefa Biochemie) supplemented with 0.5% Sucrose (Duchefa Biochemie) and 0.8% agar (Duchefa Biochemie). Media was allowed to cool to 50°C before adding hormone treatments.

2.1.2 *Arabidopsis thaliana* Sterilization for Tissue Culture

Arabidopsis seeds were sterilized in a closed box in a fume hood using chlorine gas generated from the addition of 3ml concentrated hydrochloric acid to 100ml of 13% hypochlorite solution. The seeds were left for 12 hours before being ventilated to render the box safe and placed on plates under sterile conditions (laminar flow hood). The ½ MS plates were then sealed with micropore tape (3M) and stratified for 3 days at 4°C. The plates were then placed vertically at room temperature in 24hr light to induce germination and growth.

2.1.3 *Arabidopsis thaliana* Hormone Treatment

The following auxin stock solutions were made:

TABLE 2.1| HORMONE STOCK SOLUTION CONCENTRATIONS

Auxin	Solvent	Stock Conc. (mM)
Indole-3-Acetic Acid (IAA)	1N NaOH	100
1-Naphthaleneacetic Acid (NAA)	1N NaOH	100
2,4-Dichlorophenoxyacetic Acid (2,4-D)	100% EtOH	100
2,3,5-Diidobenzoic Acid (TIBA)	DMSO	100

A table showing the hormones used.

The stock solutions were diluted to working concentration (various) using ddH_2O. ½ MS plates were supplemented with the appropriate treatment.

3 days after germination on standard ½ MS plates, seedlings were transferred to the hormone-supplemented plates. The plates were then placed vertically at room temperature in 24hr light to allow germination and growth. After 3 days, images of the seedlings were taken and the images analysed in ImageJ.

2.1.4 *Arabidopsis thaliana* Growth

Arabidopsis thaliana seeds were sown in moist Levington F2 plus sand compost treated with Calypso SC 480 insecticide (Bayer). The seeds were then stratified for 3 days at 4°C before being transferred to MLR Plant Growth Chambers (Panasonic). The plants were grown under long day conditions: 16 light hours at 22°C and 8 dark hours at 20°C with a constant relative humidity of 70%.

2.1.5 Floral Dipping of *Arabidopsis thaliana*

Generated constructs in GV3101 were dipped into *Arabidopsis thaliana* to create transgenic seeds using the protocol specified in Clough & Bent (1998).

2.1.6 Crossing of *Arabidopsis thaliana*

Selected *Arabidopsis* lines were manually crossed to create new mutant lines using the protocol specified in Weigel & Glazebrook (2006).

2.1.7 Selection of Transgenic *Arabidopsis thaliana*

Primary transformants were selected for by spreading seed on soil soaked with 0.1% Glufosinate (marketed as Basta, Bayer). After 9 days, resistant seedlings were pricked out onto fresh soil with no selection and grown under long day conditions. Once siliques formed, the plants were bagged individually and allowed to set seed.

Secondary transgenic seed was sterilized (see, 2.1.2) and spread aseptically on ½ MS plates supplemented with 20µg/ml final glufosinate-ammonium. The plates were sealed with micropore tape (3M) and the seeds stratified at 4°C for 3 days. The plates were then moved to growth cabinets and grown for eleven days (see, 2.1.4). The seedlings were then screened for resistance at a ratio of 3:1 (resistant : susceptible) in order to select for transgenics containing a single transformation insert. Selected lines were then pricked out onto fresh soil with no selection. Again, individual plants were bagged to collect seed once siliques had formed.

Tertiary transgenic seed was sterilized (see, 2.1.2) and spread aseptically on ½ MS plates supplemented with 20µg/ml final glufosinate-ammonium. The plates were sealed with micropore tape (3M) and the seeds stratified at 4°C for 3 days. The plates were then moved to growth cabinets and grown for eleven days (see, 2.1.4). Plants were then screened for complete

resistance, indicating homozygous transgenics. Selected lines were then pricked out onto fresh soil with no selection. Again, individual plants were bagged to collect seed once siliques had formed.

2.2 Microbiological Procedures

2.2.1 Generation of Chemically Competent *E. coli*

The selected *E. coli* strain (e.g. DH5α) was streaked out onto a fresh LB agar plate with no selection and incubated at 37°C for 24 hours. A single colony was selected using a sterile loop and used to inoculate 10ml of LB liquid. The culture was grown for 16 hours at 37°C. 1ml of the culture was then used to inoculate 200ml of LB liquid, with shaking at 220rpm, at 37°C for a further 6 hours. The culture was transferred to chilled centrifuge tubes and centrifuged at 4000rpm for 15 minutes at 4°C. The supernatant was removed and the cells resuspend in 10ml of ice-cold TE buffer. The culture was re-centrifuged under the same conditions, the supernatant removed and the cells resuspended in 20ml of ice-cold liquid LB. The cells were then stored at -80°C in 100µl aliquots.

2.2.2 Generation of Chemically Competent *Agrobactierum tumefaciens*

The selected *Agrobacterium* strain (e.g. GV3101) was streaked out onto a fresh LB agar plate with rifampicin and gentamycin selection and incubated at 28°C for 48 hours. A single colony was selected using a sterile loop and used to inoculate 10ml of LB liquid plus rifampicin and gentamycin. The culture was grown for 24 hours at 28°C. 1ml of the culture was then used to inoculate 200ml of LB liquid plus rifampicin and gentamycin and incubated, with shaking at 220rpm, at 28°C for a further 18 hours. The culture was transferred to chilled centrifuge tubes and centrifuged at 4000rpm for 15 minutes at 4°C. The supernatant was removed and the cells resuspend in 10ml of ice-cold TE buffer. The culture was re-centrifuged under the same conditions, the supernatant removed and the cells resuspended in 20ml of ice-cold liquid LB. The cells were then stored at -80°C in 200µl aliquots.

2.2.3 Transformation of Chemically Competent Bacterial Cells

Transformation and growth of bacterial cells with recombinant plasmids were used to 'bulk up' and select said plasmids (using *E.coli* strain DH5α), to express recombinant protein (using *E.coli*

strain BL21 (DE3)) or to act as a vector in transient expression systems (using *Agrobacterium* strain GV3101).

For a typical chemical transformation:

100 – 200ng Plasmid DNA

40/200µl Chemically competent *E.coli/Agrobacterium,* respectively.

For *E. coli:*

Cells were thawed on ice for 10min, plasmid DNA added and incubated on ice for 30min . Cells were placed 42°C for 30sec then returned to ice for a further 5min. 1ml of SOC (at RT) was added and the cells incubated in an orbital incubator shaker at 220rpm for 1 hour at 37°C.

For *Agrobacterium:*

Cells were thawed on ice for 20min, plasmid DNA added incubated on ice for 5min . Cells were flash frozen in liquid nitrogen for 5min then transferred to 37°C for 5 min. 1ml of LB (at RT) was added. The cells were incubated in an orbital incubator shaker at 220rpm for 2 hours at 28°C.

50µl culture was spread upon an LB plate with antibiotic selection. The rest of the culture was centrifuged at 14,000rpm for 30sec and the majority of the supernatant removed. The cells were resuspended in the remaining 50µl supernatant and spread upon an LB plate with antibiotic selection. The plates were incubated overnight at 37°C for *E. coli* and over a period of two days at 28°C for *Agrobacterium*. Colony PCRs were then performed to check for the presence of the recombinant gene (see 2.3.1)

2.2.4 Recombinant Plasmid Purification

Recombinant plasmids were purified from 10ml *E. coli* DH5α cultures incubated overnight at 37°C using a ZR Plasmid Miniprep Kit - Classic (Zymo Research). The amount of DNA obtained was then quantified using a NanoDrop^{TM} 1000 Spectrophotometer (Thermo Scientific).

2.3 Nucleic Acid

2.3.1 Polymerase Chain Reaction

Q5™ (NEB) cloning PCR was used to amplify the enzymatic components (see tables 2.2 and 2.3) using primers with CACC added to the 5' end of the forward primer. Colony PCR with vector-specific AttB primers was used to check for the recombinant gene insert after bacterial transformation (see tables 2.4 and 2.5). For colony PCR, individual bacterial colonies were picked using pipette tips and diluted in 20μl sterile water. 2μl was used as template.

TABLE 2.2| Q5 PCR SETUP

Component	Per Reaction
5x Q5™ Reaction Buffer	5μl
5mM dNTPs	0.5μl
Upper Primer (10pM/μl)	1.25μl
Lower Primer (10pM/μl)	1.25μl
Template	100-200ng
Q5™	0.25μl
Sterile Water	to 25μl

A table showing the compositions of cloning and site-directed mutagenesis PCRs.

TABLE 2.3| Q5 PCR CLONING CONDITIONS

Temperature	Time	Number of Cycles
98°C	1 min 30 sec	-
98°C	15 sec	X40
~2°C Lower Than Primer Tm	15 sec	
72°C	15 sec per kb	
72°C	7 min	-
10°C	∞	-

A table showing the cycling programmes used during cloning and site-directed mutagenesis PCR.

TABLE 2.4| COLONY PCR SETUP

Component	Per Reaction
2x TaqMan® Fast Universal Master Mix (Invitrogen)	2.5µl
AttB Upper Primer (10pM/µl)	0.25µl
AttB Lower Primer (10pM/µl)	0.25µl
DNA Template	10-20ng
Sterile Water	to 10µl

A table showing the compositions of colony PCRs.

TABLE 2.5| COLONY PCR CLONING CONDITIONS

Temperature	Time	Number of Cycles
94°C	3 min	-
94°C	30 sec	x35
55°C	15 sec	
72°C	30 sec per kb	
72°C	7 min	-
4°C	∞	-

A table showing the cycling programmes used during colony PCR.

Gene amplification was observed using agarose gel electrophoresis. Cloning and mutagenesis PCR gene products of the correct size were then cut from the gel using a sharp scalpel and the DNA purified using a Zymoclean Gel DNA Recovery Kit (Zymo).

2.3.2 Agarose Gel Electrophoresis

Agarose was added to 1xTAE buffer to make a 0.8-2.5% solution. The solution was then microwaved at full power until the agarose had dissolved. The solution was allowed to cool before ethidium bromide was added to a final concentration of 0.0001%. The solution was then poured into an appropriate sized gel mould, a 20/30 well comb added and the solution allowed to set. The gel was then placed into an electrophoresis tank filled with 1xTAE. Prior to sample loading, 5X

Sample Buffer (NEB) was added to the DNA samples (step omitted if using Master Mix Taq). Samples were loaded into the wells along with Hyperladder 1kb Plus (Bioline) and the gels were run at 70-110V, dependent upon agarose percentage used. The gels were imaged using a BioRad Gel Doc 2000.

2.3.3 pENTR/D-TOPO Reaction

A pENTR/D-TOPO reaction with clean PCR product containing the recombinant gene was performed following the instructions provided in the supplied kit (Invitrogen). The reaction contents were then transformed into *E. coli* DH5α (see, 2.2.3).

2.3.4 Restriction Digestion

Restriction digestion of purified DNA was used to remove template DNA from mutagenesis PCR products (DpnI (NEB)) and to cut the pENTR™/D-TOPO vector ready for LR reaction (MluI (NEB)). For a standard restriction digest, see table 2.6.

TABLE 2.6| RESTRICTION DIGESTION SETUP

Component	Per Reaction
10x Compatible NEB Buffer	20μl
DNA	1-10μg
Restriction Endonuclease (NEB)	5U per μg DNA
Sterile Water	To 200μl

A table showing the components used in a standard restriction digest with NEB enzymes.

The reactions were incubated at 37°C temperature for 1 hour, transferred to a fresh tube, and incubated for a second hour.

Restriction endonucleases are stored in 50%(v/v) glycerol-containing storage buffer. Care must be taken to ensure that the total glycerol concentration for each reaction does not exceed 5%(v/v) glycerol due to increased star activity of the enzyme.

2.3.5 LR Reaction into Gateway® Destination Vectors

An LR reaction with MluI-digested pENTR™/D-TOPO vector containing the recombinant gene was performed following the instructions provided in the supplied kit (Invitrogen) with an appropriate Gateway® Destination Vector for protein expression in either *E. coli* BL21 (DE3) or *Agrobacterium.* The reaction contents were then transformed into *E. coli* DH5α (see, 2.2.3).

2.3.6 gDNA Extraction from *Arabidopsis thaliana*

A single leaf disc was cut using the end of a p10 pipette tip. The disc was ground briefly in a 1.5ml eppendorf tube using a mini-pestle. 150µl of extraction buffer was added and the mix ground again until homogenous. The sample was centrifuged at 13,500 rpm for 5 minutes. 100µl of the supernatant was transferred to a fresh tube and 100µl of neat isopropanol was added and mixed via inversion. The mixture was incubated at room temperature for 5 minutes. Samples were centrifuged at 13,500 rpm for 10 minutes and the supernatant discarded. The pellet was mixed gently with 500µl of 70% EtOH and centrifuged at 13,500 rpm for 5 minutes. The supernatant was discarded and the pellet left to air-dry for 15 minutes. The dry pellet was then dissolved in 50µl of 10mM Tris (pH 8.5 at 25°C). The quality of the gDNA extraction was then checked via PCR using actin primers.

2.3.7 RNA Extraction from *Arabidopsis thaliana*

Frozen plant tissue was ground into a fine powder using a pre-cooled mortar and pestle. The Spectrum™ Plant Total RNA Kit (Sigma-Aldrich) was used to extract RNA. All extractions were performed following the instructions provided in the supplied kit. RNA was quantified by measuring absorbance at λ260nm and λ280nm using a NanoDrop™ 1000 Spectrophotometer (Thermo Scientific).

2.3.8 cDNA Synthesis

1.5µg of RNA was treated with 1µl DNase RQ1 (Promega) in a 10ul reaction made with DEPC water. The reaction was incubated at 37°C for 30 minutes. 1µl RQ1 Stop Solution and the reaction incubated for a further 10 minutes at 65°C. 1µl of oligo dT (500µg/ml) and 1µl dNTP mix (10µM each) was added to the reaction and incubated at 65°C for a further 5 minutes. The reaction was then chilled briefly on ice and spun down. 4µl 5X First Strand Buffer, 2µl 0.1M DTT and 1µl RNaseOUT was added to the reaction and mixed gently. The reaction was incubated at 42°C for 2 minutes before 1µl SuperScript® II Reverse Transcriptase was added to the reaction. The reaction was then incubated at 42°C for a further 50 minutes. Finally, the reaction was heated to 70°C for 15 minutes to terminate the reaction. The resultant cDNA was made up to 100µl using ultra-pure water. The quality of the resultant cDNA was tested by qPCR with *ACTIN8* primers.

2.4 Protein

2.4.1 SDS-PAGE

Acrylamide gel electrophoresis is used to separate and visualise proteins that differ in molecular weight. The tertiary structure of the loaded proteins is denatured by SDS, which coats the protein in a negative charge, allowing for separation by size alone. The application of an electric field upon a gel causes separation of the proteins into discrete bands that can be seen using coomassie staining or transferred to a PVDF membrane for western blotting (see 2.4.2). The gels consist of a stacking and running gel, the latter of which can vary in acrylamide percentage depending on the weight of proteins that require separation (see table 2.7).

TABLE 2.7| SDS-PAGE GEL COMPOSITIONS

Running Gel	**8%**	**10%**	**12%**	**14%**
1.5M Tris (pH8.8 at 25°C)	2.5ml	2.5ml	2.5ml	2.5ml
10%(w/v) SDS	100µl	100µl	100µl	100µl
30%(w/v) 29:1 Acrylamide:Bis-acrylamide	2.7ml	3.33ml	4.0ml	5.4ml
Water	4.65ml	4.02ml	3.35ml	1.95ml
TEMED	15µl	15µl	15µl	15µl
10%(w/v) APS	40µl	40µl	40µl	40µl

Stacking Gel	**5%**
1.5M Tris (pH6.8 at 25°C)	0.5ml
10% (w/v) SDS	50µl
30% (w/v) Acrylamide	0.833ml
Water	3.5ml
TEMED	7.5µl
10% (w/v) APS	20µl

A table showing the composition of the running gel (top) in which the protein bands are resolved, and the stacking gel (bottom) in which the proteins are loaded.

Lysed samples were mixed with 1x SDS Loading Buffer, heated to 95°C for 5min and loaded onto a gel. Gels were run at 100V to resolve the proteins.

2.4.2 Western Blotting

Western blotting is used to visualise specific proteins within homogenised cell or tissue extracts. A PVDF membrane was submersed methanol for 2 min then soaked in 1x transfer buffer for up to 15 min with blotting paper and sponges. The blotting cassette was prepared and proteins transferred overnight at 20V at 4°C from an SDS-PAGE gel onto the membrane. The membrane was incubated in blocking solution for 1 hour to prevent non-specific binding of the primary antibody (Bergendahl, Glaser and Burgess, 2003). The membrane was washed 1xTBST and incubated with primary antibodies in 1x TBST as per the instructions in table 2. The membrane was washed with 1xTBST and incubated with secondary antibodies (HRP). The membrane was washed again with 1xTBST and developed using ECL solution.

2.4.3 Infiltration of *Nicotiana benthamiana*

Agrobacterium containing recombinant plasmid was incubated overnight in an orbital incubator shaker at 28°C and 220rpm. The cells were pelleted at RT at 5000rpm and resuspended in 20ml 10mM sterile $MgCl_2$. The cells were diluted using 10mM sterile $MgCl_2$ to an OD_{600} 0.1-1 and infiltrated into a single *Nicotiana benthamiana* leaf (provided by Mr. John Simpson) using a 1ml sterile syringe. The plant was then kept at 18°C on a long day cycle for 3 days.

2.4.4 Protein Extraction from *Nicotiana benthamiana* Leaves

1g of infiltrated *Nicotiana benthamiana* leaves were cut at the stem from the plant, wrapped in aluminum foil and flash frozen in liquid nitrogen. The leaves were then powdered in a liquid nitrogen-cooled mortar and pestle and 1g of PVPP added.

For SUMO:

2ml of ice-cold SUMO buffer was added to the powdered tissue and ground further using the mortar and pestle to form a paste. Upon melting, the now liquid paste was then transferred to a pre-cooled eppendorf tube. The tubes were centrifuged at 4°C and 8,000rpm for 12 min. The supernatant was transferred to a fresh pre-cooled tube and was either prepared for loading onto an SDS-PAGE gel by the addition of 1xSDS Buffer or immunoprecipitated using the MACS® microbead system (Miltenyi Biotech) as per the instructions included in the kit. The tubes were incubated on ice for 15 minutes and the SUMOylated protein extracted using a µMACs multistand and separator. The eluted protein was then loaded onto an SDS-PAGE gel for western blotting.

For CO-IP:

2ml of ice-cold CO-IP buffer was added to the powdered tissue and ground further using the mortar and pestle to form a paste. Upon melting, the now liquid paste was then transferred to a pre-cooled eppendorf tube. The tubes were centrifuged at 4°C and 10,000rpm for 15 min. The supernatant was transferred to a fresh pre-cooled tube and was either prepared for loading onto an SDS-PAGE gel by the addition of 1xSDS Buffer or immunoprecipitated using the MACS® microbead system (Miltenyi Biotech) as per the instructions included in the kit. The tubes were incubated on ice for 30 minutes to 1 hour and the SUMOylated protein extracted using a µMACs multistand and separator. The eluted protein was then loaded onto an SDS-PAGE gel for western blotting.

1ml of ice –cold SUMO extraction buffer was added to 1ml powder and centrifuged at 4°C and 8000rpm for 12 min. The supernatant was removed into a fresh tube and was either prepared for loading onto an SDS-PAGE gel by the addition of 1xSDS Buffer or immunoprecipitated using the MACS® microbead system (Miltenyi Biotech) as per the instructions included in the kit.

2.5 Imaging

2.5.1 Cell Clearing

In order to minimise light scattering during observation of deep tissue structures using light microscopy, *Arabidopsis* roots were cleared using the following protocol. The seedlings were placed in acidified methanol (20% MeOH, 4% conc. HCl) and incubated at 55°C for 15 minutes. The roots were then transferred to a basic solution (7% NaOH, 60% EtOH) for neutralisation and incubated at room temperature for 15 minutes. The roots were then rehydrated over the course of several EtOH incubation steps. The roots were first incubated in 60% EtOH at room temperature for 5 minutes, then transferred to a 40% EtOH solution and the incubation step repeated. The roots were moved through 20% and 10% EtOH solutions before being moved to a 50% glycerol solution. The roots were incubated at room temperature for 30 minutes before being mounted ready for imaging.

2.5.2 LR Primordia

The cleared seedlings were mounted onto slides in 50% glycerol. The roots were imaged using bright field microscopy using a NA 60x oil objective. The lateral root primordia were then counted and classified according to stage.

2.5.3 Confocal Imaging

The subcellular localisation of YFP-tagged constructs and relative expression of DR5:VENUS was visualised using a confocal laser scanning microscope (Zeiss 880 with Airyscan) with a NA 60x oil objective. YFP and VENUS fluorescent tags were excited using an argon laser at λ488nm and transmission collected between λ505nm and λ530 to prevent crosstalk from chloroplast auto-fluorescence.

2.6 Software Packages

2.6.1 Sequence Analysis and Primer Design

Serial Cloner Version 2.6.1 © 2004-2016 Frank Perez (SerialBasics)

Finch TV Version 1.4 © 2013 Geospiza®

2.6.2 Image Capture

Quantity One® 1-D Analysis Software Version 4.6.5 © Bio-Rad Laboratories.

2.6.3 Figure Preparation

ImageJ Version 1.47

Zen Imaging Software © Version 2.3 Ziess Ltd.

Photoshop CC 2014 Version 15.0 © Adobe

PyMOL Molecular Graphics System, Version 1.8. Schrodinger LLC. (Delano, 2002)

2.6.4 Manuscript Compilation

Microsoft Word © Office 2016, Microsoft.

2.7 Materials

2.7.1 Buffers

All buffers were made with ultrapure deionised water.

4x SDS Loading Buffer: 200mM Tris-HCl (pH 6.8 at 25°C), 8% (w/v) SDS, 50mM EDTA, 20mg Bromophenol blue, 4% (w/v) β-mercaptoethanol, 40% (v/v) glycerol.
10x SDS-PAGE RunningBuffer: 250mM Tris-HCl (pH 8.3 at 25°C), 1.9M glycine, 1% (w/v) SDS.
Coomassie Stain: 0.25% (w/v) Coomassie Brilliant Blue R-250, 10% (v/v) MeOH, 10% (v/v) glacial acetic acid.
Coomassie Destain: 10% (v/v) MeOH, 10% (v/v) glacial acetic acid.
1x Transfer Buffer: 25mM Tris, 190mM glycine, 20% (v/v) MeOH.
10x TBS: 500mM Tris (pH 7.4 at 25°C), 9% (w/v) NaCl.
1x TBST: 50mM Tris (pH 7.4 at 25°C), 0.9% (w/v) NaCl, 0.1% (v/v) Tween20.
Blocking Solution: 5% (w/v) non-fat milk powder in 1xTBST.
SUMO Extraction Buffer: 50mM NaCl, 50mM Tris-HCl (pH 8 at 25°C), 1mM EDTA, 1% (v/v) NP-40, 0.5% (w/v) Sodium deoxycholate, 0.2% (w/v) SDS, 20mM NEM, 1 per final 10ml protease inhibitor cocktail.
CO-IP Buffer: 150mM NaCl, 50mM Tris-HCl (pH 8 at 25°C), 5mM EDTA, 10% (v/v) glycerol, 0.1% (v/v) Triton-X, 10mM DTT, 1 per final 10ml protease inhibitor cocktail.
Ponceau S Stain: 0.5% (w/v) Ponceau S, 1% (v/v) glacial acetic acid.

2.7.2 Enzymes

MyTaq™ Red Mix (Bioline: BIO-25044)

Q5® Hot Start High-Fidelity DNA Polymerase (New England Biolabs: MD493L)

Life Technologies pENTR/D-TOPO (Fisher: 10780335)

Life Technologies Gateway Cassette LR Clonase II (Fisher: 11791020)

Invitrogen SuperScript® II Reverse Transcriptase (Fisher: 18064014)

Invitrogen RNaseOUT™ Recombinant Ribonuclease Inhibitor (Fisher: 10777019)

HF-MluI Restriction Enzyme (New England Biolabs: R3198S)

2.7.3 Chemicals

1-Naphthaleneacetic acid (Sigma: N0640-25G)

1,4-Dithiothreitol (Sigma: 000000010197777001)

2,4-Dichlorophenoxyacetic acid (Sigma: D7299-100G)

50X TAE (Fisher: 10490264)

Acetic Acid, glacial (Fisher: 10394970)

Acrylamide, Bis-Acrylamide (Sigma: A3574)

Agarose (Melford: MB1200)

Agar (Melford: M1002)

Ammonium persulfate (Fisher: 10396503)

Brilliant Blue R250 (Fisher: 10573165)

Bromophenol Blue (Fisher: 10679733)

cOmplete™, Mini, EDTA-free Protease Inhibitor Cocktail (Sigma: 000000004693159001)

Ethanol (School of Biology, Durham)

Ethidium bromide (Fisher: 10132863)

Ethylenediaminetetraacetic acid (Sigma: E5134)

Glufosinate-ammonium (Sigma: 45520)

Glycerol (Fisher: 10021083)

Glycine (Fisher: 10773644)

Hydrochloric acid, 36-8% (Fisher: 10000180)

Indole-3-acetic acid (Sigma: I3750-5G-A)

IPTG (Sigma: I6758-5G)

LB (Fisher: 12871650)

Liquid herbicide BASTA (marketed as Harvest) was kindly supplied by Ian Cookram, Technical enquiry at Bayer CropScience Ltd.

Magnesium chloride, hexahydrate (Melford: M05333)

Methanol (Fisher: 10785484)

Murashige & Skoog medium, basal salt mixture (Duchefa Biochemie: M0221.0050)

N-ethylmaleimide (Sigma: E3876)

NP-40 (Sigma: I8896-50ML)

Phytoagar (Duchefa Biochemie: P1003.5000)

Silwet-L77® surfactant

Sodium chloride (VWR: 27810.364)

Sodium deoxycholate (Sigma: D6750-10G)

Sodium dodecyl sulfate (Melford: B2008)

Sodium hyperchlorite (Fisher: 10296650)

Sucrose (Duchefa Biochemie: S0809.5000)

TEMED (Fisher: 10549960)

Tris base (VWR: 28811.364)

Tween-20 (Sigma: P2287)

β-mercaptoethanol (Sigma: M3148)

2.7.4 Antibiotics

Kanamycin monosulphate (Melford: K0126) – 50mg/ml in H_2O

Rifampicin (Fisher: 10562975) – 25mg/ml in MeOH

Gentamicin sulphate (Melford: G0124) – 25mg/ml in 70% EtOH

2.7.5 Kits

Sigma Plant Spectrum Total RNA Extraction kit (Sigma: STRN250)

Gel DNA Recovery Kit - Zymoclean™ (Cambridge Bioscience: D4002)

ZR Plasmid Miniprep™- Classic (Cambridge Bioscience: D4054)

2.7.6. Ladders

DNA Hyperladder™ 1KB plus (Bioline: BIO-33069)

Thermo Scientific™ PageRuler™ Plus Prestained Protein Ladder (Fisher: 26620)

2.7.7 Vectors

Life Technologies pENTR/D-TOPO (Fisher: K240020)

pEARLYGATE 104/201/203 (Earley, et al., 2006)

2.7.8 Bacterial Strains

GV3101:pMP90; *Agrobacterium tumefaciens* (Rif/Gent)

DH5α; *Escherichia coli* (No selection)

Storage Conditions:

All bacterial strains were grown in LB liquid culture before storage. 2ml of culture was transferred to an eppendorf and mixed with glycerol to a final concentration of 15%. The eppendorfs were snap frozen using liquid nitrogen and stored at -80°C ready for revival.

2.7.9 Antibodies

α-HA (3F10, Rat); working concentration 1:5,000 (Roche: 11867423002)

α-GFP (Mouse); working concentration 1:5,000 (Clonetech: 632381)

α-c-MYC (9E10, Mouse); working concentration 1:5,000 (Fisher: 13-2500)

α-SUMO (Rabbit); working concentration 1:3,000 (Generated in-house)

α-RAT-HRP; working concentration 1:10,000 (Sigma: A5795)

α-MOUSE-HRP; working concentration 1:10,000 (Sigma: A9044)

α-RABBIT-HRP; working concentration 1:10,000 (Sigma: A0545)

3. The Characterisation of the Auxin Response in the OTS SUMO Protease Mutants

3.1 Introduction

In 2006, Chosed, et al. (2006), demonstrated the *in vitro* catalytic activity of four ULP1-like SUMO proteases in *Arabidopsis thaliana.* Later work by Conti, et al. (2008), identified the role of one of these proteases, ULP1d, in salt tolerance. Overexpression of ULP1d, consequently known as OVERLY TOLERANT TO SALT1 (OTS1), through an insertion in the promoter region caused a dramatic increase in salt tolerance in *Arabidopsis thaliana*. The group also identified a homologue of OTS1, OVERLY TOLERANT TO SALT 2 (OTS2), which was shown to regulate the response to salt stress in a redundant fashion with OTS1. The *Arabidopsis* double knock out mutant line of these two proteases, *ots1 ots2*, showed an increase in sensitivity to salt.

Previous work conducted by Dr. Beatriz Orosa and Dr. Mark Bailey regarding the *ots1 ots2* mutant line has shown a difference in auxin-related gene expression in comparison to WT. RNA-seq data generated from the *ots1 ots2* line, under control conditions (Bailey, 2014), shows a number of auxin genes are differentially expressed in the mutant line, with 12 up-regulated by more than 0.5-fold in comparison to WT, and 26 down-regulated by more than 0.5-fold. Compared to the number of differentially expressed genes involved in other hormone signalling pathways, such as ethylene, cytokinin, ABA, etc. (fig. 3.1), the higher number of differentially expressed auxin-related genes suggest that OTS1 and OTS2 may play an important role in auxin homeostasis and signalling.

In *Arabidopsis thaliana*, two SUMO conjugating enzymes, the E3 Ligases SIZ1 and HPY2, have been identified to date (Ishida, et al., 2012). Research by Ishida, et al. (2009) and Huang, et al. (2009) has suggested that these E3 ligases, and thus SUMOylation, may be involved in auxin signalling and response (see. Section 1.2.3).

Auxin plays an important role in the development and maintenance of essential root architecture. Through auxin-mediated signalling systems, plants are able to control several aspects of root development, such as the length of the primary root (Rahman, et al., 2007), the priming and development of lateral roots (Fukaki, et al., 2007), changes in root hair length (Pitts, et al., 1998), the response to differences in water potential (Kaneyasu, et al., 2007), and the response to both gravitropic and thigmotropic stimuli (Philosoph-Hadas, et al., 2005; Reinhold, et al., 1972). These effects are achieved through the finely-tuned control of endogenous auxin levels, which oscillate in order to guide development in a spatiotemporal fashion (Scheres & Laskowski, 2016). The disruption of auxin homeostasis and signalling leads to the development of very distinct root phenotypes.

In order to test the hypothesis that SUMOylation plays a role in auxin signalling, here I characterised the auxin-related root phenotypes of the *Arabidopsis* SUMO protease double knock out line, *ots1 ots2*.

FIGURE 3.1| A NUMBER AUXIN-RELATED GENES ARE DIFFERENTIALLY EXPRESSED IN THE *OTS1 OTS2* KNOCK-OUT MUTANT LINE IN COMPARISON TO WT

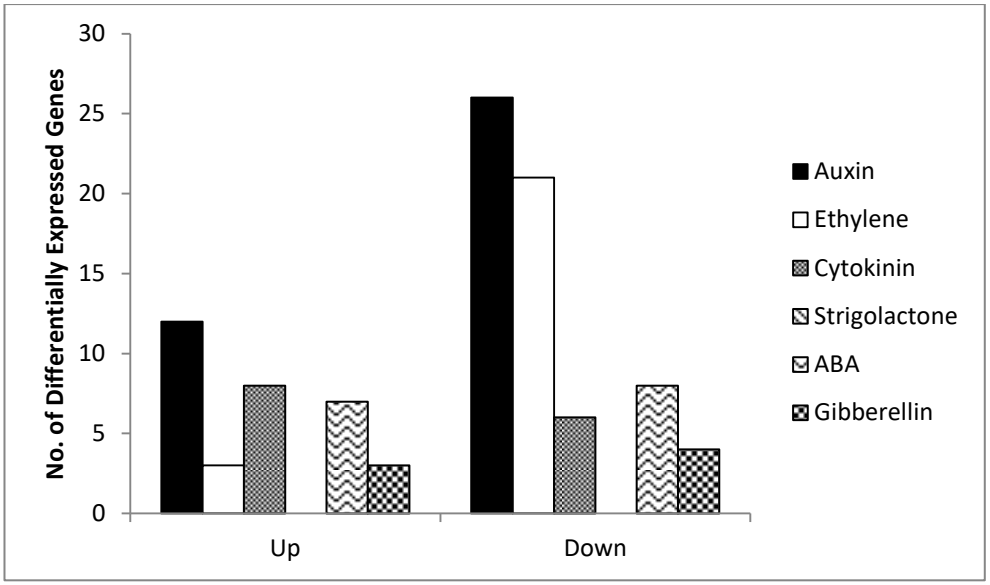

A comparison of the number of differentially expressed genes (logFC = >0.5, P values = <0.01) in the Arabidopsis knock-out line ots1 ots2 in comparison to WT in untreated seedlings. ots1 ots2 show an increase in the number of both up- and down-regulated auxin-related genes when compared to Col-0. The number of genes differentially expressed with regards to auxin is higher than those involved in other hormone pathways, such as ethylene, cytokinin, strigolactone, ABA and gibberellin, suggesting that SUMO may play a role in the auxin pathway.

Chart generated from RNAseq data obtained by Dr. Mark Bailey and Dr. Beatriz Orosa (Bailey, 2014).

3.2 The Arabidopsis SUMO protease mutant shows a reduction in primary root length under auxin stimulus

One of the most well-characterised auxin associated phenotypes is that of primary root length. Auxin has a bimodal effect on primary root length (Overvoorde, et al., 2010); at low concentrations, auxin promotes the growth of the primary root, resulting in an increase in primary root length. However, at high concentrations, primary root growth is inhibited. To investigate the role of SUMOylation in the auxin response, the effects of auxin on primary root length in a hyper-SUMOylated environment, such as that of the SUMO protease knock out mutant line *ots1 ots2*, were studied.

The SUMO protease knock out mutant line, *ots1 ots2*, along with a WT control (Col-0) and an auxin insensitive mutant line, *tir1 afb2 afb3*, was germinated on ½ MS plates and grown under 24 hour light conditions for three days (see, Methods 2.1.1). Three days after germination, the seedlings were then transferred to assay plates containing either 0.1uM IAA, 0.1uM 2,4-D, or no auxin stimulus (control) and grown under 24 hour light conditions for a further 3 days.

In the absence of exogenous auxin stimulation, *ots1 ots2* primary root length is indistinguishable from wild type primary root length (fig. 3.2 & 3.3). This suggests that the *ots1 ots2* mutant is able to produce and respond appropriately to internal auxin cues. The auxin signalling triple mutant, *tir1 afb2 afb3*, is significantly shorter under control conditions, as previously described in (Dharmasiri, et al., 2005).

Upon the application of the auxinic compounds indole-3-acetic acid (IAA) and 2,4-dichlorophenoxyacetic acid (2,4-D) to the assay plates, a significant difference in primary root length between wild type and the SUMO protease mutant line *ots1 ots2* was observed (fig. 3.2 & 3.3). A reduction of primary root length was seen in both the wild type and the *ots1 ots2* mutant. However, the reduction in primary root length was significantly more severe in the *ots1 ots2* line. This suggests that the *ots1 ots2* mutant is more sensitive to exogenous auxin stimulus than the wild type. As expected, no reduction in primary root length was observed for the auxin insensitive triple mutant, *tir1 afb2 afb3.*

Further experiments to determine the auxin sensitivity of the *ots1 ots2* mutant line were conducted using a range of concentrations of IAA. Due to the bimodal nature of the auxin response with regards to primary root length, at lower IAA concentrations, such as 0.01uM IAA (Booker, et al., 2010), very little difference in primary root length is to be expected in comparison to control conditions. However, as the concentration of auxin increases, the length of the primary root should decrease. This well characterised phenotype was observed, as expected, for the WT (Col-0), with the length of the primary root decreasing dramatically as the concentration of auxin increased (fig. 3.4). However, the *ots1 ots2* line did not follow the expected pattern, with the length of the primary root showing a significant higher level of decrease compared to WT even at extremely low levels of auxin (fig. 3.5). This suggests that an increased level of SUMOylation leads to an increase in sensitivity to stimulation by auxinic compounds, therefore resulting in the dramatic reduction in primary root length observed after exposure to 0.01uM IAA. No discernible difference in primary root length was observed for the auxin insensitive triple mutant line, *tir1 afb2 afb3*, between the control conditions and all tested auxin concentrations, as expected.

In order to further explore the role of SUMOylation plays in the auxin response, the *ots1 ots2* mutant line was exposed to the auxin transport inhibitor, 2,3,5-triiodobenzoic acid (TIBA). TIBA blocks the polar transport of auxin through the disruption of PIN1 membrane localisation (Geldner, et al., 2001). No significant difference was observed with regards to primary root length between WT and the *ots1 ots2* mutant line upon exposure to both high (30uM) and low (3uM) concentrations of TIBA (fig. 3.6 & 3.7). This suggests that whilst an increase in SUMOylation leads to an increase in auxin sensitivity, this is not due to SUMO-mediated alterations in polar auxin transport via the PIN1 auxin efflux protein.

FIGURE 3.2| *ots1 ots2* SHOWS A REDUCTION IN PRIMARY ROOT LENGTH IN RESPONSE TO EXPOSURE TO THE AUXINIC COMPOUNDS INDOLE-3-ACETIC ACID (IAA) AND 2,4-DICHLOROPHENOXYACETIC ACID (2,4-D)

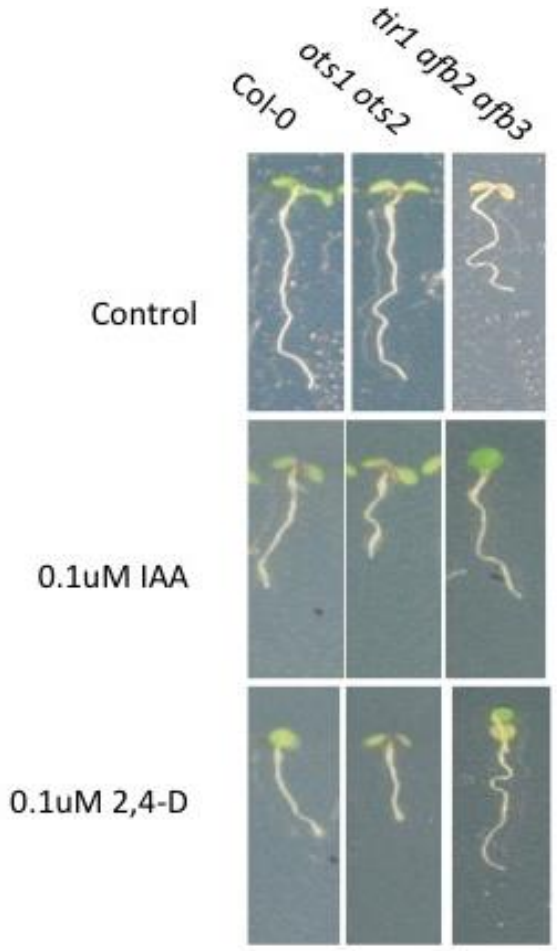

5-day-old ots1 ots2 seedlings showing the effect of exogenous auxin application (IAA and 2,4-D) on primary root length compared to WT (Col-0) and an auxin-signalling mutant (tir1 afb2 afb3). A decrease in primary root length is observed, in comparison to WT, in the ots1 ots2 mutant line after auxin treatment. No decrease is observed for the auxin insensitive mutant line, tir1 afb2 afb3.

Seedlings were germinated on 1/2MS and 0.8% phytoagar plates supplemented with 0.5% sucrose under 24 hour light conditions. At 2 days old, the seedlings were transferred to the prepared assay plates: 1/2MS with 0.8% phytoagar and 0.5% sucrose, supplemented with either 0.1uM IAA, or 0.1uM 2,4-D, or no hormone treatment (control). Seedlings were then grown under 24hr light conditions for a further 3 days before the root length was measured. n = 125 per genotype, per treatment.

FIGURE 3.3| *ots1 ots2* EXHIBITS A STATISTICALLY SIGNIFICANT REDUCTION IN PRIMARY ROOT LENGTH UPON EXPOSURE TO THE AUXINS IAA AND 2,4-D

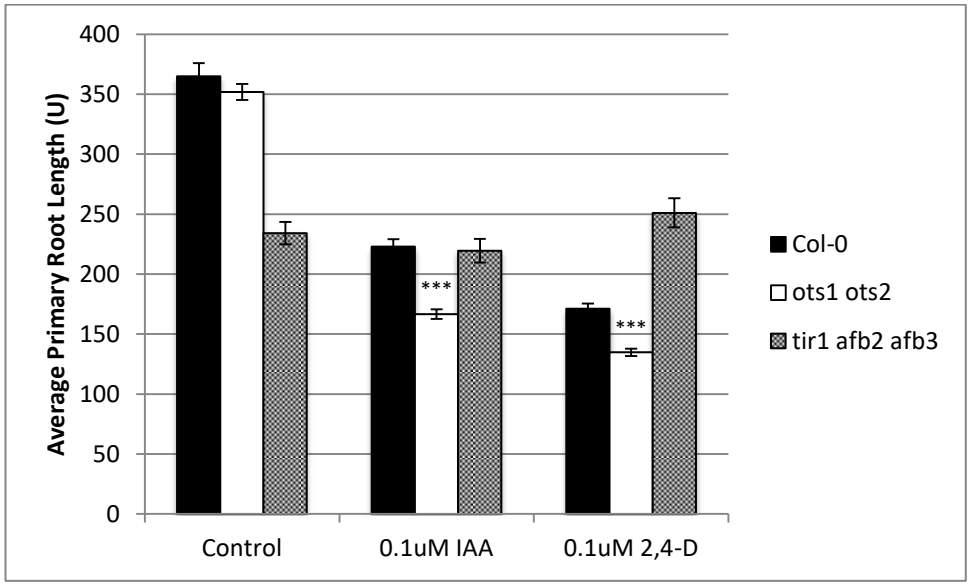

Analysis of the primary root length of 5-day-old Col-0, ots1 ots2, and tir1 afb2 afb3 Arabidopsis seedlings in response to exogenous auxin application (0.1uM IAA and 0.1uM 2,4-D). A statistically significant decrease in primary root length is observed, in comparison to WT, in the ots1 ots2 mutant line after auxin treatment. No significant decrease is observed for the auxin insensitive mutant line, tir1 afb2 afb3.

*Seedlings were germinated on 1/2MS and 0.8% phytoagar plates supplemented with 0.5% sucrose under 24 hour light conditions. At 2 days old, the seedlings were transferred to the prepared assay plates: 1/2MS with 0.8% phytoagar and 0.5% sucrose, supplemented with either 0.1uM IAA, or 0.1uM 2,4-D, or no hormone treatment (control). Seedlings were then grown under 24hr light conditions for a further 3 days before the root length was measured. Error bars represent standard error of the mean. P values for differences between Col-0 and ots1 ots2 for each treatment: *** ≤ 0.001 (multi-way ANOVA with Tukey test post hoc). n = 75 per genotype, per treatment. Three repeats conducted.*

FIGURE 3.4| *ots1 ots2* SHOWS A DOSE-DEPENDENT REDUCTION IN PRIMARY ROOT LENGTH UPON EXPOSURE TO IAA

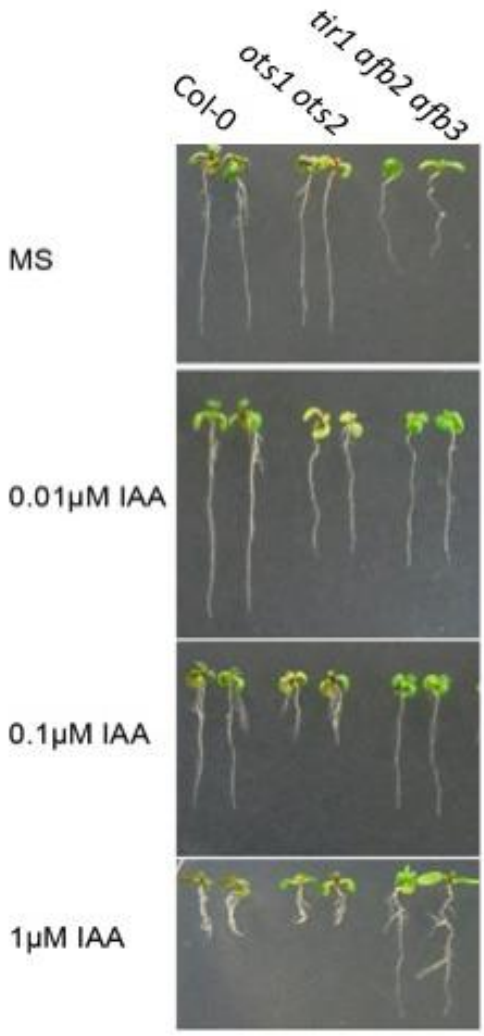

6-day-old ots1 ots2 seedlings showing the effect of various concentrations of exogenous auxin (IAA) on primary root length compared to WT (Col-0), and an auxin-signalling mutant (tir1 afb2 afb3). ots1 ots2 showed significant a decrease in primary root length in comparison to WT, even at low concentrations of auxin (0.01uM), where a slight increase in primary root length is observed in WT seedlings due to the bimodal nature of auxin. No significant change in primary root length is observed for the auxin insensitive mutant line, tir1 afb2 afb3, between treatments.

Seedlings were germinated on 1/2MS and 0.8% phytoagar plates supplemented with 0.5% sucrose under 24 hour light conditions. At 2 days old, the seedlings were transferred to the prepared assay plates: 1/2MS with 0.8% phytoagar and 0.5% sucrose, supplemented with either 0.01uM/0.1uM/1uM IAA, or no hormone treatment (control). Seedlings were then grown under 24hr light conditions for a further 5 days before the root length was measured. n = 80 per genotype, per treatment. Three repeats conducted.

FIGURE 3.5| *ots1 ots2* EXHIBITS A STATISTICALLY SIGNIFICANT DOSE-DEPENDENT REDUCTION IN PRIMARY ROOT LENGTH UPON EXPOSURE TO IAA

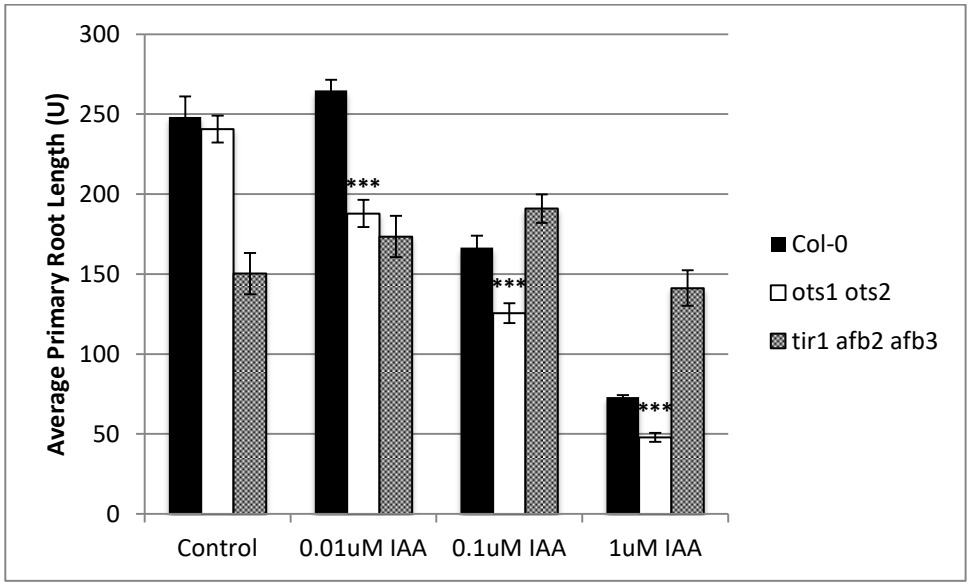

Analysis of the primary root length of 6-day-old Col-0, ots1 ots2, and tir1 afb2 afb3 Arabidopsis seedlings in response to differing concentrations of exogenous auxin (0.01/0.1/1uM IAA). ots1 ots2 showed significant a decrease in primary root length in comparison to WT, even at low concentrations of auxin (0.01uM), where a slight increase in primary root length is observed in WT seedlings due to the bimodal nature of auxin. No significant change in primary root length is observed for the auxin insensitive mutant line, tir1 afb2 afb3, between treatments.

*Seedlings were germinated on 1/2MS and 0.8% phytoagar plates supplemented with 0.5% sucrose under 24 hour light conditions. At 2 days old, the seedlings were transferred to the prepared assay plates: 1/2MS with 0.8% phytoagar and 0.5% sucrose, supplemented with either 0.01uM/0.1uM/1uM IAA, or no hormone treatment (control). Seedlings were then grown under 24hr light conditions for a further 5 days before the root length was measured. Error bars represent standard error of the mean. P values for differences between Col-0 and ots1 ots2 for each treatment: *** ≤ 0.001 (multi-way ANOVA with Tukey test post hoc). n = 80 per genotype, per treatment. Three repeats conducted.*

FIGURE 3.6| *ots1 ots2* SHOWS NO DIFFERENCE IN RESPONSE TO TREATMENT WITH THE AUXIN EFFLUX INHIBITOR 2,3,5-TRIIODOBENZOIC ACID (TIBA) COMPARED TO WILD TYPE

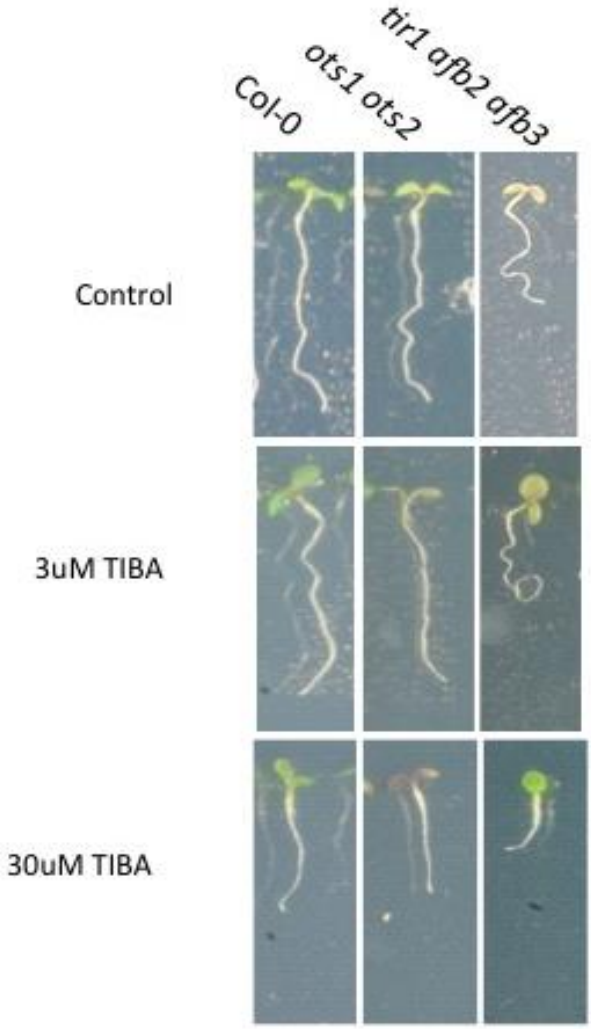

5-day-old ots1 ots2 seedlings showing the effect of auxin signalling inhibition (TIBA) on primary root length compared to WT (Col-0) and an auxin-signalling mutant (tir1 afb2 afb3). No statistically significant decrease in primary root length is observed in the ots1 ots2 mutant upon TIBA treatment.

Seedlings were germinated on 1/2MS and 0.8% phytoagar plates supplemented with 0.5% sucrose under 24 hour light conditions. At 2 days old, the seedlings were transferred to the prepared assay plates: 1/2MS with 0.8% phytoagar and 0.5% sucrose, supplemented with either 3uM TIBA, 30uM TIBA, or no hormone treatment (control). Seedlings were then grown under 24hr light conditions for a further 3 days before the root length was measured. n = 75 per genotype, per treatment. Three repeats conducted.

FIGURE 3.7| *OTS1 OTS2* EXHIBITS NO STATISTICALLY SIGNIFICANT DIFFERENCE IN RESPONSE TO TREATMENT WITH TIBA IN COMPARISON TO WILD TYPE

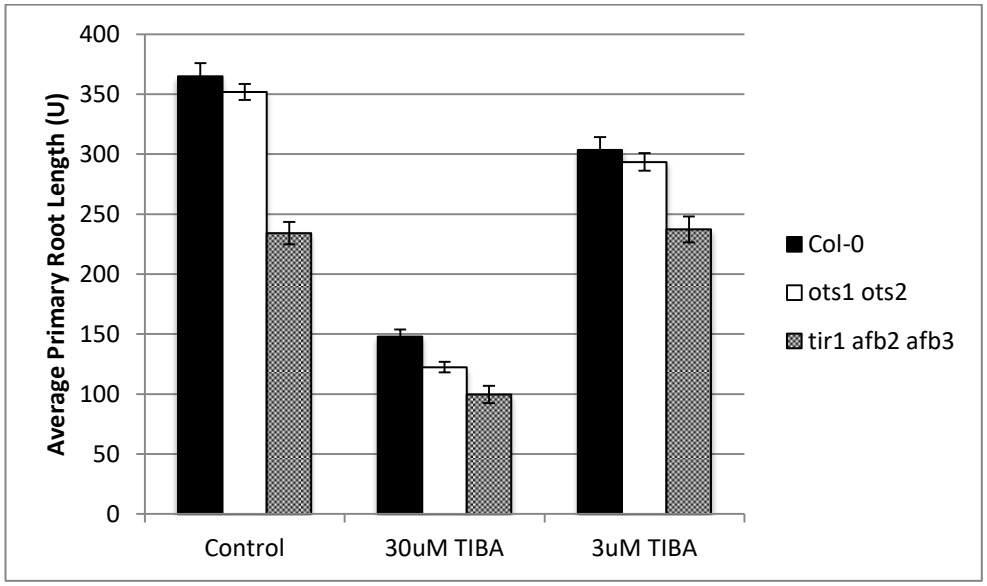

Analysis of the primary root length of 5-day-old Col-0, ots1 ots2, and tir1 afb2 afb3 Arabidopsis seedlings in response to auxin signalling inhibition (TIBA). No statistically significant decrease in primary root length is observed in the ots1 ots2 mutant upon TIBA treatment.

Seedlings were germinated on 1/2MS and 0.8% phytoagar plates supplemented with 0.5% sucrose under 24 hour light conditions. At 2 days old, the seedlings were transferred to the prepared assay plates: 1/2MS with 0.8% phytoagar and 0.5% sucrose, supplemented with either 3uM TIBA, 30uM TIBA, or no hormone treatment (control). Seedlings were then grown under 24hr light conditions for a further 3 days before the root length was measured. Error bars represent standard error of the mean. Analysis by multi-way ANOVA (with Tukey test post hoc) indicates no statistical significance between treatments. n = 75 per genotype, per treatment. Three repeats conducted

3.3 The Arabidopsis SUMO protease mutant shows a reduction in lateral root primordia

The effects of auxin upon the growth and development of the lateral root in *Arabidopsis* have been extensively studied (reviewed in Lavenus, et al., 2013). To further investigate the role of SUMOylation in the auxin response, the effects of auxin on the growth and development of lateral roots in a hyper-SUMOylated environment, such as that of the SUMO protease knock out mutant line *ots1 ots2*, were studied.

In the absence of auxin stimulation, the *ots1 ots2* mutant line displays a reduction in the number of emerged lateral roots compared to WT (fig. 3.8 & 3.10). Under 24 hour light conditions, the *ots1 ots2* mutant line produced half the number of lateral roots compared to Col-0; the observed ratio of 1:2 emerged lateral roots between *ots1 ots2* and the Col-0 seedlings persisted over the course of the observed time period, with the same ratio observed at both 6 and 9 days growth (fig. 3.9). These observations suggest that increased levels of SUMOylation have a detrimental effect on the production of lateral roots, possibly through alterations in either the regulation of endogenous auxin oscillations through which the LR founder cells are primed (Moreno-Risueno, et al., 2010), or the regulation of lateral root development from primed LR founder cells via IAA3/14 and ARF7/19 (Okushima, et al., 2007).

To assess whether the reduction in emerged lateral roots observed for the *ots1 ots2* mutant line was due to aberrations in LR priming or emergence, the LR primordia of this line were studied. Seedlings were grown under 24 hour light conditions on ½ MS plates for 7 days before undergoing cell clearing (see, Methods 2.5.1). The cleared roots were mounted in 50% glycerol and the LR primordia counted and staged via white light microscopy at 60x magnification. The *ots1 ots2* line showed no irregularities in LR formation, with normal LR primordia of all stages (I-VII) observed compared to WT (fig. 3.11) and no increase in the number of arrested LR observed compared to WT. However, the *ots1 ots2* line appeared to have significantly fewer LR primordia at all stages of development, save Stages I and II, compared to WT (fig. 3.12). A >2-fold increase in stage I and II LR primordia was observed in the SUMO protease mutant line; these LR primordia did not appear to be developmentally arrested, located near the root tip rather than further up the root (as would indicate arrest). It is possible that the difference in LR primordia observed at these stages is due to issues successfully identifying early stage LR primordia in the WT: due to the nature of the

establishment of the LR initialisation site, consisting of a small amount of asymmetric division within a single cell layer, the early stages can be difficult to identify within the root. At all other stages, more LR primordia were observed in the WT roots, with a >3-fold increase in stage VII/emerged LRs seen in comparison to the *ots1 ots2* mutant line. This data indicates that increased SUMOylation does not affect the growth and development of LR primordia, but appears instead to affect the establishment of the LR founder cells from which lateral roots are produced, potentially through SUMO-mediated alterations in the establishment of auxin maxima and minima (Dubrovsky, et al., 2001) or through abnormalities in root cap formation (Xuan, et al., 2015).

The application of exogenous auxin to *Arabidopsis* roots causes an increase in lateral root production. This is due to increased cell division in the pericycle; lateral roots develop from auxin-primed triplets of Xylem Pole Pericycle (XPP) cells located within the pericycle (De Smet, et al., 2007), therefore an increase in pericycle cell proliferation leads to an increase in lateral root number. To further confirm the role of SUMO in the lateral root phenotype observed above for the *ots1 ots2* mutant line, 3-day-old seedlings grown under 24 hour light conditions were transferred to ½ MS plates supplemented with varying concentrations of IAA (0.01uM-1uM). The seedlings were incubated on the assay plates for 3 days under 24 hour light conditions and the number of emerged lateral roots counted (fig. 3.4 & 3.13).

As expected, the number of emerged lateral roots for the WT plants increased dramatically after auxin treatment. This phenotype was not observed for the auxin insensitive triple knock out line, *tir1 afb2 afb3*, again as expected, with the occasional lateral root only produced at very high levels of auxin concentration (1uM). Surprisingly, the number of emerged lateral roots observed after auxin treatment for the *ots1 ots2* mutant line doubled compared to the number observed under control conditions for the genotype. However, the number of lateral roots produced by the *ots1 ots2* line remained far below that of the WT, regardless of auxin concentration. This data suggests that the *ots1 ots2* mutant line is not insensitive to exogenous auxin stimulus, further supporting the findings regarding auxin sensitivity observed in chapter 3.2, but that increased background SUMOylation does affect the priming of lateral root primordia.

FIGURE 3.8| *ots1 ots2* PRODUCES FEWER LATERAL ROOTS AT 6 AND 9 DAY POST-GERMINATION IN COMPARISON TO WILD TYPE

6-day-old and 9-day-old Col-0 and ots1 ots2 seedlings showing the number of emerged lateral roots between genotypes. The ots1 ots2 mutant shows fewer emerged lateral roots at all both 6 and 9 days old.

Seedlings were germinated on 1/2MS plates with 0.8% phytoagar and supplemented with 0.5% sucrose. The seedlings were germinated and grown under 24 hour light conditions for 6 and 9 days, respectively. n = 50 per genotype. Three repeats conducted.

FIGURE 3.9| *ots1 ots2* PRODUCES SIGNIFICANTLY FEWER LATERAL ROOTS IN COMPARISON TO WILD TYPE AT BOTH 6 AND 9 DAYS POST-GERMINATION

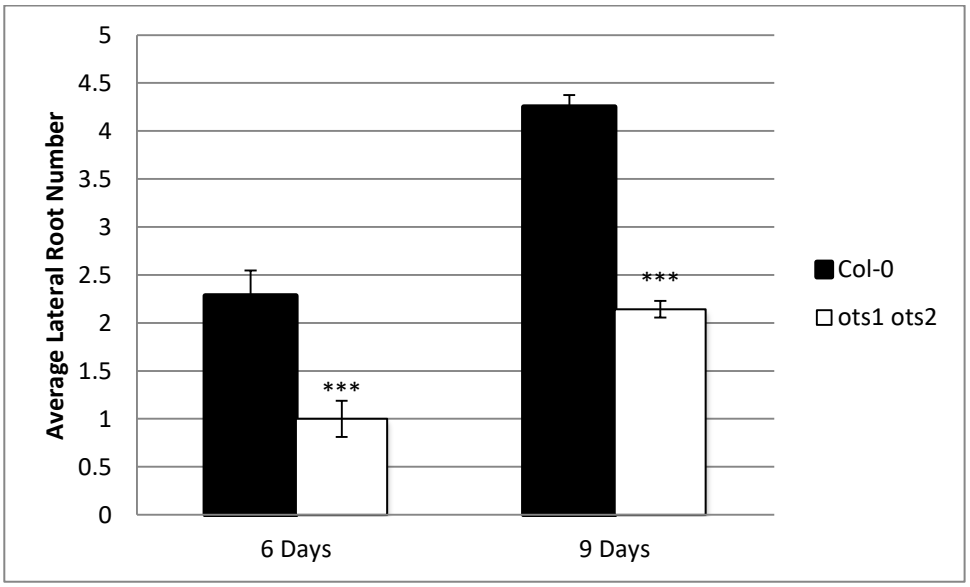

Analysis of the emerged lateral root number of Col-0 and ots1 ots2, Arabidopsis seedlings at 6 days and 9 days post-germination. The ots1 ots2 mutant shows fewer emerged lateral roots at all both 6 and 9 days old.

*Seedlings were germinated on 1/2MS plates with 0.8% phytoagar and supplemented with 0.5% sucrose. The seedlings were germinated and grown under 24 hour light conditions for 6 and 9 days, respectively. Error bars represent standard error of the mean. P values for differences between Col-0 and ots1 ots2 at 6 days and 9 days: ** ≤ 0.01 and *** ≤ 0.001, respectively (one-way ANOVA). n = 50 per genotype. Three repeats conducted.*

FIGURE 3.10| *ots1 ots2* PRODUCES FEWER LATERAL ROOTS PER SEEDLING IN COMPARISON TO WILD TYPE

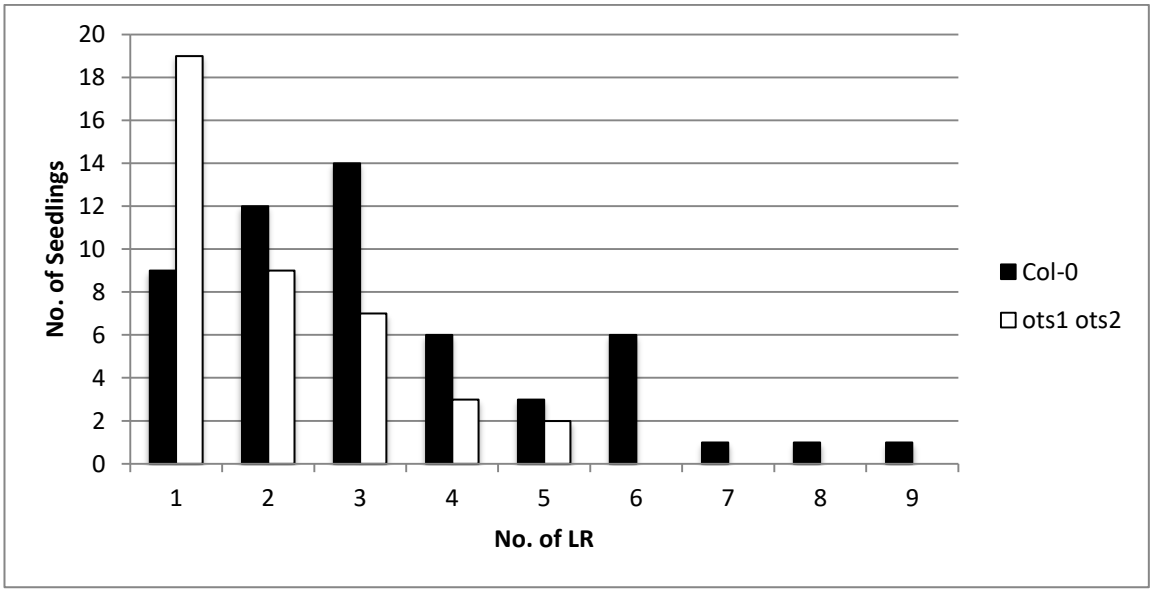

The distribution of lateral root numbers between Col-0 and ots1 ots2 Arabidopsis seedlings at 6 days post-germination. ots1 ots2 has a larger number of seedlings with only one emerged lateral root at 6 days post germination in comparison to WT. ots1 ots2 has no seedlings with 6 or more emerged lateral roots at day 6, with all seedlings showing 5 or fewer emerged lateral roots.

Seedlings were germinated on 1/2MS plates with 0.8% phytoagar and supplemented with 0.5% sucrose. The seedlings were germinated and grown under 24 hour light conditions for 6 days before counting. n = 50 per genotype.

FIGURE 3.11| *THE STAGING OF LATERAL ROOT PRIMORDIA*

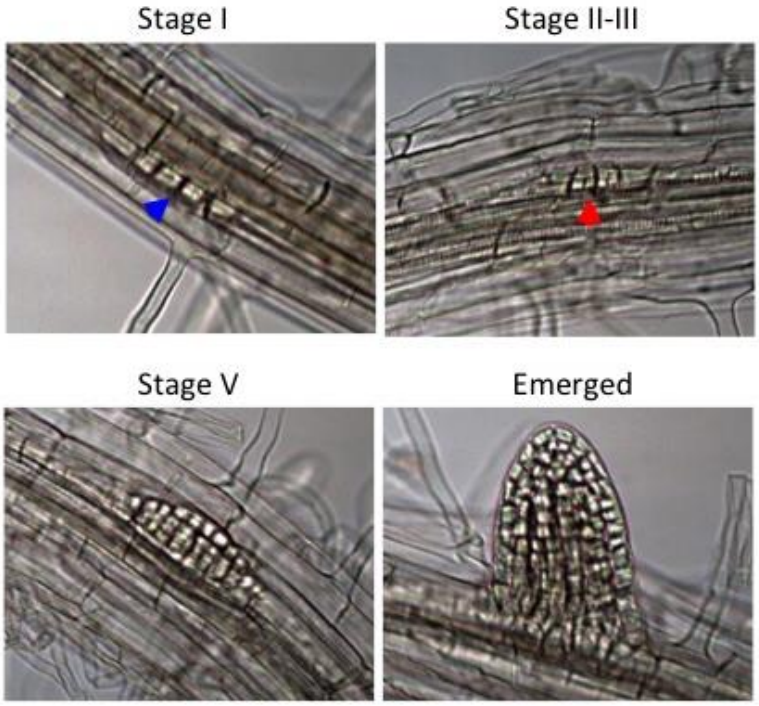

Composite figure showing the staging of lateral root primordia of 7-day-old seedlings. WT seedlings were germinated on ½ MS plates with 0.8% phytoagar and supplemented with 0.5% sucrose. The seedlings were grown under 24 hour light conditions for 7 days. The roots were cleared and the lateral root primordia staged via white-light microscopy at 60x magnification. Stage I shows the initial assymertric anticlinial division of the XPP cells in the pericycle (blue arrowhead) giving rise to the lateral root initiation site. The cells then divide in a periclinal fashion to form two (stage II) (red arrowhead), three (stage III), four (Stage IV) and five (Stage V) layers. As the cells in the primordia continue to divide, they break through the casparian strip (Stage V-VI), eventually emerging as a new lateral root.

FIGURE 3.12| *ots1 ots2* PRODUCES SIGNIFICANTLY FEWER ROOT PRIMORDIA IN COMPARISON TO WT

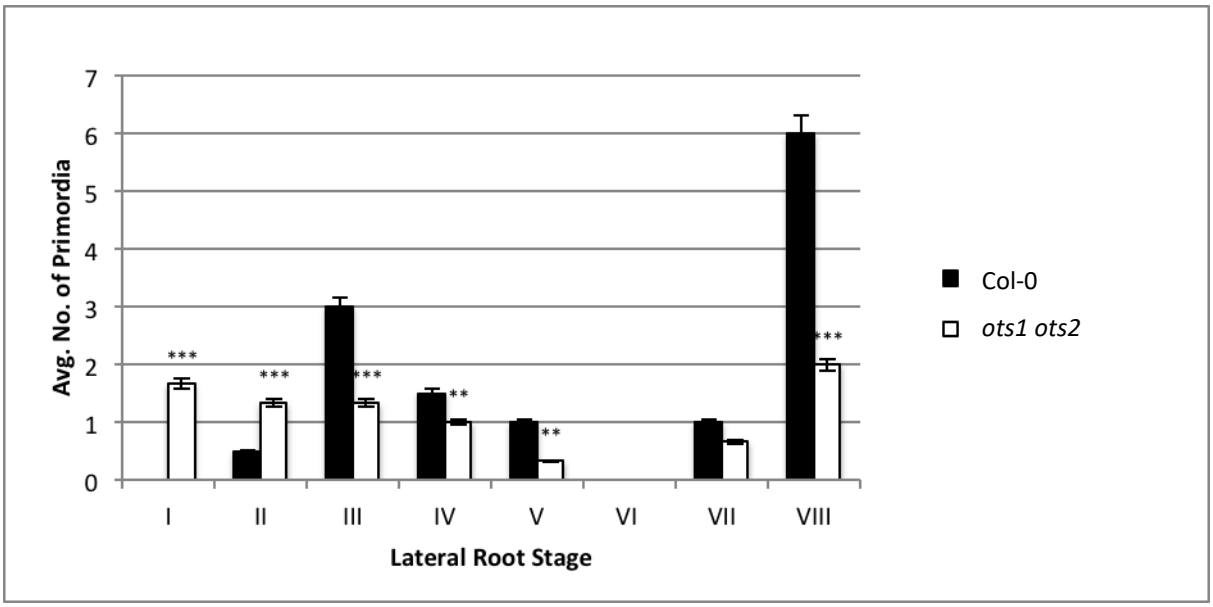

Analysis of the average number of lateral root primordia categorised by stage between Col-0 and ots1 ots2 Arabidopsis seedlings at 7 days post-germination. ots1 ots2 shows a significantly fewer number of late-stage LR primordia, in comparison to WT. ots1 ots2, however, does not show a dramatic increase in the number of LR primordia at the earlier stages, suggesting that the decrease in emerged lateral roots observed for the mutant line is not due to LR primordia arrest at the earlier stages.

*WT seedlings were germinated on ½ MS plates with 0.8% phytoagar and supplemented with 0.5% sucrose. The seedlings were grown under 24 hour light conditions for 7 days. The roots were cleared and the lateral root primordia staged via white-light microscopy at 60x magnification. Error bars represent standard error of the mean. P values for differences in the number of LR primordia at different stages between Col-0 and ots1 ots2: ** ≤ 0.01 and *** ≤ 0.001, respectively (one-way ANOVA). n = 10 seedlings for each genotype. Two repeats conducted.*

FIGURE 3.13| *ots1 ots2* EXHIBITS A STATISTICALLY SIGNIFICANT DOSE-DEPENDENT INCREASE IN LATERAL ROOT EMERGENCE UPON EXPOSURE TO IAA

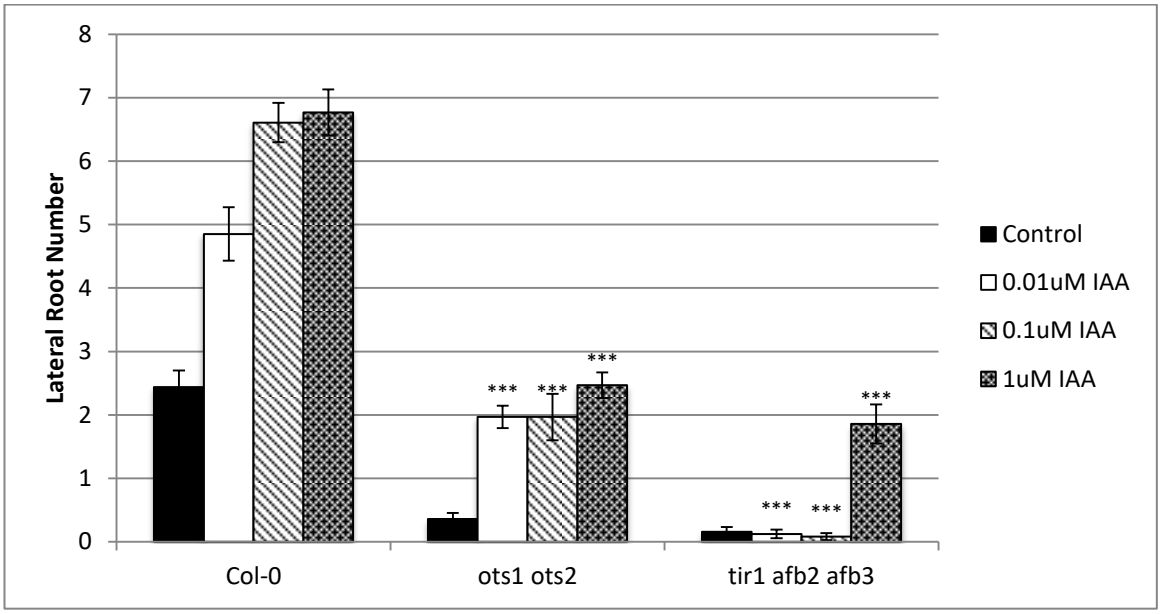

Analysis of the number of emerged lateral roots (LR) of 6-day-old Col-0, ots1 ots2, and tir1 afb2 afb3 Arabidopsis seedlings in response to differing concentrations of exogenous auxin (0.01/0.1/1uM IAA). ots1 ots2 shows significantly fewer emerged LR, in comparison to WT, for all treatments (control, 0.01-1uM IAA). An increase in LR emergence is observed for ots1 ots2 upon treatment with IAA in comparison to the ots1 ots2 untreated control, suggesting that ots1 ots2 is not insensitive to auxin with regards to the lateral root.

*Seedlings were germinated on 1/2MS and 0.8% phytoagar plates supplemented with 0.5% sucrose under 24 hour light conditions. At 2 days old, the seedlings were transferred to the prepared assay plates: 1/2MS with 0.8% phytoagar and 0.5% sucrose, supplemented with either 0.01uM/0.1uM/1uM IAA, or no hormone treatment (control). Seedlings were then grown under 24hr light conditions for a further 5 days before the number of emerged KR were counted. Error bars represent standard error of the mean. P values for differences between Col-0 and ots1 ots2 and tir1 afb2 afb3 for each treatment: *** ≤ 0.001 (multi-way ANOVA with Tukey test post hoc). n = 80 per genotype, per treatment. Three repeats conducted.*

3.4 The Arabidopsis SUMO protease mutant shows a reduction in the production of root hairs

Root hairs are an important part of plant root architecture. These subcellular extensions from root epidermal cells allow the plant root system to dramatically increase its surface area, thereby increasing the soil volume, and thus nutrient content, available to the plant. The growth and development of these root hairs is mediated through the action of several phytohormones, such as auxin, ethylene, jasmonic acid, brassinosteroids and strigolactone (Lee & Cho, 2013), with the roles of auxin and ethylene perhaps the most well studied.

The density of root hairs has been shown to be dependent upon several factors, such as Pi content (Bates & Lynch, 2000), and exposure to the ethylene precursor 1-aminocyclopropane-1-carboxylic acid (ACC) (Dolan, 1996). Pi deficiency is a major driver in root architecture remodelling, with changes to the plant root structure in response to low soil Pi content observed across a wide variety of plant species, such as maize (*Zea mays*), tomato (*Solanum lycopersicum*) and rice *(Oryza sativa*) (Li, et al., 2012; Kim, et al., 2008; Niu, et al., 2013).

Under control conditions, 7-day-old seedlings from the SUMO protease mutant line *ots1 ots2* produced significantly fewer root hairs in comparison to WT (Col-0) (fig. 3.14 & 3.15). This suggests that high levels of background SUMOylation may also possibly affect the nutrient stress and ethylene signalling pathways. These observations further support findings that SUMO plays an important role in the Pi-starvation response; knock out mutants of the SUMO E3 ligase SIZ1, *siz1-1/2/3* and *siz1-1 sos3-1,* display hypersensitivity to Pi starvation through an increase in root hair density via modification of the MYB transcription factor PHOSPHATE STARVATION RESPONSE 1 (PHR1) (Miura, et al., 2005). Further work involving the *siz1* knock out mutant has shown SIZ1 to be a negative regulator Pi deficiency-induced root architecture remodelling through the involvement of the auxin response pathway (Miura, et al., 2011). The root hair phenotype displayed here suggests that SUMO may play a role in the remodelling of plant root architecture in response to Pi deficiency and auxin.

Auxin modulates root hair growth, working downstream of the transcription factor involved in root hair initiation, ROOT HAIR DEFECTIVE 6 (RDH6) (Masucci & Schiefelbein, 1996). Changes in

auxin homeostasis affect root hair elongation; in the auxin insensitive mutant *tir1*, and its paralogues *(afb1, afb2,* and *afb3)*, root hair length is dramatically reduced (Dharmasiri, et al., 2005). The opposite is observed for the TIR1 RHS-over-expression line, where an increase in root hair growth is seen (Ganguly, et al., 2010). Under control conditions, 7-day-old seedlings from the SUMO protease mutant line *ots1 ots2* produced significantly longer root hairs in comparison to WT (Col-0) (fig. 3.16), with the opposite phenotype observed, as expected, for the auxin insensitive triple knock out line, *tir1 afb2 afb3*. This observation is consistent with the data regarding auxin sensitivity obtained in chapters 3.2 and 3.3; the statistically significant (one-way ANOVA) increase in root hair length confirms the hypothesis that an increase in background SUMOylation levels leads to an increase in auxin sensitivity.

FIGURE 3.14| THE *ots1 ots2* MUTANT SHOWS DIFFERENCES IN ROOT HAIR LENGTH AND DENSITY IN COMPARISON TO WT

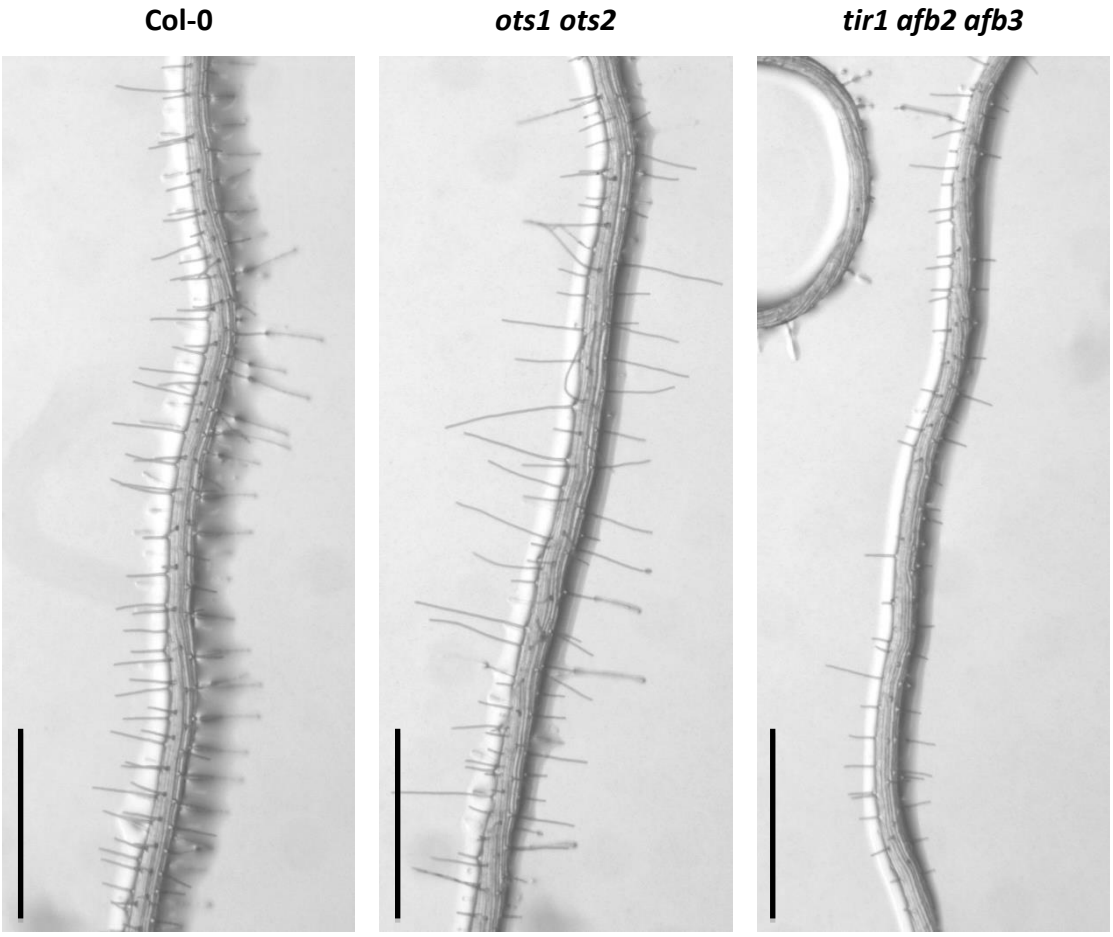

Roots of 7-day-old Col-0 (WT), ots1 ots2 and tir1 afb2 afb3 seedlings at 2x magnification showing morphological differences in root hairs between Arabidopsis mutant lines. ots1 ots2 shows a decrease in number of root hairs, in comparison to WT, and an increase in root hair length. The auxin insensitive mutant, tir1 afb2 afb3, shows a dramatic decrease in root hair density and length in comparison to WT.

Seedlings were germinated on 1/2MS and 0.8% phytoagar plates supplemented with 0.5% sucrose under 24 hour light conditions. Seedlings were then grown under 24hr light conditions for 7 days before the number of root hairs were counted. Error bars represent standard error of the mean. n = 20 per genotype. Three repeats conducted. Scale 1mm. Magnification = 2x.

FIGURE 3.15 | *ots1 ots2* PRODUCES SIGNIFICANTLY FEWER ROOT HAIRS IN COMPARISON TO WT

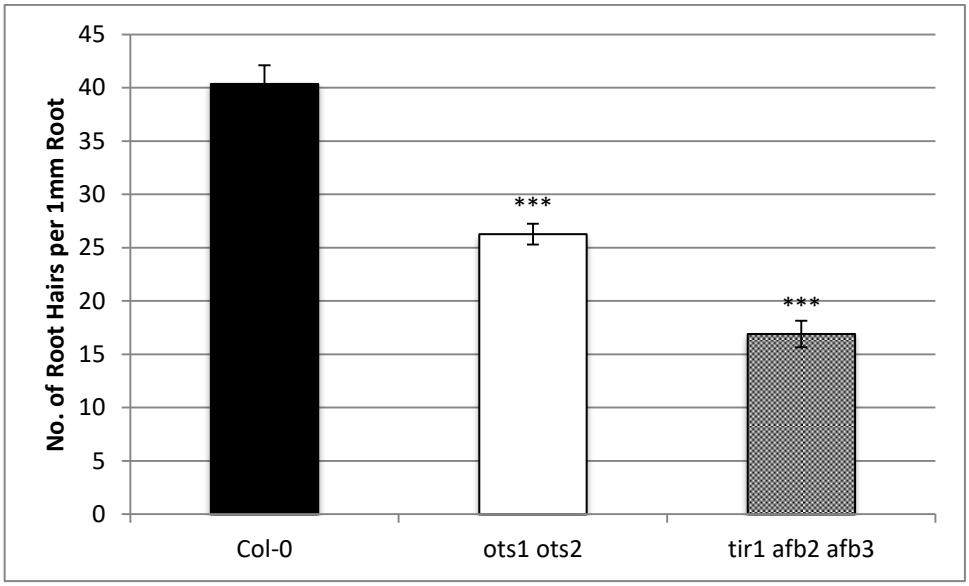

Analysis of average root hair number of 7-day old Col-0, ots1 ots2 and tir1 afb2 afb3 Arabidopsis lines. ots1 ots2 shows a statistically significant decrease in number of root hairs, in comparison to WT. The auxin insensitive mutant, tir1 afb2 afb3, shows a dramatic decrease in root hair density in comparison to WT.

*Seedlings were germinated on 1/2MS and 0.8% phytoagar plates supplemented with 0.5% sucrose under 24 hour light conditions. Seedlings were then grown under 24hr light conditions for 7 days before the number of root hairs were counted. Error bars represent standard error of the mean. P values for differences between Col-0 and the two mutant lines (ots1 ots2, tir1 afb2 afb3): *** ≤ 0.001 (one-way ANOVA with Tukey test post hoc). n = 20 per genotype. Three repeats conducted.*

FIGURE 3.16| *ots1 ots2* PRODUCES SIGNIFICANTLY LONGER ROOT HAIRS IN COMPARISON TO WT

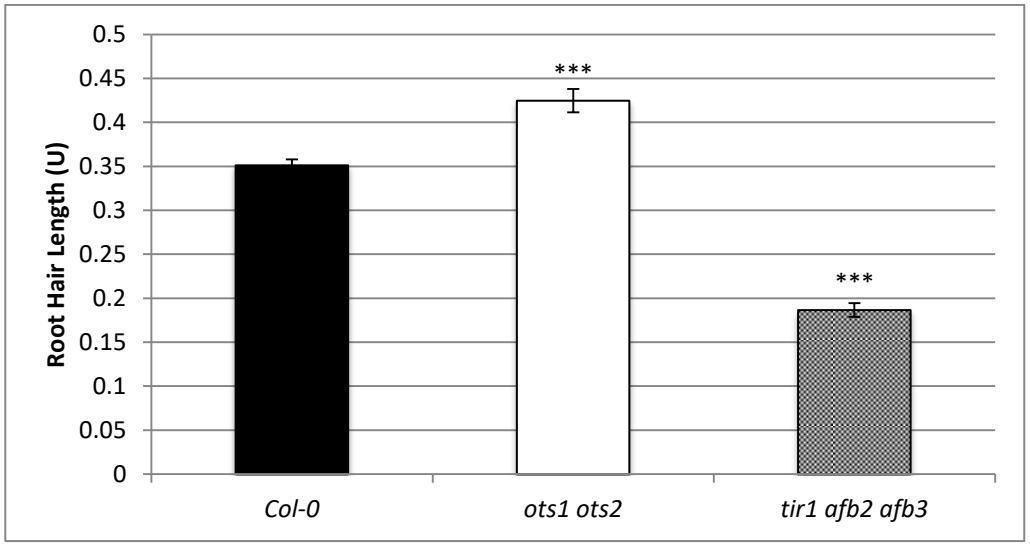

Analysis of average root hair length of 7-day old Col-0, ots1 ots2 and tir1 afb2 afb3 Arabidopsis lines. ots1 ots2 shows a statistically significant increase in average root hair length, in comparison to WT. The auxin insensitive mutant, tir1 afb2 afb3, shows a dramatic decrease in root hair length in comparison to WT.

*Seedlings were germinated on 1/2MS and 0.8% phytoagar plates supplemented with 0.5% sucrose under 24 hour light conditions. Seedlings were then grown under 24hr light conditions for 7 days before the number of root hairs were counted. Error bars represent standard error of the mean. P values for differences between Col-0 and the two mutant lines (ots1 ots2, tir1 afb2 afb3): *** ≤ 0.001 (one-way ANOVA with Tukey test post hoc). n = 20 per genotype. Three repeats conducted.*

3.5 The Arabidopsis SUMO protease mutant shows an increased hydrotropic response

Due to the sessile nature of plants, members of this kingdom have evolved several intricate mechanisms to deal with their ever changing environments. Through these mechanisms, plants are able to perceive and respond appropriately to varied environmental stimuli, such as drought, gravity and light, by growing to/from the point of stimulus. This morphological plasticity exhibited in response to perceived environmental change is known as a tropic response.

The hydrotropic response is the morphological change induced in response to fluctuations in the surrounding moisture gradient (Eapen, et al., 2005). Unlike many of the other tropisms, such as gravitropism (Chen, et al., 1999) and phototropism (Liscum, et al., 2014), hydrotropism has been less extensively studied, with relatively little research conducted in this area until the turn of the 21st century, despite its perceived importance in the prevention of crop yield losses due to water shortage (Cassab, et al., 2013). This apparent oversight is due to the interplay between gravitropism and hydrotropism; due to the former tropism interfering with the subtler influence of the latter, the establishment of this tropism as a distinct response was not achieved until the mid-1980s (Jaffe, et al., 1985).

Classical thinking attributes root hydrotropism to the Cholodny-Went hypothesis (Went & Thimann, 1937); upon the detection of specific environmental stimuli, the lateral redistribution of auxin occurs within the plant, leading to alterations in growth. Whilst this has been shown generally to hold true for gravitational stimulus (Gutjahr, et al., 2005), current research regarding the role of auxin in the hydrotropic response renders this hypothesis less than favourable (see, 3.8 Discussion) (Shkolnik, et al., 2016).

Despite the lack of definitive evidence linking auxin to hydrotropism, the responses of the SUMO protease double knock out mutant line, *ots1 ots2*, and the SUMO protease over expression line, *35S:OTS1:HA,* to changes in water potential were tested. In order to determine whether increased background SUMOylation levels affect the response to changes in water potential, a split-plate assay was used (see, fig. 3.17) (Antoni, et al., 2016). The lower half of the split ½ MS plate was

supplemented with 400mM sorbitol to decrease the water potential, thereby creating a water gradient through which the hydrotropic response could be stimulated.

WT (Col-0), *ots1 ots2,* and *35S;OTS1:HA* seedlings were germinated and grown on ½ MS plates under 24 hour light conditions. At 5 days old, the seedlings were transferred to the split assay plate and incubated vertically under 24 hour light conditions for 12 hours (fig. 3.18), after which the angle of bend, and therefore the strength of the tropic response, was measured. Upon exposure to the moisture gradient, the *ots1 ots2* line showed a significant increase (one-way ANOVA) in the average angle of bend compared to WT (fig. 3.19). This indicates that increased SUMOylation levels leads to an increase in hydrotropism in *Arabidopsis*.

The hydrotropic response of the 35S:OTS1:HA overexpression line was also tested. Due to the hydrotropic phenotype exhibited by the knock out line, it was expected that the 35S:OTS1:HA line would show a significant decrease in hydrotropic response. However, overexpression of the OTS1 SUMO protease appeared to result in a slight increase in angle of bend compared to WT, though not as extreme as that observed for the *ots1 ots2* knock out line. This increase was not found to be statistically significant (one-way ANOVA). This seemingly contradictory phenotype observed for the overexpression line could be due to the molecular quirks of overexpression. For example, the activity of OTS1 may not be dependent upon its expression level, meaning any restoration of OTS1 function results in a return to the WT phenotype. It is also possible that the increase in hydrotropic response observed for the knock out line is due to the loss of the *ots2* gene only; overexpression of the OTS1 gene, therefore, would not significantly affect the hydrotropic response.

FIGURE 3.17| SCHEMATIC DEMONSTRATING EXPERIMENTAL SETUP FOR THE HYDROTROPIC RESPONSE ASSAY

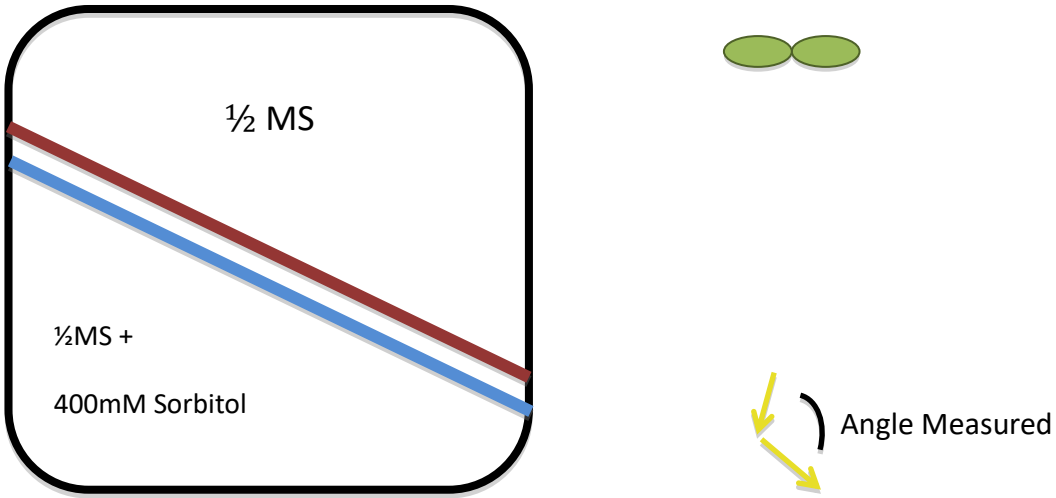

Schematic showing the split-plate hydrotropism assay setup. 1/2MS plates were poured and all media from the lower half of the plate (indicated by the blue line) removed and replaced with 1/2MS supplemented with 400mM sorbitol (thereby providing the hydrotropic stimulus). 5-day-old seedlings were transferred to the assay plate; seedlings were positioned upon the plate with the root tips situated at the red line (2mm above the start of the hydrotropic stimulus). After 12 hours, the angle of bend was then measured (indicated by the yellow arrows).

FIGURE 3.18| THE *ots1 ots2* MUTANT IS POSITIVELY HYDROTROPIC

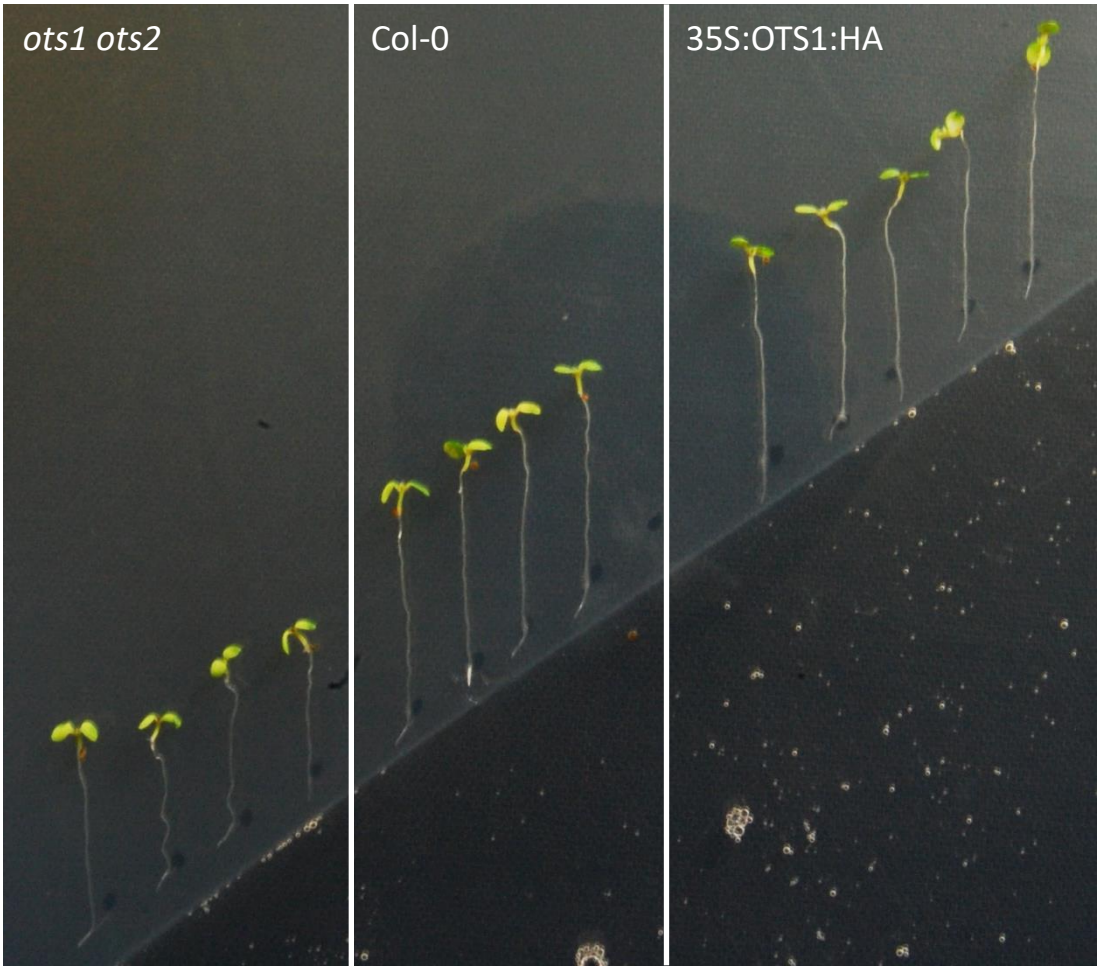

5-day-old ots1 ots2 seedlings showing the increased response to hydrotropic stimulus (400mM sorbitol) after 12 hours compared to WT (Col-0), and the SUMO protease overexpression line (OTS1-OE). The ots1 ots2 mutant line shows a slight decrease in bend angle in comparison to WT, indicating a positively hydrotropic phenotype.

Seedlings were germinated on 1/2MS and 0.8% phytoagar plates supplemented with 0.5% sucrose under 24 hour light conditions. At 5 days old, the seedlings were transferred to the prepared assay plates: 1/2MS with 0.8% phytoagar and 0.5% sucrose, with the lower half of the split plate supplemented with 400mM sorbitol. Seedlings were then grown under 24hr light conditions for a further 12 hours before the root bend angle was measured. n = 60 per genotype. Three repeats conducted.

FIGURE 3.19| *ots1 ots2* SHOWS A SIGNIFICANT INCREASE IN HYDROTROPIC RESPONSE IN COMPARISON TO WT

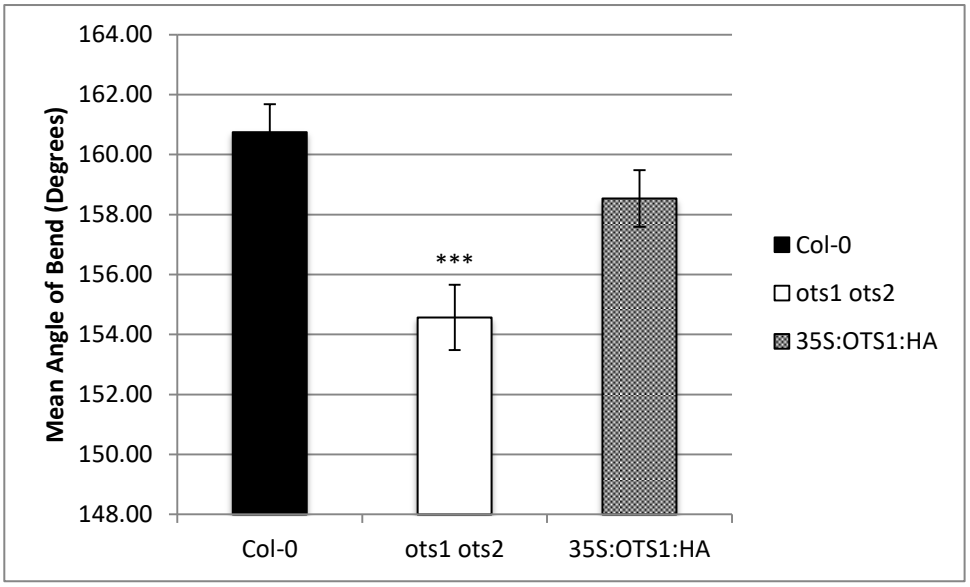

Analysis of mean angle of bend of 5-day old Col-0, ots1 ots2 and OTS1 overexpressor, 35S:OTS1:HA, Arabidopsis lines in response to hydrotropic stimulus (400mM sorbitol). The ots1 ots2 mutant line shows a statistically significant decrease in bend angle in comparison to WT, indicating a positively hydrotropic phenotype.

*Seedlings were germinated on 1/2MS and 0.8% phytoagar plates supplemented with 0.5% sucrose under 24 hour light conditions. At 5 days old, the seedlings were transferred to the prepared assay plates: 1/2MS with 0.8% phytoagar and 0.5% sucrose, with the lower half of the split plate supplemented with 400mM sorbitol. Seedlings were then grown under 24hr light conditions for a further 12 hours before the root bend angle was measured. Error bars represent standard error of the mean. P values for differences between Col-0 and ots1 ots2 lines: ** ≤ 0.01 (one-way ANOVA with Tukey test post hoc). n = 60 per genotype. Three repeats conducted.*

3.8 Discussion

The control of root architecture is inextricably linked with plant phytohormones. The most well studied of these hormones is auxin. Auxin is a major player in practically all forms of plant growth and development, from embryogenesis and organogenesis to tropisms and stress responses (Saini, et al., 2013). Research conducted by Ishida, et al. (2009) and Huang, et al. (2009) regarding the SUMO E3 ligases SIZ1 and HPY2 has shown that the auxin response may be regulated, in part, through SUMOylation. Here, through the use of *Arabidopsis* seedlings unable to express two members of the SUMO protease family, OTS1 and OTS2, that link has been confirmed.

The *ots1 ots2* knock out mutant line shows a distinct and statistically significant increase in sensitivity to auxin compared to WT (fig. 3.2, 3.4, 3.13, & 3.14). The mutant line displays many of the classical auxin-sensitive phenotypes, such as a decrease in primary root length upon the application of exogenous auxin (Eliasson, et al., 1989), an increase in lateral root number upon application of exogenous auxin (Reed, et al., 1989), and an increase in root hair length under control conditions (Pitts, et al., 1998). These phenotypes suggest that an increase in background levels of SUMOylation within *Arabidopsis* lead to an increase in auxin sensitivity within the plant. However, how this increase in sensitivity is achieved is not yet known.

The lack of phenotype observed for the *ots1 ots2* mutant line when exposed to TIBA suggests that whilst increased SUMOylation levels effect auxin sensitivity, this is not due to SUMO-mediated alterations in polar auxin transport. This leads to the assumption that the changes in auxin sensitivity observed for the *ots1 ots2* mutant line may be due to increased SUMOylation of the auxin cascade machinery, e.g. the TIR1, AUX/IAA and ARF protein families. This hypothesis is explored in later chapters (see, chapter 4 &5).

Alongside the clear auxin phenotype documented in this chapter, the *ots1 ots2* mutant line also appears to exhibit a root cap-related phenotype. In comparison to WT *Arabidopsis*, the *ots1 ots2* mutant line produces significantly fewer lateral roots under control conditions. Whilst initially this appears to undermine the hypothesis, and associated experimental data regarding the primary root and root hair length, that increased levels of background SUMOylation result in an increase in auxin sensitivity, this is not the case. Upon the application of exogenous auxin to the seedlings,

an increase in lateral root number is observed for the *ots1 ots2* mutant (fig. 3.13) compared to the untreated *ots1 ots2* seedlings. However, this increase only extends to a doubling in number of emerged lateral roots; unlike its WT counterpart, the *ots1 ots2* mutant does not conform to the pattern of producing increasing numbers of lateral roots with increasing auxin concentration, but is instead only able to increase the number of lateral roots it produces to by a finite number (twice that observed under control conditions) regardless of exogenous auxin concentration. This deviation from the expected pattern suggests that, whilst the *ots1 ots2* mutant is indeed auxin sensitive, as demonstrated by its increase in lateral root production upon auxin application, it is defective in the priming of lateral root precursor cells.

Recent research by Xuan, et al. (2015) has indicated that the root cap is responsible for the modulation of the auxin signal responsible for the priming of lateral root precursor cells. The priming of the XPP cells that eventually form the lateral root primordia occurs via periodic oscillations in cellular auxin concentration (Laskowski, 2013). This oscillation is modulated by the auxin precursor IBA; through the root-cap specific conversion of IBA to IAA and the subsequent induction of MEMBRANE-ASSOCIATED KINASE REGULATOR 4 (MAKR4), the plant is able to tightly regulate spatiotemporal root patterning (Xuan, et al., 2015).

This information combined with the experimental data shown here regarding the increased hydrotropic response of the *ots1 ots2* mutant line (fig. 3.18 & 3.19) suggests increased levels of SUMOylation alter the perception and signalling of the primary root cap. Changes in water potential are sensed by root cap cells (Kiss, 2007), with removal of the root cap resulting in the complete abolition of the hydrotropic response (Jaffe, et al., 1985). It is therefore likely that the reduction in lateral roots observed for the *ots1 ots2* mutant line, and the increase in hydrotropic response, is due to defects in the primary root cap and not SUMO-mediated alterations in the auxin signalling cascade.

3.9 Conclusion

In this chapter, it has been demonstrated that hyper-SUMOylated cellular environment of the SUMO protease knock out mutant line, ots1 ots2, may induce an increase in sensitivity to the phytohormone auxin.

Phenotypic analysis of the *ots1 ots2* mutant line revealed an increased level of response to exogenous auxin stimulus, with a reduction in primary root length and an increase in lateral root number observed after exposure to the auxinic compounds IAA and 2,4-D. Analysis of root hair length under control conditions further confirmed a potential increase in auxin sensitivity within the mutant line, with increased root hair length observed for the mutant in comparison to WT. The absence of a differential response between WT and the *ots1 ots2* mutant line upon exposure to the auxin efflux inhibitor, TIBA, lead to the hypothesis that this potential increase in auxin sensitivity may be due to SUMO-mediated alterations in the auxin signalling cascade rather than auxin transport. This hypothesis is further explored in subsequent chapters (see, chapters 4 & 5).

A secondary phenotype possibly regarding the root cap was observed for this mutant line. A reduction in lateral root primordia and emerged lateral roots under control conditions, alongside an increase in hydrotropic response, lead to the hypothesis that root cap perception and/or signalling may be altered in the *ots1 ots2* mutant background.

4. The SUMOylation of the Auxin Receptor TIR1

4.1 Introduction

The results presented in Chapter 3 indicate that SUMOylation plays a role in auxin signalling in *Arabidopsis thaliana*. The root phenotype data from the *ots1 ots2* double mutant shows that there is an increase in auxin sensitivity in a hyper-SUMOylated background. This leads to the hypothesis that SUMOylation of the auxin cascade machinery, either in part or as a whole, increases auxin sensitivity.

In this chapter, the SUMOylation status and the effects thereof of the auxin receptor TIR1 are investigated.

4.2 SUMOylation of the Auxin Receptor TIR1

To investigate the hypothesis (see, Introduction 1.3) that SUMOylation of the primary auxin receptor, TIR1, is involved in the increase in auxin sensitivity observed in the hyper-SUMOylated *ots1 ots2* mutant, the protein sequences of the TIR1/AFB family members were scanned for potential SUMO binding sites using the bioinformatics software, HyperSUMO (Nelis, 2014) as shown in fig. 4.1. Potential SUMO binding sites were identified in all family members, with three such sites (K373, K457 and K485) predicted in the main auxin receptor protein, TIR1.

Arabidopsis TIR1 homologues were identified in other plant species using BLASTp (Gish & States, 1993). From the TIR1 homologues identified by BLASTp, under the standard parameter settings, proteins from the following species were used in a bioinformatic analysis with HyperSUMO to determine the conservation of predicted SUMO binding sites: *C. sativa* (XP_010512696), *E. salsugeineum* (XP_006402320), *B. rapa* (XP_009116967), *O. sativa* (XP_015635915), *Z. mays* (XP_008669494), *S. tuberosum* (XP_006359432), *N. tabacum* (ACT53268), and *C. annuum* (XP_016565699). The results of this analysis indicate that the three SUMO binding sites predicted in *Arabidopsis* are conserved in *C. sativa*, *E. salsugeineum* and *B. rapa*. In all homologues, the predicted SUMO binding site corresponding to *At*TIR1 K485 was present, the sequence remaining highly conserved amongst all analysed proteins (fig. 4.2). These results suggest that the K485 binding site is the most likely candidate for the SUMO binding site of TIR1.

Whilst primary protein sequence analysis by HyperSUMO is useful in identifying potential SUMO binding sites, it does not take into account the 3D structure of the protein. SUMO can only bind to lysine residues exposed to the external environment, no matter how favourable the amino acid sequence. It is therefore important to map predicted SUMO binding sites onto the 3D structure of the protein in question, where possible, in order to eliminate any predicted sites buried within the protein or rendered inaccessible through steric hindrance. The three predicted TIR1 SUMO binding sites, K373, K457 and K485, were located on the structure of the crystallised TIR1-ASK1 complex (pdb file: 2P1M; Tan, et al., 2007) using the protein structure modelling software PyMOL. All three sites are present on the lower side of the LRR domain, with residues K373 and K457 angled away from the underside of the protein, and residue K485 angled in towards the auxin-binding pocket located in the barrel of the solenoid formed by the LRR domain (fig. 4.3). The location of all three potential SUMO binding residues renders them suitable for SUMO binding.

The four Auxin Receptor F-box proteins were successfully amplified using the proofreading DNA polymerase Q5 (NEB) plus 0.3% DMSO from cDNA generated from 7 day old Col-0 seedlings (fig. 4.4) (see, Methods 3.3.1 & 3.3.7/8). The PCR product was purified using a Zymoclean™ Gel DNA Recovery Kit (Zymo) and cloned into the entry vector pENTR/D-TOPO (see, Methods 3.3.3). The constructs were transformed into *E. coli* DH5α and the colonies screened for successful clones by PCR using AttB primers. Two clones for each construct were selected for plasmid purification followed by in-house sequencing via DBS Genomics. Constructs containing the correct gene sequence were digested with MluI (NEB) and transferred via recombination into the 35S, N-terminal GFP-tag Gateway® destination vector pEARLYGATE104 and into the 35S, N-terminal 4xMyc-tag pEARLYGATE203 (see, Methods 3.3.4 & 3.3.5). Confirmed TIR1, AFB1, AFB2 and AFB3 clones in pEARLYGATE104/203, identified via colony PCR with AttB primers, were transformed into the *Agrobacterium* strain GV3101 ready for transient expression (see, Methods 3.2.3).

A transient assay in *N. benthamiana* using 35S:GFP:TIR1 was conducted to confirm the SUMOylation status of the auxin receptor E3 ligase (see, Methods 3.4). Recombinant YFP:TIR1 transient expression was confirmed by western blotting with α-GFP monoclonal antibodies (Clonetech); α-GFP was used as it is reactive to all GFP variants, such as YFP and CFP (Kaltwasser, et al., 2002). A large band corresponding to YFP:TIR1 was observed in the IP sample lane (see, fig. 4.5:A). The SUMOylation status of recombinant YFP:TIR1 was shown via western blotting with α-HA antibodies (Sigma). A faint band was observed at ~200kDa in the lane corresponding to YFP:TIR1 (fig 4.5:B). This band suggests that YFP:TIR1 is SUMOylated *in planta*, with the mass of the observed band implying that YFP:TIR1 is decorated by multiple SUMO moieties.

To confirm TIR1 SUMOylation *in vivo*, *tir1* knockout *Arabidopsis* lines containing C-terminal VENUS-tagged TIR1 under control of the TIR1 promoter (pTIR1:TIR1:VENUS, obtained from Malcolm Bennett, Nottingham University) were used. Mutants were confirmed before use via PCR from genomic extracts (see, Methods 3.3.1 & 3.3.6) using 3 sets of primers (Fig. 4.6). pTIR1:TIR1:VENUS seeds were germinated on MS medium (see, Methods 3.1.1 & 3.1.2) and allowed to grow for 12 days before harvesting. Protein was extracted from the harvested tissue and expression of the recombinant protein observed by western blot with α-GFP monoclonal antibodies (Clonetech) (fig. 4.7). No TIR1:VENUS was identified in the extract or IP. Unfortunately,

cleavage of the VENUS tag from TIR1 was observed in the IP; no band corresponding to TIR1:VENUS was seen in the pTIR1:TIR1:VENUS IP lane, only that of the free VENUS.

FIGURE 4.1| SUMO SITE PREDICTION FOR THE TIR1/AFB FAMILY

A.

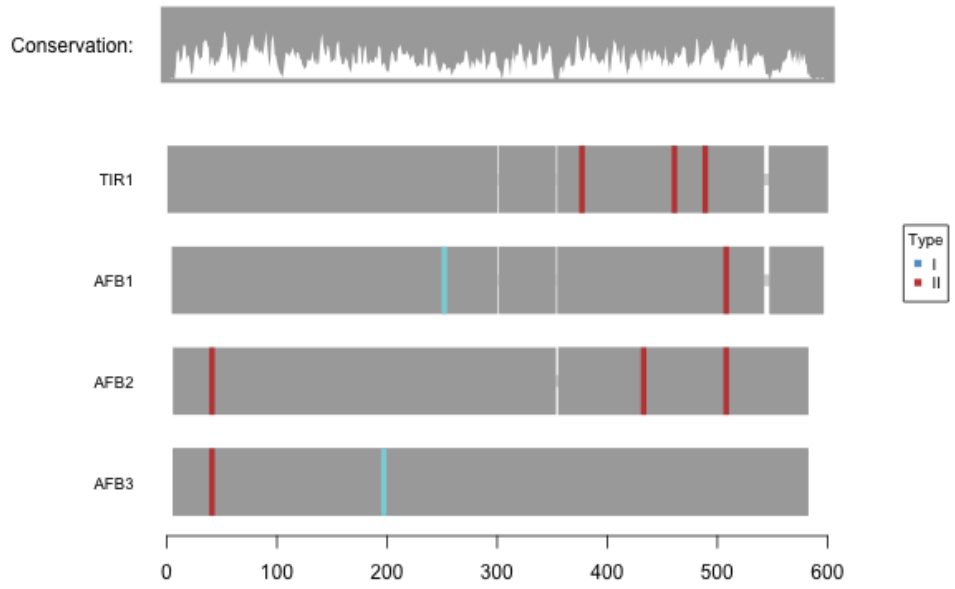

B.

Protein	Position	Type	Confidence	Sequence
AFB1	K246	I	100	QLKPEA
AFB3	K190	I	99	CLKGET
TIR1	K373	II	100	CPKLES
TIR1	K457	II	100	AKKMEM
TIR1	K485	II	99	LRKLEI
AFB1	K500	II	99	AAKLET
AFB2	K34	II	100	WYKIER
AFB2	K424	II	95	IVKACK
AFB2	K499	II	99	VSKYET
AFB3	K34	II	99	WHKIER

A. *Schematic showing the highly predicted (85%+) SUMOylation sites in the Auxin-Responsive F-box family of proteins. The predicted SUMOylation sites located within this protein family differ between members.*

B. *A table showing the location, type, percentage prediction and sequence of the predicted SUMO sites in the Auxin-Responsive F-Box Family of proteins.*

FIGURE 4.2| SUMO SITE PREDICTION FOR CROSS-SPECIES ATTIR1 HOMOLOGUES

A.

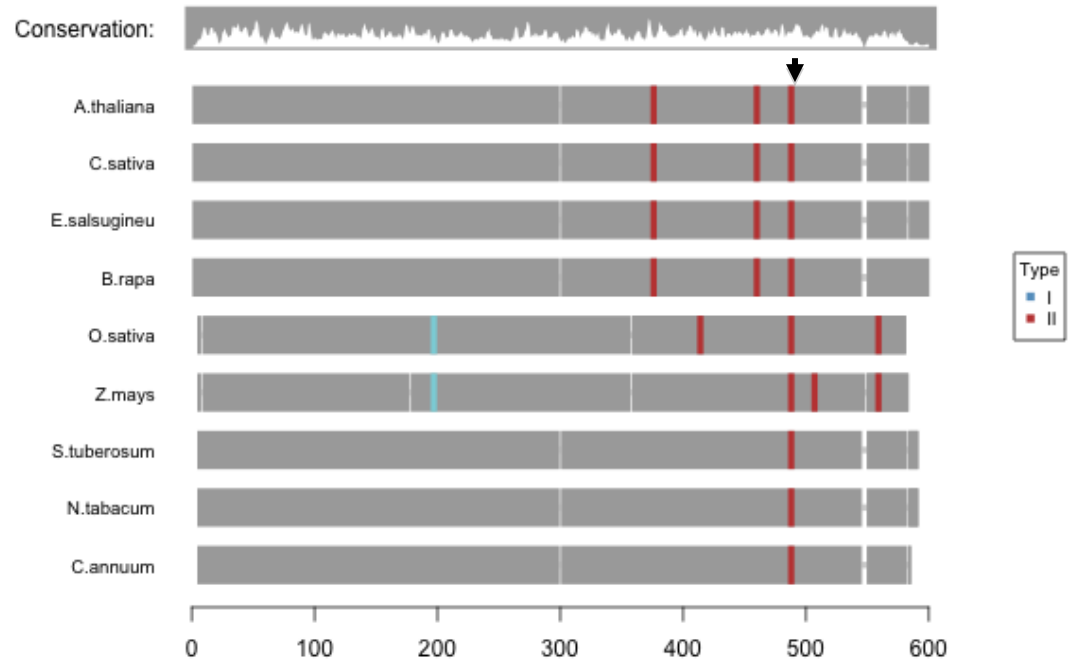

B.

Protein	Position	Type	Confidence	Sequence
A. thaliana (AT3G62980)	K485	II	99	LRKLEI
C. sativa (XP_010512696)	K485	II	99	LRKLEI
E. salsugeineum (XP_006402320)	K485	II	99	LRKLEI
B. rapa (XP_009116967)	K485	II	99	LRKLEI
O. sativa (XP_015635915)	K480	II	99	LRKLEI
Z. mays (XP_008669494)	K479	II	99	LRKLEI
S. tuberosum (XP_006359432)	K481	II	99	LRKLEI
N. tabacum (ACT53268)	K481	II	99	LRKLEI
C. annuum (XP_016565699)	K481	II	99	LRKLEI

A. *Schematic showing the highly predicted (85%+) SUMOylation sites in TIR1 homologues identified using BLASTp. All homologues show a highly conserved SUMOylation site at the C-terminal end of the protein (AtTIR1 K485), indicated by a black arrow.*

B. *A table showing the location, type, percentage prediction and sequence of the AtTIR predicted SUMO site K485 homologues. All predicted sites have the same, highly conserved amino acid sequence.*

FIGURE 4.3| SUMO SITE LOCATION IN THE 3D STRUCTURE OF ATTIR1

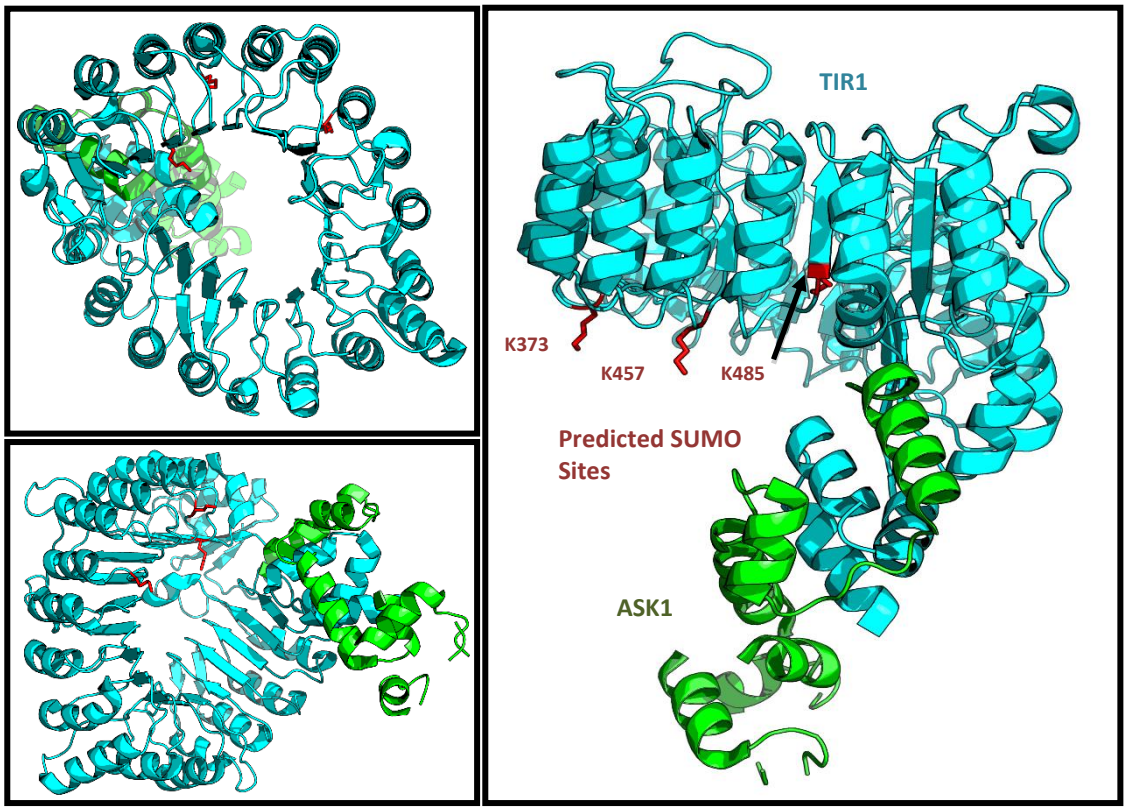

The 3D-structure of the ASK1-TIR1 auxin-receptor complex, with each component shown in green and blue respectively. The three lysine residues predicted to be involved in the SUMOylation of TIR1 are highlighted in red. These residues are located on the underside of the main barrel of TIR1, opposite the AUX/IAA binding location. The side-chains of K373 and K457 are pointing away from the main body of the TIR1 protein. The side-chain of the K485 residue is pointing inwards through the main barrel, towards the auxin-binding site. Co-ordinates from pdb file 2P1M (Tan, et al., 2007)*. Figure generated in PyMOL (Delano, 2002) modelling software, Version 1.8.*

FIGURE 4.4| CLONING OF *ARABIDOPSIS THALIANA* TIR1 AND AFB PROTEIN FAMILY

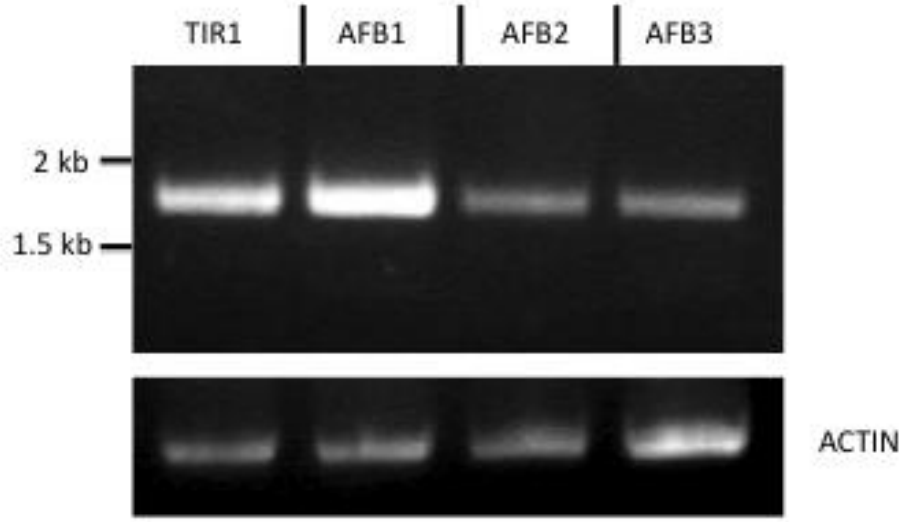

Gel image showing the cloning of TIR1 (AT3G62980), AFB1 (AT4G03190), AFB2 (AT3G26810) and AFB3 (AT1G12820). Genes were cloned from Col-0 cDNA extracted from 7-day old seedlings The PCR was conducted with the proof-reading polymerase Q5 (New England Biolabs) supplemented with 0.3% DMSO, and was run for 30 cycles.

FIGURE 4.5| YFP:TIR1 APPEARS TO UNDERGO SUMOYLATION IN TRANSIENT ASSAY

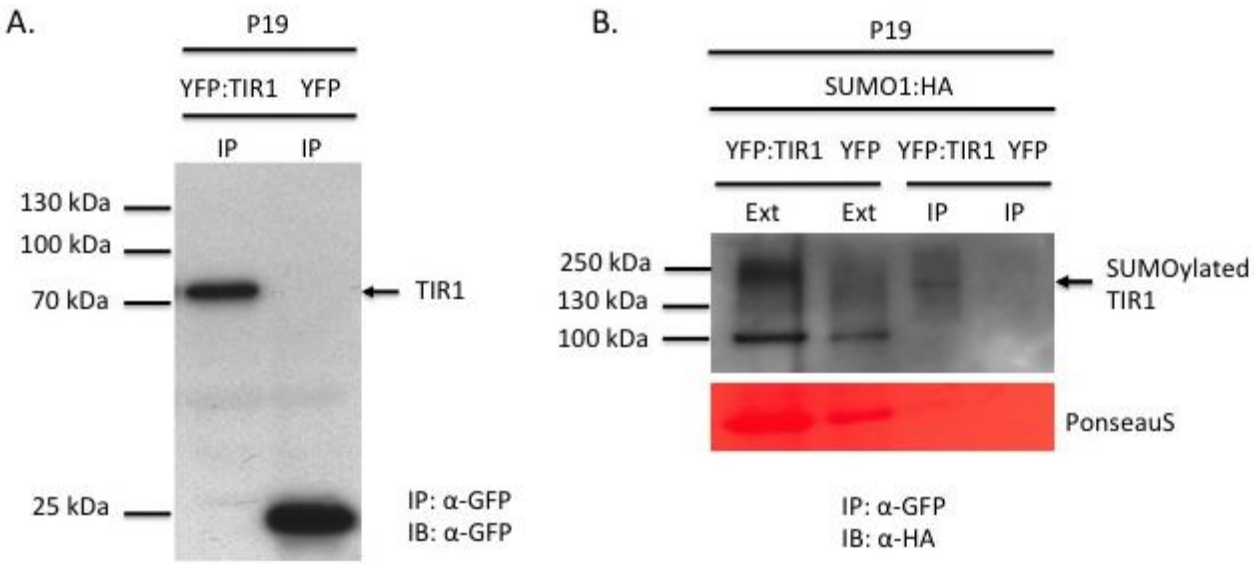

A. *Western blot showing α-GFP IP and α-GFP IB of YFP:TIR1 plus a YFP control infiltrated with P19 suppressor protein and recombinant SUMO1:HA in a 1:1:3 ratio. Bands can be seen in all lanes, showing expression and successful immunoprecipitation of TIR1 and the GFP control. 10ul of IP was loaded.*

B. *Western blot showing α-GFP IP and α-HA IB of YFP:TIR1 and YFP control infiltrated with P19 suppressor protein and recombinant SUMO1:HA. A faint band can be seen in the IP lane of YFP:TIR1, indicating SUMOylation of TIR1. 20ul of extract and 20ul of IP was loaded. Ponceau S-stained RuBisCO is shown as loading control.*

FIGURE 4.6| GENOTYPING OF THE *ARABIDOPSIS THALIANA* PTIR1:TIR1:VENUS LINE

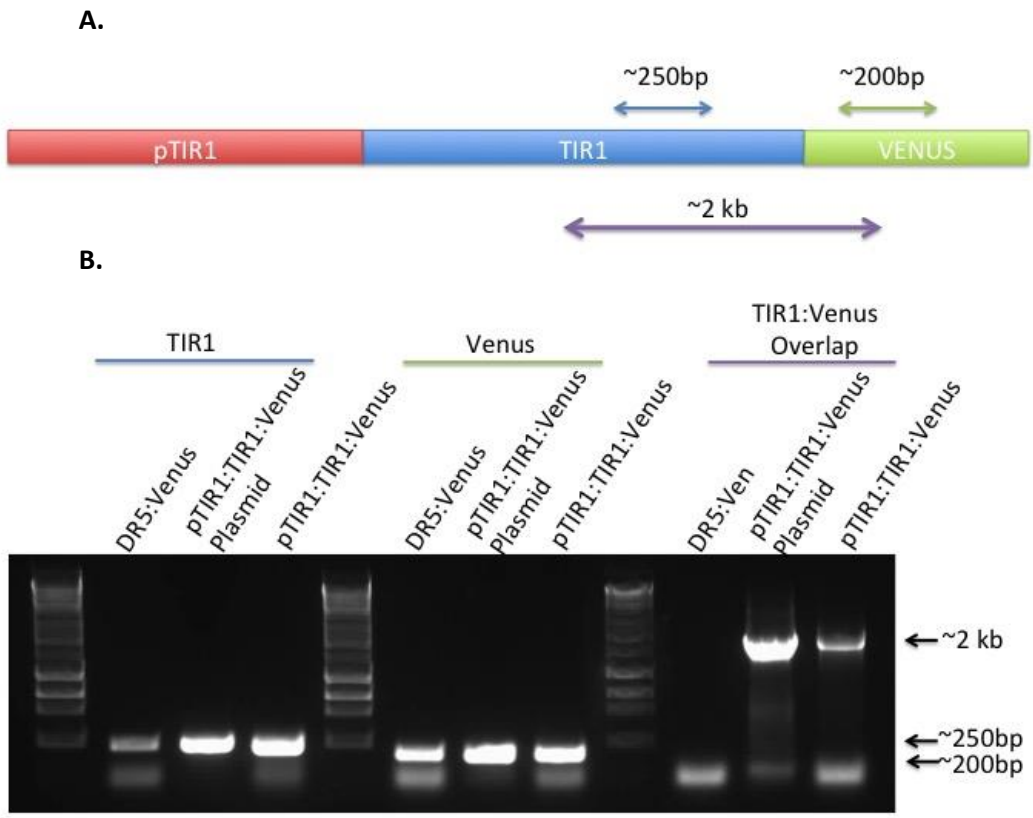

A. *A schematic showing the location and PCR product size of the primers used in the genotyping of the Arabidopsis pTIR1:TIR1:VENUS mutant line.*

B. *Gel image showing the genotyping of the pTIR1:TIR1:VENUS line alongside a VENUS-only control (DR5:VENUS) and the pTIR1:TIR1:VENUS plasmid used to generate the mutant line.*

FIGURE 4.7| THE VENUS TAG IS CLEAVED FROM TIR1 IN THE PTIR1:TIR1:VENUS LINE

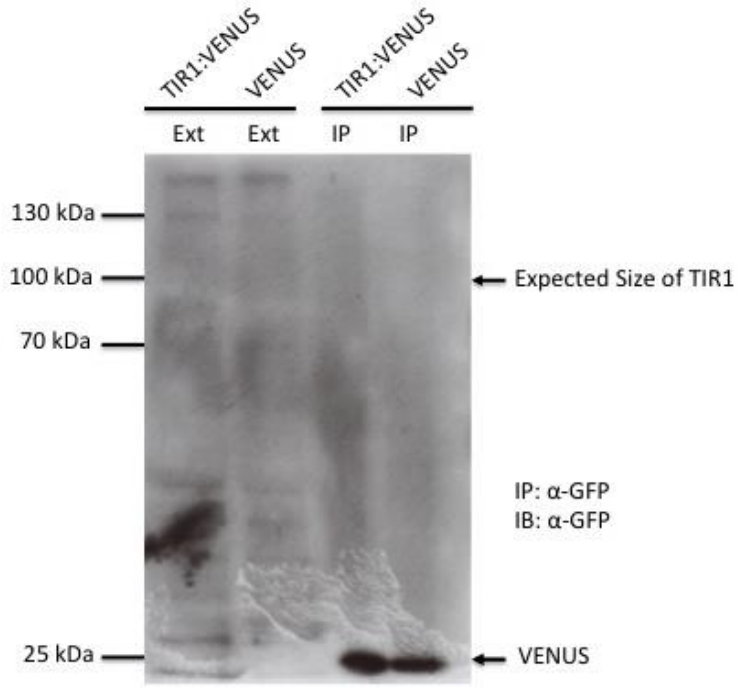

Western blot showing α-GFP IP and α-GFP IB of protein extracted from Arabidopsis thaliana mutant line pTIR1:TIR1:VENUS and a VENUS only control line (DR5:VENUS). No TIR1:VENUS was detected in the total protein extract or in the IP elution. Free VENUS was detected in the elution from the IP, indicating that the tag is undergoing cleavage.

4.3 Generation of the Non-SUMOylatable TIR1^{3KR} Mutant

In order to identify the predicted SUMO binding sites involved in the conjugation of SUMO moieties to TIR1, site directed mutagenesis was used to remove each of the predicted SUMO binding residues in turn (see, Appendix A.1). Through the use of specially designed overlapping mismatch primers (see, Appendix A.2), the lysine residues at each of the predicted binding sites were changed to arginine, thus preventing the binding of SUMO whilst maintaining the structural environment of the surrounding area. The three single TIR1 SUMOylation mutants (K373R, K457R and K485R) were successfully amplified using the proofreading DNA polymerase Q5 (NEB) plus 0.3% DMSO from purified recombinant TIR1 pENTR/D-TOPO (see, fig. 4.8) (see, Methods 3.3.1). The PCR product was then digested and transformed into *E. coli* DH5α. Mutant clones were identified through sequencing by DBS Genomics, with successfully mutated clones used to make the double SUMO-site mutants: K373/457R, K373/485R and K457/5485R, via the same process. The final, triple SUMO-site mutant, TIR1 3KR, was generated as above from successfully mutated double mutant clones.

Upon confirmation of the generation of the TIR1 3KR triple mutant, the clone was then digested with MluI (NEB) and transferred via recombination into the 35S, N-terminal GFP-tag Gateway® destination vector pEARLYGATE104 and into the 35S, N-terminal 4xMyc-tag pEARLYGATE203. Confirmed TIR1^{3KR} clones in pEARLYGATE104/203, identified via colony PCR with AttB primers, were transformed into the *Agrobacterium* strain GV3101 ready for transient expression.

In order to confirm the loss of SUMOylation in the TIR1^{3KR} mutant, a transient assay in *N. benthamiana* was performed. Recombinant YFP:TIR1^{3KR} and YFP:TIR1 transient expression was confirmed by western blotting with α-GFP monoclonal antibodies (Clonetech). Two large bands corresponding to YFP:TIR1^{3KR} and YFP:TIR1 respectively were observed in both the IP sample lanes (see, fig. 4.9:A). The SUMOylation status of recombinant YFP:TIR1^{3KR} in comparison to YFP:TIR1 was confirmed via western blotting with α-HA antibodies (Sigma). A large band was observed at ~200kDa in the lane corresponding to YFP:TIR1, again confirming that YFP:TIR1 is SUMOylated *in planta* (see, fig. 4.9:B). No equivalent band was observed in the lane corresponding to the YFP:TIR1^{3KR} mutant, confirming the loss of SUMOylation, as predicted, with the removal of the lysine residues identified by HyperSUMO.

To assess the role the SUMOylation of TIR1 plays in auxin signalling, a stability assay was conducted. c-MYC:TIR1 and c-MYC:TIR1^{3KR} were transiently expressed in *N. benthamiana* and the leaves treated with the auxinic compound 1-Naphthaleneacetic acid (NAA) before collection. 10uM NAA was infiltrated into leaves expressing c-MYC:TIR1 and c-MYC:TIR1^{3KR}, with samples taken at 30 minutes and 2 hour time points alongside a non-auxin treated control. The stability of c-MYC:TIR1^{3KR} compared to c-MYC:TIR1 was assessed via western blot with α-c-MYC monoclonal antibodies (Sigma). In transient assay, c-MYC:TIR1^{3KR} was shown to be less stable than c-MYC:TIR1, with the stability of the non-SUMOylatable protein decreasing upon the addition of auxin (fig. 4.10). The result of this blot provides a potential explanation for the increased auxin sensitivity observed in the hyper SUMOylated *ots1 ots2* line (see, chapter 3); the SUMOylation of the auxin receptor TIR1 stabilises the protein, resulting in an increase in sensitivity to auxin.

To fully confirm SUMOylation of TIR1 and investigate its role *in planta*, N-terminal c-MYC-tagged 35S:TIR1 constructs (pEARLYGATE203) of TIR1 and the TIR1^{3KR} mutant, were dipped into wild-type (Col-0) *Arabidopsis*, the SUMO protease double knock out mutant line *ots1 ots2*, and the auxin insensitive triple knock out mutant line *tir1 afb2 afb3* (see, Methods 3.1.5 & 3.1.6). Seeds from the dipped plant lines were collected and germinated on MS media supplemented with BASTA. F1 transformants were then moved to soil and their seeds collected. F2 seeds were again germinated on MS media supplemented with BASTA and transformants selected for growth on soil.

FIGURE 4.8| GENERATION OF SINGLE, DOUBLE AND TRIPLE K->R SUMO SITE TIR1 CLONES

A.

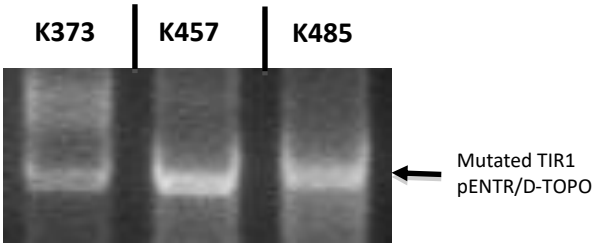

B.

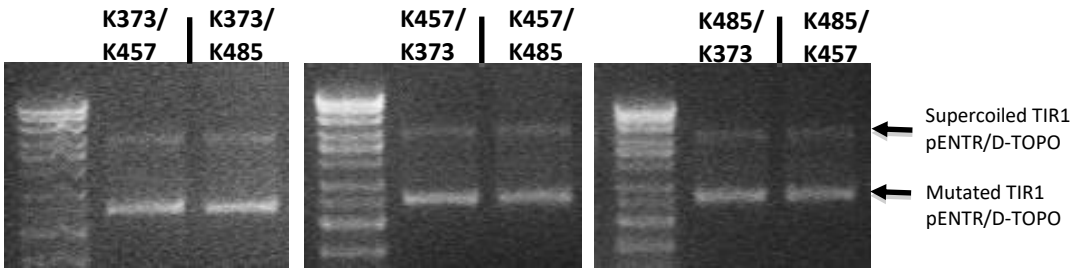

C.

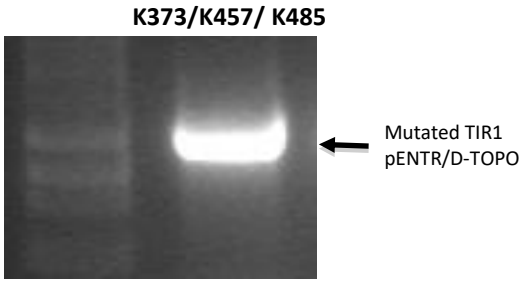

A. *Gel image showing the introduction of the three SUMO site mutations of TIR1 (AT3G62980) to make the TIR1 single SUMO site mutants. Genes were mutated from a confirmed TIR1 pENTR/D-TOPO clone. The PCR was conducted with the proof-reading polymerase Q5 (New England Biolabs) supplemented with 0.3% DMSO, and was run for 25 cycles.*

B. *Gel image showing the introduction of the three SUMO site mutations of TIR1 (AT3G62980) into confirmed single SUMO site mutant clones to make the TIR1 double SUMO site mutants. Genes were*

mutated from a confirmed TIR1^{K373R}, TIR1^{K457R} and TIR1^{K485R} pENTR/D-TOPO clones. The PCR was conducted as stated previously (see, Fg.4.6, A.).

C. *Gel image showing the introduction of the missing SUMO site mutation of TIR1 (AT3G62980) into confirmed double SUMO site mutant clones to make the TIR1 triple SUMO site mutant, TIR1^{3KR}. Genes were mutated from a confirmed TIR1$^{K373R/K457R}$, TIR1$^{K373R/K485R}$ and TIR1$^{K457R/K485R}$ pENTR/D-TOPO clones. The PCR was conducted as stated previously (see Fig. 4.6, A.).*

FIGURE 4.9| THE TIR1^{3KR} SUMO SITE MUTANT IS NOT SUMOYLATED IN TRANSIENT ASSAY

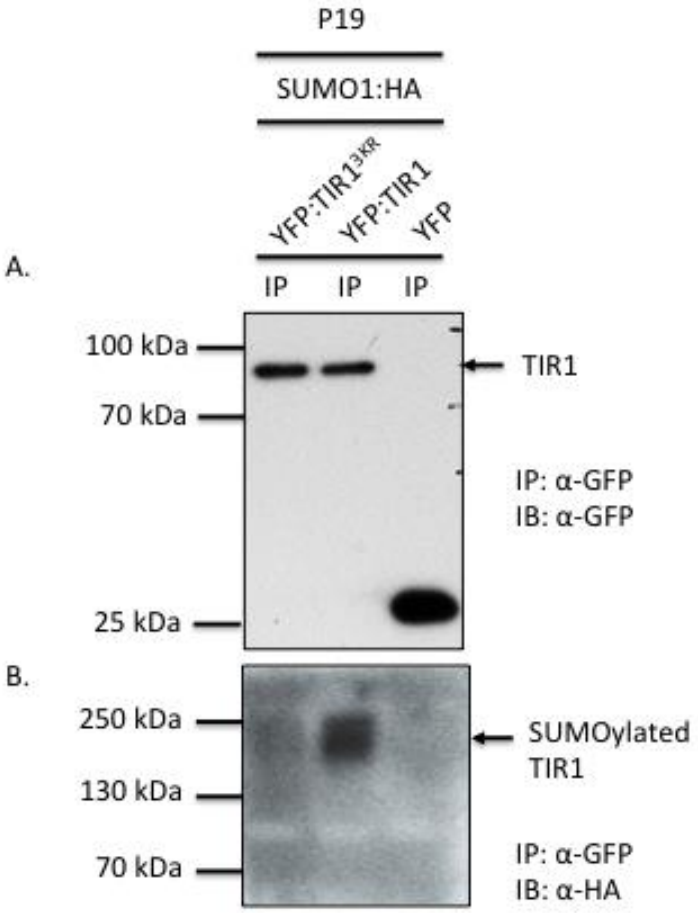

A. *Western blot showing α-GFP IP and α-GFP IB of recombinant YFP:TIR1^{3KR}, YFP:TIR1 and a YFP control infiltrated with P19 suppressor protein and recombinant SUMO:HA in a 1:1:3 ratio. Bands can be seen in all lanes, showing successful immunoprecipitation of YFP:TIR1^{3KR}, YFP:TIR1 and the YFP control. 15ul of IP was loaded.*

B. *Western blot showing α-GFP IP and α-HA IB of recombinant YFP:TIR1^{3KR}, YFP:TIR1 and YFP control infiltrated with P19 suppressor protein and recombinant SUMO:HA. A large band can be seen in the IP lane of YFP:TIR1, indicating SUMOylation of YFP:TIR1. No corresponding band can be seen in the IP lane of YFP:TIR1^{3KR}, indicating the successful removal of the SUMO sites. 20ul of IP was loaded.*

FIGURE 4.10| THE TIR1 3KR MUTANT SHOWS A DECREASE IN STABILITY UPON THE ADDITION OF AUXIN

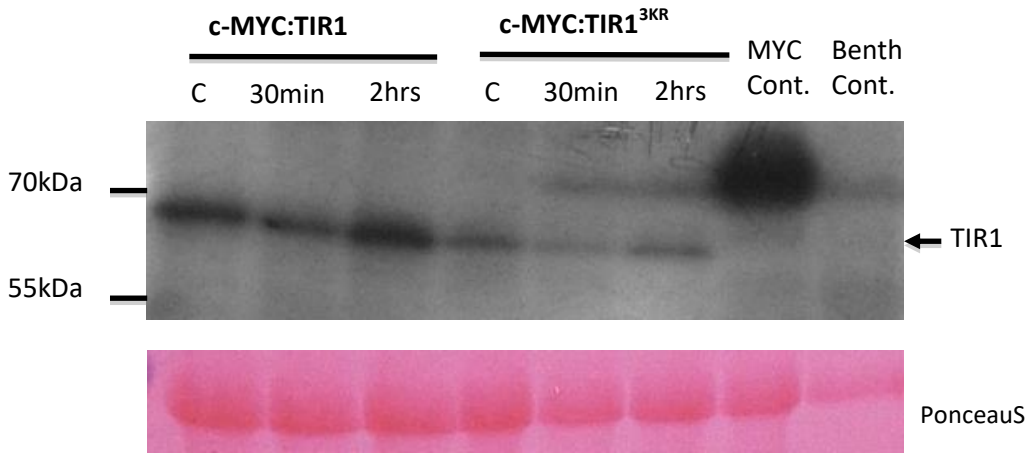

Western blot showing α-c-MYC IB of c-MYC:TIR1 and c-MYC:TIR1^{3KR} alongside a MYC-tag control and uninfiltrated N. benthamiana extract in transient assay. Leaves were treated with 1uM NAA and samples collected at 30 minute and 2 hour time points. 20ul of protein extract was loaded. Ponceau-stained RuBisCO is shown as loading control.

4.4 SUMOylation and TIR1 interaction data

To further probe the effects of the SUMOylation of TIR1 on the auxin response, the interaction of both the YFP:TIR1 and non-SUMOylatable YFP:TIR1^{3KR} mutant with several proteins involved in the auxin signalling cascade and SUMOylation machinery were studied.

In order to act as ubiquitin E3 ligase, the auxin receptor F-box protein, TIR1, forms a complex with three others: ASK1, CUL1 and RBX1 (Yu, et al., 2015). To assess the effects of SUMOylation on the assembly of the SCF^{TIR} E3 ligase complex, ASK1 and CUL1 were cloned for use in transient assay (fig. 4.11). Both ASK1 and CUL1 were successfully amplified using the proofreading DNA polymerase Q5 (NEB) plus 0.3% DMSO from cDNA generated from 7 day old Col-0 seedlings. The PCR product was purified using a Zymoclean^{TM} Gel DNA Recovery Kit (Zymo) and cloned into the entry vector pENTR/D-TOPO. The constructs were transformed into *E. coli* DH5α and the colonies screened for successful clones by PCR using AttB primers. Two clones for each construct were selected for plasmid purification followed by in-house sequencing via DBS Genomics. Constructs containing the correct gene sequence were digested with MluI (NEB) and transferred via recombination into the 35S, N-terminal HA-tag Gateway® destination vector pEARLYGATE201. Confirmed ASK1 and CUL1 clones in pEARLYGATE201, identified via colony PCR with AttB primers, were transformed into the *Agrobacterium* strain GV3101 ready for transient expression.

To investigate the effect of SUMOylation on the assembly of the TIR1-ASK1 complex, a CO-IP of transiently expressed YFP:TIR1 and YFP:TIR1^{3KR} with HA:ASK1 was performed (fig. 4.12) (see, Methods 3.4.6). A western blot probed with α-HA monoclonal antibodies (Sigma) showed there was no difference in the interaction of ASK1 with both YFP:TIR1 and YFP:TIR1:^{3KR}. Therefore, it can be concluded that SUMOylation does not affect the assembly of the TIR1-ASK1 complex.

The experiment was repeated with HA:CUL1 and HA:RBX1, in order to determine whether SUMOylation of TIR1 affected the assembly of the rest of the E3 ligase complex. However, neither construct expressed sufficiently well in *N. benthamiana* to conduct the CO-IP.

Alongside the components of the E3 ligase complex, the effects of TIR1 SUMOylation upon the AUX/IAA repressors were also studied. In order to assess the role of TIR1 SUMOylation in auxin-induced degradation of the AUX/IAA repressor family, c-MYC:TIR1 and c-MYC:TIR1^{3KR} were transiently expressed in *N. benthamiana* alongside YFP:IAA18 (see. Chapter 5.2 for construct generation) and the leaves treated with the auxinic compound 1-Naphthaleneacetic acid (NAA) before collection. 1uM NAA was infiltrated into leaves expressing the recombinant proteins, with samples taken at 30 minutes and 2 hour time points alongside a non-auxin treated control. A CO-IP of transiently expressed c-MYC:TIR1 and c-MYC:TIR1^{3KR} with YFP:IAA18 was performed (fig. 4.13). A western blot probed with α-GFP monoclonal antibodies showed there was no difference in the interaction of YFP:IAA18 with both c-MYC:TIR1 and C-MYC:TIR1:^{3KR}. Therefore, it can be concluded that SUMOylation does not affect the stability of IAA18.

Due to the increase in auxin sensitivity observed in the *ots1 ots2* mutant line, the interaction of TIR1 and its non-SUMOylatable counterpart with the SUMO protease OTS1 was also studied. A CO-IP of transiently expressed YFP:TIR1 and YFP:TIR1:^{3KR} with OTS1:HA was performed (fig. 4.14). A western blot probed with α-HA monoclonal antibodies showed there was no interaction between OTS1:HA and either of the recombinant TIR1 proteins. This suggests that OTS1 is not the primary SUMO protease responsible for the regulation of TIR1 SUMOylation.

FIGURE 4.11| CLONING OF AUXIN-RESPONSIVE E3 LIGASE COMPLEX PROTEINS CUL1 AND ASK1

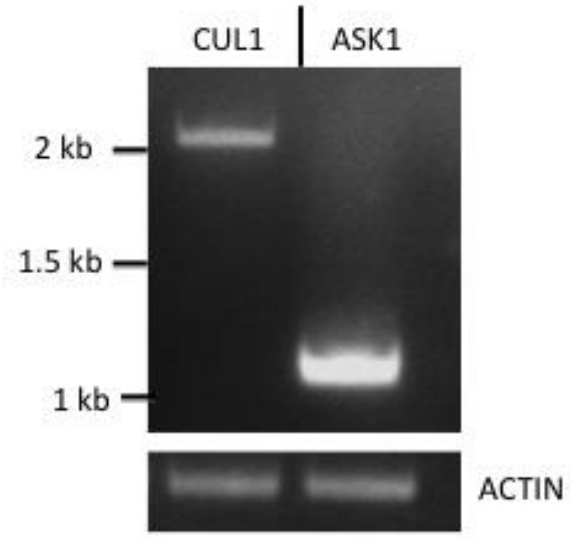

Gel image showing the cloning of CUL1 (AT3G62980) and ASK1 (AT4G03190). Genes were cloned from Col-0 cDNA extracted from 7-day old seedlings The PCR was conducted with the proof-reading polymerase Q5 (New England Biolabs) supplemented with 0.3% DMSO, and was run for 30 cycles.

FIGURE 4.12| BOTH TIR1 AND TIR1^{3KR} INTERACT WITH ASK1 IN TRANSIENT ASSAY

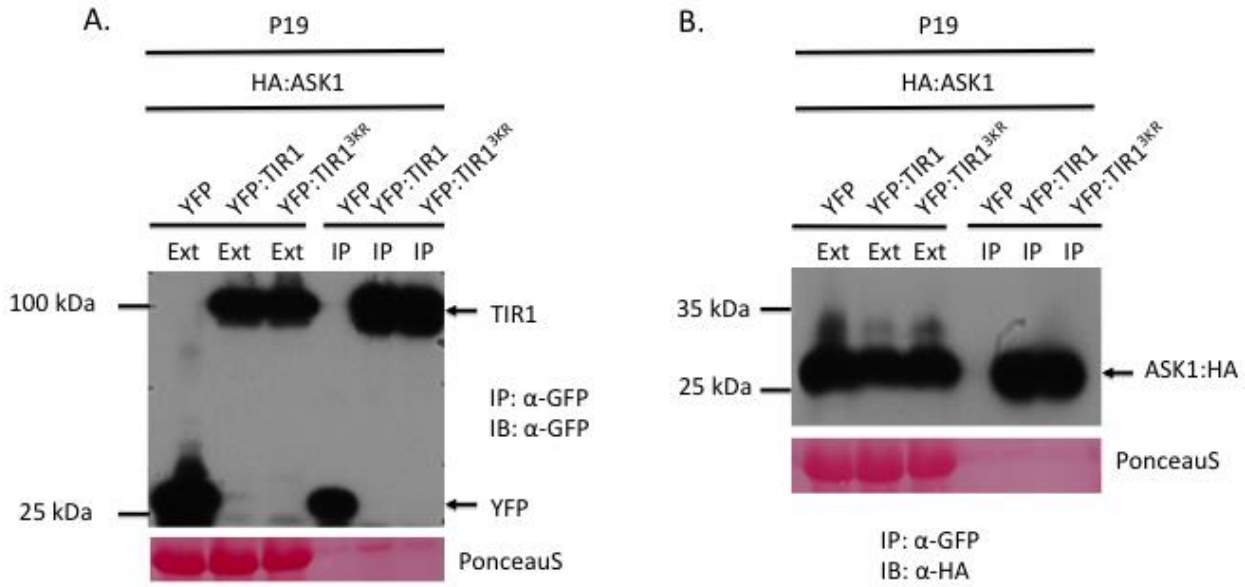

A. *Western blot showing α-GFP IP and α-GFP IB of recombinant YFP:TIR1^{3KR}, YFP:TIR1 and a YFP control infiltrated with P19 suppressor protein and recombinant HA:ASK1 in a 1:1:1 ratio. Bands can be seen in all lanes, showing successful immunoprecipitation of YFP:TIR1^{3KR}, YFP:TIR1 and the YFP control. 10ul of IP was loaded.*

B. *Western blot showing α-GFP IP and α-HA IB of recombinant YFP:TIR1^{3KR}, YFP:TIR1 and YFP control infiltrated with P19 suppressor protein and recombinant HA:ASK1. Large bands corresponding to HA:ASK1 can be seen in the YFP:TIR1 and YFP:TIR1^{3KR} lanes, indicating interaction with HA:ASK1. No corresponding band can be seen in theYGFP control. 5ul of IP was loaded.*

FIGURE 4.13| THE TIR1^{3KR} MUTANT INTERACTS WITH IAA18 IN TRANSIENT ASSAY

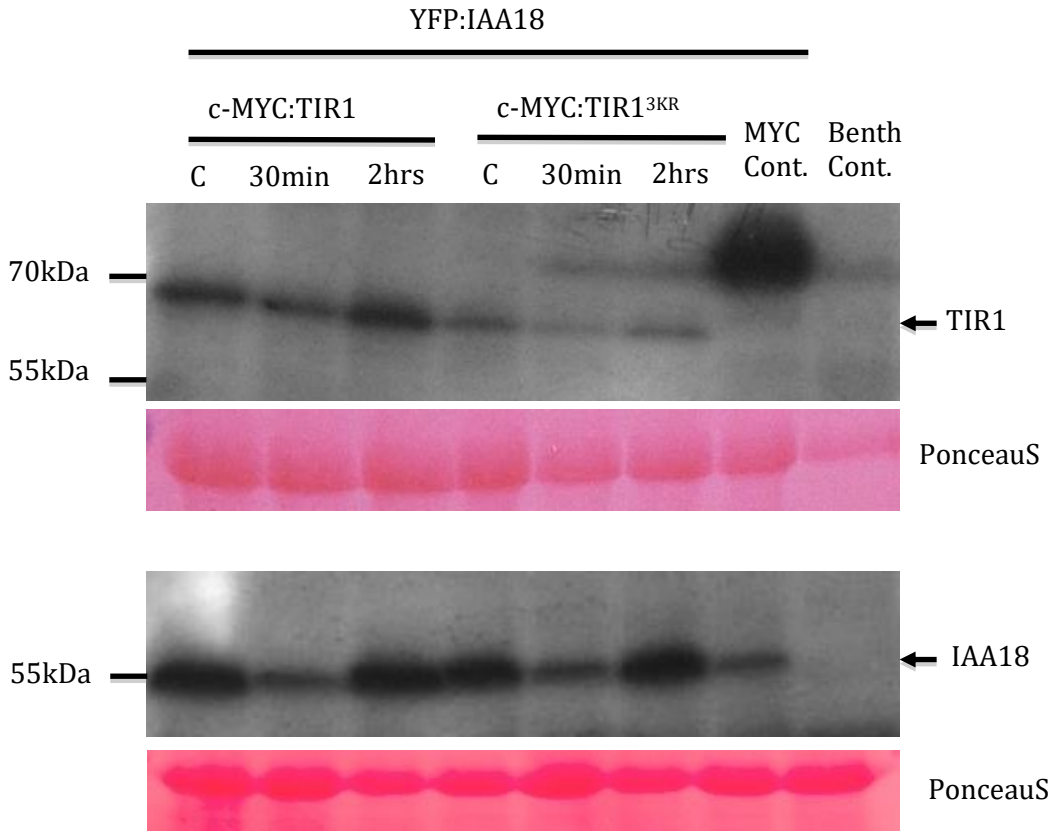

Western blot showing transient expression and stability of YFP:IAA18 after treatment with 1uM NAA. α-c-MYC IB (Top) and α-GFP IB (bottom) show recombinant c-MYC:TIR1, c-MYC:TIR1^{3KR} and a c-MYC control infiltrated with P19 suppressor protein and recombinant YFP:IAA18 in a 1:1:1 ratio. Bands corresponding to YFP:IAA18 can be seen in all lanes. 20ul of protein extract was loaded.

FIGURE 4.14| TIR1 DOES NOT INTERACT WITH OTS1 IN TRANSIENT ASSAY

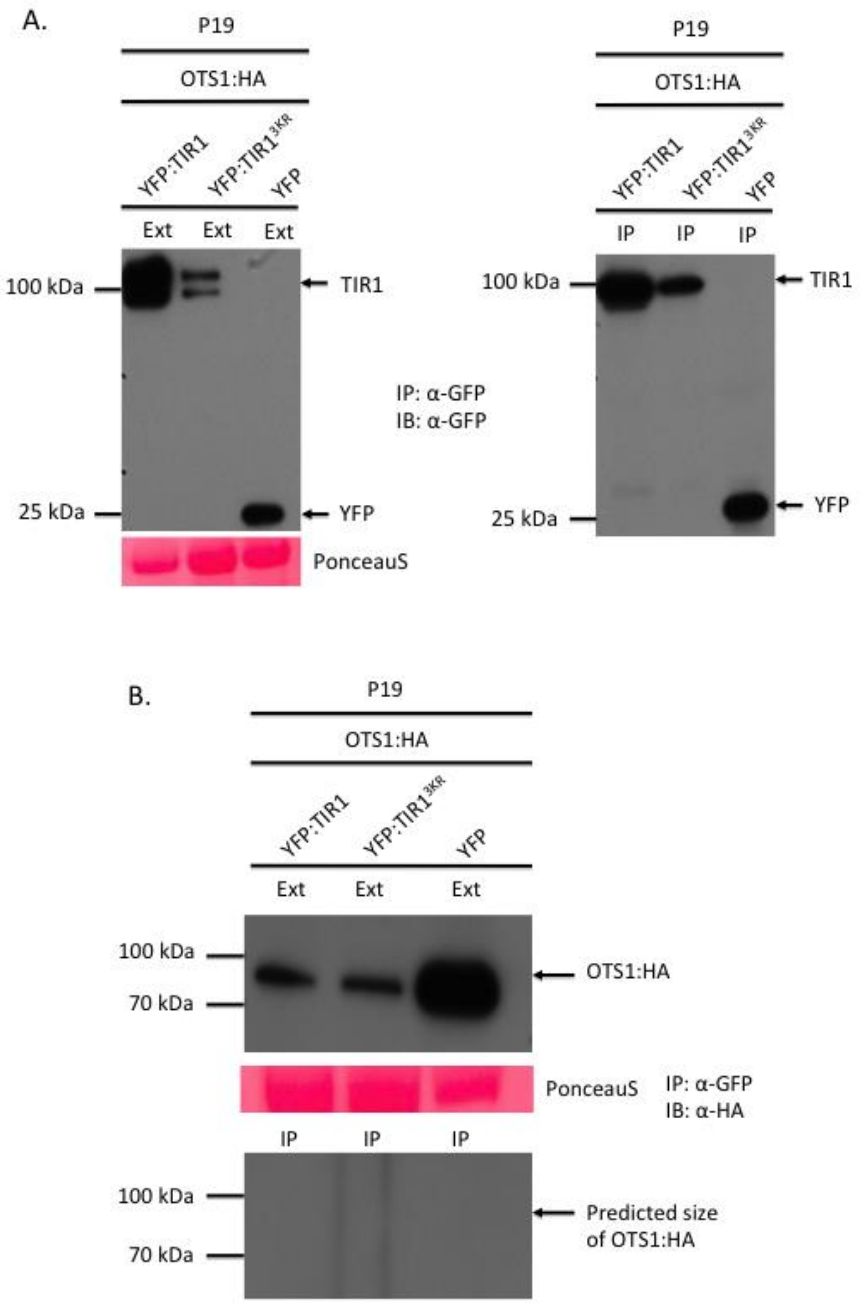

A. *Western blot showing α-GFP IP and α-GFP IB of recombinant YFP:TIR1^{3KR}, YFP:TIR1 and a YFP control infiltrated with P19 suppressor protein and recombinant OTS1:HA in a 1:1:1 ratio. Bands can be seen in all lanes, showing successful immunoprecipitation of YFP:TIR1^{3KR}, YFP:TIR1 and the YFP control. 20ul of IP was loaded.*

B. *Western blot showing α-GFP IP and α-HA IB of recombinant YFP:TIR1^{3KR}, YFP:TIR1 and YFP control infiltrated with P19 suppressor protein and recombinant OTS1:HA. No bands corresponding to OTS1:HA can be seen when probed with α-HA. 20ul of IP was loaded.*

4.4 SIM of TIR1

Aside from conjugation through its C-terminal di-glycine motif, SUMO is also able to interact with and influence the function of target proteins in a non-covalent manner via SUMO-Interacting Motifs (SIMs) (Hecker, et al., 2006). Previous work by Conti, *et al.* (2014), identified potential *Arabidopsis* SIM sites using peptide arrays, which were then used to educate the HyperSUMO programme created by Dr. Stuart Nelis (Nelis, 2014). Using the HyperSUMO programme, several potential SIM sites were identified in the TIR1/AFB protein family (fig. 4.15).

To investigate the potential role of non-covalent SUMO interaction in the auxin signalling cascade, a CO-IP of transiently expressed YFP:TIR1 with SUMO1:HA was performed (fig. 4.17). A western blot probed with α-HA monoclonal antibodies showed there was no non-covalent interaction between YFP:TIR1 and SUMO1 (fig. 4.16). Therefore, it can be concluded that TIR1 does not possess a functioning SIM.

FIGURE 4.15| SIM SITE PREDICTION FOR THE TIR1/AFB FAMILY

A.

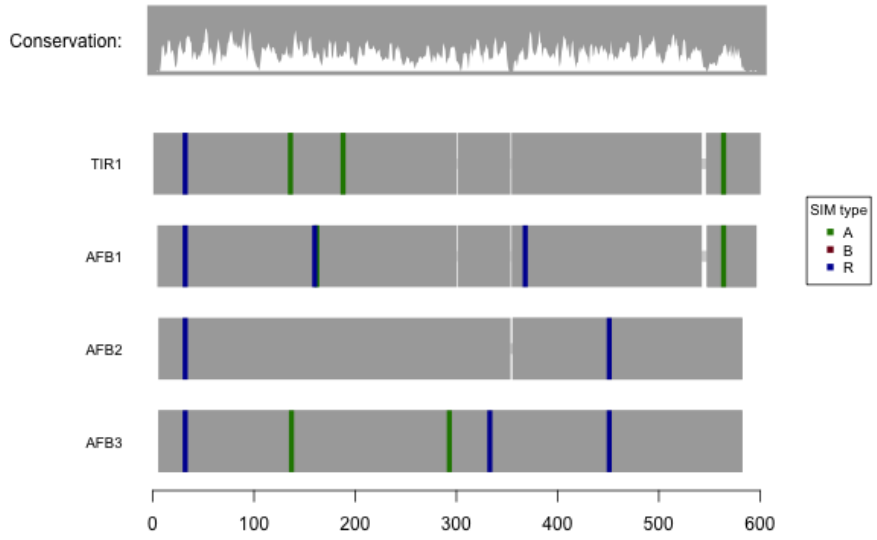

B.

Protein	Position	Type	Confidence	Sequence
TIR1	132 to 144	A	94	FK**VLVL**SSCEGFS
TIR1	184 to 196	A	98	TS**LVSL**NISCLAS
TIR1	554 to 566	A	93	ER**VFIY**RTVAGPR
AFB1	154 to 166	A	94	LR**VLEL**RECIVED
AFB1	549 to 561	A	92	ER**IYIY**RTVAGPR
AFB3	128 to 140	A	98	KS**LVLV**SCEGFTT
AFB3	284 to 296	A	99	QN**LISL**NLSYAAE
TIR1	23 to 35	R	92	LDKDRNS**VSLV**CK
AFB1	19 to 31	R	92	SNEDRNS**VSLV**CK
AFB1	147 to 159	R	87	IAATCRN**LRVL**EL
AFB1	353 to 365	R	87	IPLTEQG**LVFV**SK
AFB2	18 to 30	R	91	SHKDRNA**ISLV**CK
AFB2	435 to 447	R	93	SGLLTDQ**VFLY**IG
AFB3	18 to 30	R	93	SHKDRNS**ISLV**CK
AFB3	319 to 331	R	88	DSIGDKG**LAVV**AA
AFB3	437 to 449	R	93	SGLLTDQ**VFLY**IG

A. *Schematic showing the highly predicted (85%+) SUMO INTERACTION MOTIFs (SIMs) in the Auxin-Responsive F-box family of proteins. The predicted SIMs located within this protein family differ between members.*

B. *A table showing the location, type, percentage prediction and sequence of the predicted SIMs in the Auxin-Responsive F-Box Family of proteins.*

FIGURE 4.16| NO SIM SITE BINDING IS OBSERVED FOR TIR1 UNDER TRANSIENT ASSAY CONDITIONS

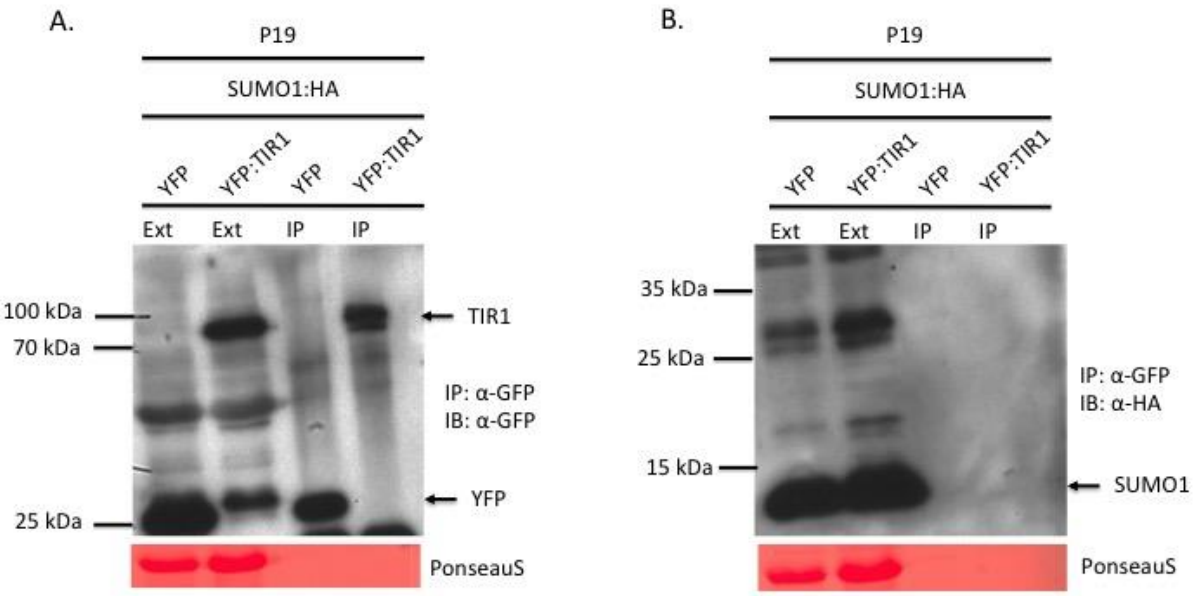

A. *Western blot showing α-GFP IP and α-GFP IB of recombinant YFP:TIR1 and a YFP control infiltrated with P19 suppressor protein and recombinant SUMO1:HA in a 1:1 ratio. Bands can be seen in all lanes, showing successful immunoprecipitation of YFP:TIR1 and the YFP control. 20ul of IP was loaded.*

B. *Western blot showing α-GFP IP and α-HA IB of recombinant YFP:TIR1 and YFP control infiltrated with P19 suppressor protein and recombinant SUMO1:HA. No bands corresponding to SUMO1:HA can be seen in the IP lanes when probed with α-HA. 20ul of IP was loaded.*

4.6 Discussion

Analysis of the protein sequences of the F-box auxin receptor family of proteins by the programme HyperSUMO revealed the presence of several SUMO sites for each member. Despite the relatively high level of protein sequence conservation between the members of this protein family (fig. 4.1), there was little in the way of similarity in the location and motif of the predicted SUMO binding sites; of the four proteins, only the C-terminal Type II SUMO-binding sites of AFB1 and AFB2, and the N-terminal Type II SUMO binding sites of AFB2 and AFB3 were conserved. And of this, only the latter showed any form of binding motif similarity between sites. This difference in predicted SUMO binding suggests that despite their relative redundancy in terms of auxin perception, SUMOylation plays a very different role for each protein.

Further bioinformatic analysis revealed the conservation of one of the predicted SUMO binding sites amongst inter-species homologues of the *At*TIR1 auxin receptor protein (fig. 4.2). The predicted K485 SUMO binding site was identified in all homologues, ranging from closely related dicots such as *B. rapa* (Tiffin & Hahn, 2002) to commercially important monocot species such as *O. sativa*. The high level of conservation amongst the TIR1 homologues indicated that of all auxin receptor F-box family members, TIR1 was perhaps the most promising candidate to help elucidate the role SUMOylation plays in auxin signalling.

Consequently, transient expression of TIR1 was used to confirm the presence of covalently bound SUMO moieties to the protein. The band shift observed indicates that TIR1 is decorated with many SUMO proteins, suggesting that all three predicted sites are utilised in the binding of either a single moiety or a poly-SUMO chain (Vertegaal, 2010). Whether SUMO binding at these separate sites confers different functions to the TIR1 protein, such as the SUMO site dependent effects on localisation and stability demonstrated for mammalian POLY(A)-POLYMERASE (PAP) (Vethantham, et al., 2008), remains to be seen. Further phenotyping work using the generated single and double TIR1 SUMO site mutants (fig. 4.8) dipped into an *Arabidopsis* line of appropriate background, such as the auxin signalling triple mutant *tir1 afb2 afb3*, would allow the function of each of these sites to be determined fully.

Having established that TIR1 undergoes SUMOylation *in planta*, the generation of a mutant form of the protein with all three SUMO sites rendered impotent through the substitution of the active lysine with arginine was undertaken. Transient expression of this mutant, the $TIR1^{3KR}$, further confirmed the location of SUMO binding (as predicted by HyperSUMO) through the complete loss of SUMOylation of the protein. This un-SUMOylatable form of TIR1 was shown to be less stable, with less protein observed under control conditions and after exogenous auxin treatment. The decrease in recombinant protein level observed for the mutant suggests that SUMO is essential in the regulation of TIR1 stability, and therefore auxin signalling.

SUMO plays a large role in the response to both endogenous and external stresses, such as genotoxic shock and heat stress (Enserink, 2015). During times of stress, SUMO proteases, such as ESD4, OTS1 and OTS2, cleave SUMO moieties from their target proteins, resulting in a significant change in transcriptional regulation within the plant (Park, et al., 2011). One of the ways this change in transcriptional regulation occurs is through ubiquitin-SUMO pathway crosstalk. In plants subject to heat shock, the ubiquitination of SUMO-conjugated proteins was found to dramatically increase (Millera, et al., 2010). It is therefore possible, that the removal of SUMO from TIR1 induces ubiquitation of the protein, leading to an increase in TIR1 turnover, thus reducing the pool of readily available TIR1 within the cell. This hypothetical mechanism allows the plant to quickly and efficiently control auxin-mediated growth under stress conditions through an auxin-independent manner.

The data obtained from transient assay regarding the interaction of the non-SUMOylatable form of $TIR1^{3KR}$ with a number of its binding partners lends credence to the theory that the SUMOylation of TIR1 affects auxin signalling through maintenance of receptor stability only. No difference in interaction was observed between either from of TIR1 and ASK1 (fig. 4.12) or IAA18 (fig 4.13). This suggests that SUMO does not affect the assembly of the SCF E3 ligase complex, of which ASK1 is an integral component, or the binding and subsequent degradation of the AUX/IAA transcriptional inhibitors, such as IAA18. This assumption, however, is to be taken with a pinch of salt, as the rest of the SCF complex proteins (CUL1 and RBX1) along with other members of the AUX/IAA family have not been tested. It is possible that the SUMOylation status of TIR1 may affect the binding of these other, untested proteins.

However, due to the inherent flaws of transient expression, the data presented in this chapter may not be an entirely accurate representation of what occurs *in vivo*. Further work involving the transgenic *Arabidopsis* lines expressing c-MYC-tagged TIR1 and TIR1^{3KR} will be used to confirm both the SUMOylation status of TIR1 and the role that status plays within the plant root.

4.7 Conclusion

In this chapter, a possible process through which the increased auxin sensitivity observed in the hyper-SUMOylated *Arabidopsis* SUMO protease mutant, *ots1 ots2*, (see, Chapter 3) is achieved has been shown.

Transient assay results in *N. benthamiana* indicate that an integral part of the auxin signalling machinery, the auxin receptor TIR1, undergoes SUMOylation *in planta* (see, fig. 4.5/4.9). Subsequent removal of the predicted SUMO binding sites of TIR1 has been shown to affect the stability of the receptor (fig. 4.10). It is therefore possible to conclude that the addition of SUMO moieties to TIR1 stabilises it, consequently resulting in increased auxin signalling within the plant. This conclusion is borne out in the increased sensitivity to exogenous auxin observed in the *ots1 ots2* mutant line, where the levels of SUMO-conjugated proteins are far higher than those observed in wild type plants (Conti, et al., 2008).

5. The Role of SUMOylation in the Downstream Components of the Auxin Signalling Cascade

5.1 Introduction

The results presented in chapter 4 suggest that SUMO plays a role in auxin signalling through modification of the auxin receptor E3 ligase TIR1.

However, TIR1 may not be the only target for SUMOylation within this pathway. It is not unusual for several proteins within a pathway to become modified, either simultaneously or sequentially, by posttranslational modifiers such as SUMO. For example, many of the proteins involved in double-stranded DNA break repair undergo rapid SUMOylation, with the SUMO moieties stabilising the physical interactions necessary to successfully repair the break (Psakhye & Jentsch, 2012). It is therefore possible that other auxin signalling components downstream of TIR1 are also subject to modification by SUMO, allowing the plant to be able to more finely tune its response to environmental stress.

In this chapter, the SUMOylation status of the rest of the auxin signalling cascade machinery, the AUX/IAA and ARF protein families, is investigated. The transcriptional response to auxin in a hyper-SUMOylated environment is also studied in this chapter, allowing for further confirmation of the role SUMO plays in the auxin perception and signalling.

5.2 The AUX/IAA Repressor Proteins Do Not Undergo SUMOylation in Transient Assay

The AUX/IAA family of repressor proteins are an integral part of the auxin signalling machinery. The SUMOylation of these proteins, alongside TIR1, may also play a role in the regulation of the auxin response. SUMOylation of AUX/IAA proteins may interfere with their stability and rate of turnover, therefore modulating auxin responsive gene expression in a SUMO-dependent manner entirely independent to TIR1.

To investigate this hypothesis, the protein sequences of the AUX/IAA repressor proteins were scanned for potential SUMO binding sites using the bioinformatics software, HyperSUMO (Nelis, 2014), as shown in fig. 5.1. A large number of potential SUMO binding sites were identified by the software, with several of the more closely related AUX/IAA proteins containing two predicted SUMO binding sites located at the C-terminal end.

Given the prohibitively large number of AUX/IAA proteins and their relative functional redundancy within the auxin signalling pathway, a full investigation of the SUMOylation status of AUX/IAA family was not conducted. Instead, four AUX/IAA proteins shown to be involved in the formation of lateral roots (Marchant, et al., 2002; Goh, et al., 2012; Uehara, et al., 2008) were selected: IAA2 (AT3G23030), IAA3 (AT1G04240), IAA14 (AT4G14550) and IAA18 (AT1G51950). These AUX/IAA proteins were successfully amplified using the proofreading DNA polymerase Q5 (NEB) from cDNA generated from 7 day old Col-0 seedlings (fig. 5.2) (see, Methods 3.3.1&3.3.7/8). The PCR product was purified using a Zymoclean™ Gel DNA Recovery Kit (Zymo) and cloned into the entry vector pENTR/D-TOPO. The constructs were transformed into *E. coli* DH5α and the colonies screened for successful clones by PCR using AttB primers. Two clones for each construct were selected for plasmid purification followed by in-house sequencing via DBS Genomics. Constructs containing the correct gene sequence were digested with MluI (NEB) and transferred via recombination into the 35S, N-terminal GFP-tag Gateway® destination vector pEARLYGATE104 (see, Methods 3.3.4 & 3.3.5). Confirmed IAA2, IAA3, IAA14 and IAA18 clones in pEARLYGATE104, identified via colony PCR with AttB primers, were transformed into the *Agrobacterium* strain GV3101 ready for transient expression (see, Methods 3.2.3).

Transient assays in *N. benthamiana* using 35S:YFP:IAA3 and 35S:YFP:IAA18 were conducted to confirm the SUMOylation status of IAA3 and IAA18 (see, Methods 3.4). YFP:IAA3 and YFP:IAA18 transient expression was confirmed by western blotting with α-GFP monoclonal antibodies (Clonetech). Specific bands corresponding to YFP:IAA3 and YFP:IAA18 were observed in both the extract and IP sample lanes (fig. 5.3). The SUMOylation status of the YFP:IAA3 and YFP:IAA18 constructs was confirmed via western blotting with α-HA antibodies (Sigma). No bands were observed in the lanes corresponding to YFP:IAA3 and YFP:IAA18, indicating that neither of these AUX/IAA proteins is SUMOylated *in planta*. However, in the total protein extracts obtained from transient expression, there is a dramatic reduction in free SUMO observed in those co-expressing recombinant AUX/IAA proteins. This may be due to an increased turnover rate of SUMO-tagged AUX/IAA proteins, with the addition of a SUMO moiety dramatically reducing the stability of the repressors.

In light of this, the SUMOylation status of a stabilised (through the mutation of the DII degron domain) IAA28 construct (obtained from Teva Vernoux, ENS de Lyons) was also investigated. YFP:IAA28 transient expression was confirmed by western blotting with α-GFP antibodies (Clonetech). A specific band corresponding to YFP:IAA28 was observed in the IP sample lane. The SUMOylation status of the YFP:IAA28 construct was confirmed via western blotting with α-HA monoclonal antibodies (Sigma). No band was observed, indicating that IAA28 is not SUMOylated *in planta* (fig. 5.4).

FIGURE 5.1| SUMO SITE PREDICTION FOR THE AUX/IAA REPRESSOR FAMILY

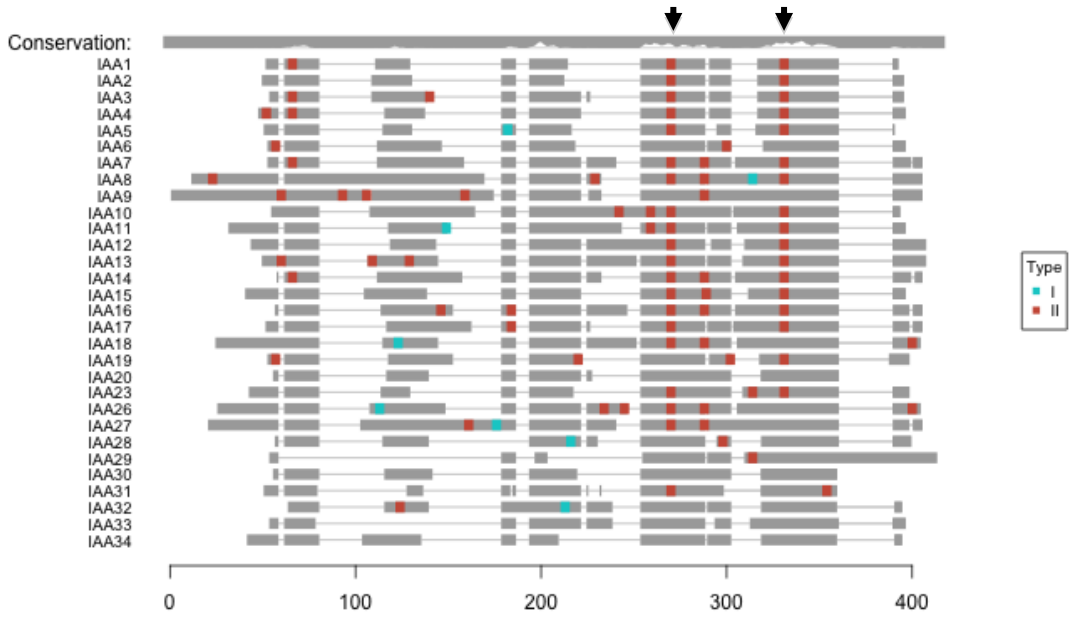

A schematic showing the highly predicted (85%+) SUMOylation sites in the AUX/IAA repressor family of proteins. Many of the AUX/IAA proteins show two highly conserved SUMOylation sites at the C-terminal end, as indicated by the two black arrows.

FIGURE 5.2| CLONING OF THE AUX/IAA PROTEINS IAA2, IAA3, IAA14 AND IAA18

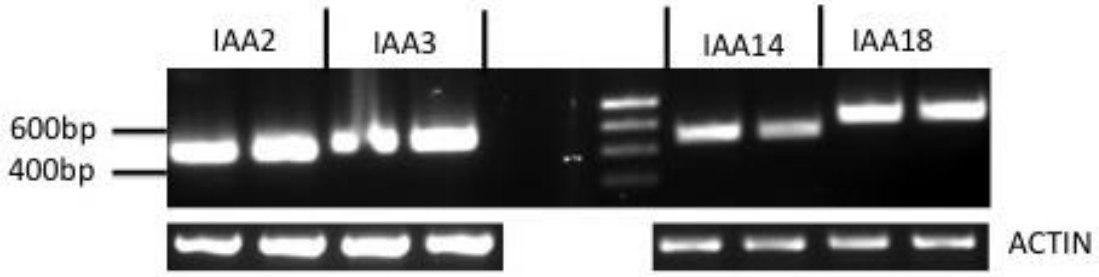

Gel image showing the cloning of IAA2 (AT3G23030), IAA3 (AT1G04240), IAA14 (AT4G14550) and IAA18 (AT1G51950). Genes were cloned from Col-0 cDNA extracted from 7-day old seedlings The PCR was conducted with the proof-reading polymerase Q5 (New England Biolabs) supplemented with 0.3% DMSO, and was run for 30 cycles.

FIGURE 5.3| THE AUX/IAA PROTEINS IAA3 AND IAA18 ARE NOT SUMOYLATED UNDER TRANSIENT ASSAY CONDITIONS

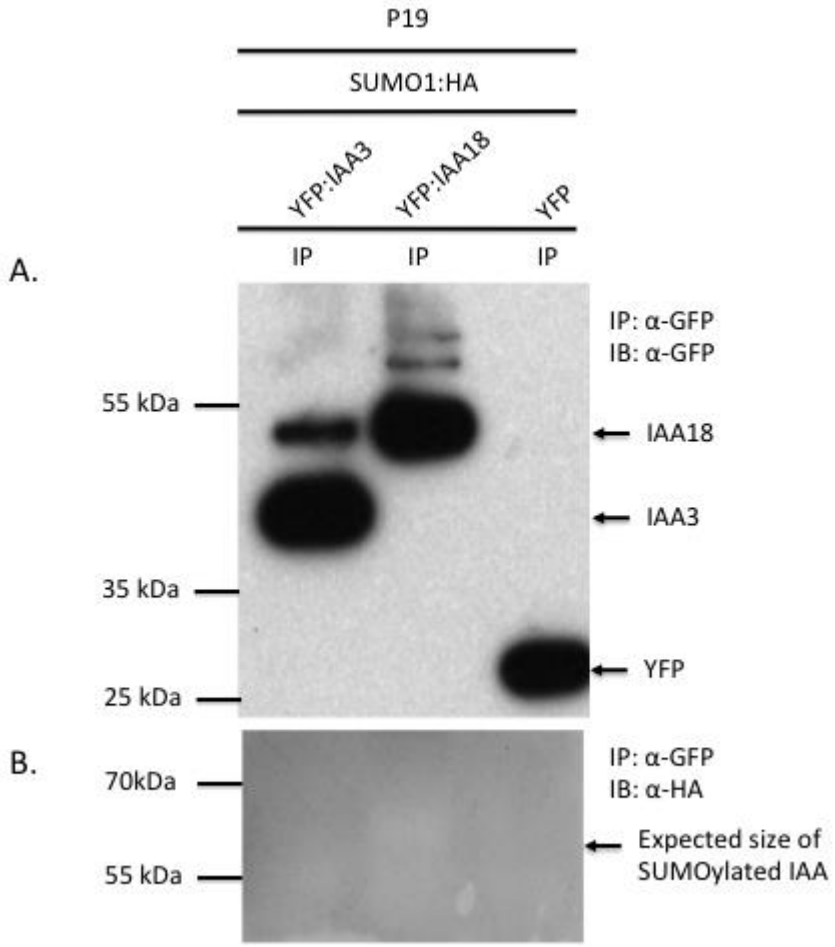

A. *Western blot showing α-GFP IP and α-GFP IB of recombinant YFP:IAA3, YFP:IAA18 and a YFP control infiltrated with P19 suppressor protein and recombinant SUMO1:HA in a 1:1:3 ratio. Bands can be seen in all lanes, showing successful immunoprecipitation of YFP:IAA3, YFP:IAA18 and the YFP control. 15ul of IP was loaded.*

B. *Western blot showing α-GFP IP and α-HA IB of recombinant YFP:IAA3, YFP:IAA18 and YFP control infiltrated with P19 suppressor protein and recombinant SUMO1:HA. No bands can be seen in any of the lanes, indicating that both YFP:IAA3 and YFP:IAA18 are not SUMOylated under transient assay conditions. 20ul of IP was loaded.*

FIGURE 5.4| STABILISED IAA28 IS NOT SUMOYLATED UNDER TRANSIENT ASSAY CONDITIONS

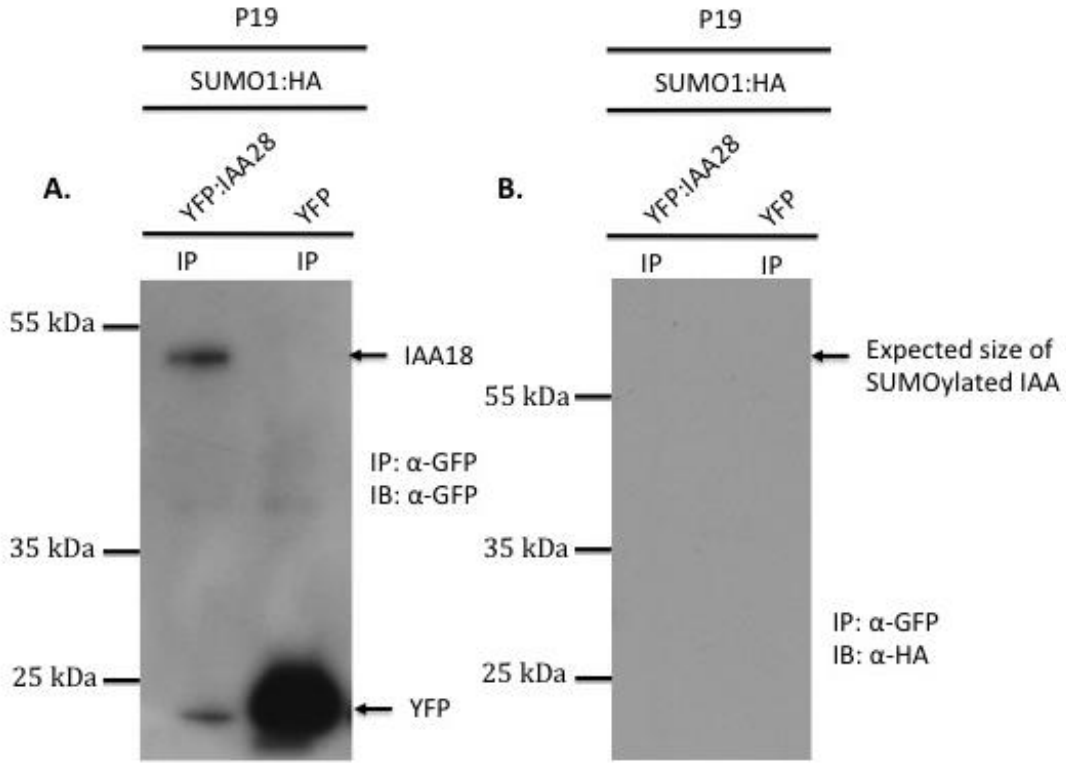

A. *Western blot showing α-GFP IP and α-GFP IB of recombinant YFP:IAA28 plus a GFP control infiltrated with P19 suppressor protein and recombinant SUMO1:HA in a 1:1:3 ratio. Bands can be seen in both lanes, showing expression and successful immunoprecipitation of YFP:IAA28 and the GFP control. 20ul of IP was loaded.*

B. *Western blot showing α-GFP IP and α-HA IB of recombinant YFP:IAA28 and GFP control infiltrated with P19 suppressor protein and recombinant SUMO1:HA. No bands can be seen, indicating that YFP:IAA28 is not SUMOylated. 20ul of IP was loaded.*

5.3 The Activating ARF Transcription Factors, ARF7 and ARF19, Undergo SUMOylation in Transient Assay

The Auxin Response Factors ARF7 and ARF19 have been shown to play a large role in the regulation of lateral root formation in *Arabidopsis thaliana* (Okushima, *et al.* 2007). The lateral root phenotype observed in the *ots1 ots2* double mutants (see, Chapter 3. 3) suggests that SUMO may also play a role in lateral root regulation, potentially through the SUMOylation of previously identified regulatory proteins, such as ARF7 and ARF19.

To investigate this hypothesis, the protein sequences of the activating ARFs (ARF5 (AT1G119850), ARF6 (AT1G30330), ARF7 (AT5G20730), ARF8 (AT5G37020) and AF19 (AT1G19220)) were scanned for potential SUMO sites using the bioinformatics software HyperSUMO (Nelis, 2014). In ARF7 and ARF19, two homologous SUMO binding sites were identified in each protein sequence (fig. 5.5). The first of these binding sites, residue K103 in ARF7 and residue K104 in ARF19, is located in the DNA binding region of the ARF proteins, making it a promising candidate for further investigation.

Transient assays in *N. benthamiana* using 35S:ARF7:4xMYC and 35S:ARF19:GFP constructs (obtained from Professor Malcolm Bennett, Nottingham University) were conducted to confirm the SUMOylation status of ARF7 and ARF19 (see, Methods 3.4). ARF7 and ARF19 transient expression was confirmed by western blotting with α-c-MYC (Sigma) and α-GFP (Clonetech) monoclonal antibodies, respectively. Specific bands corresponding to ARF7:MYC and ARF19:GFP were observed in both the extract and IP sample lanes (fig. 5.6 & 5.7). The SUMOylation status of both constructs was confirmed via western blotting with α-SUMO1 antibodies (Abcam).

The transient expression data shows that ARF7 is SUMOylated *in planta* (fig. 5.6). The level of SUMOylated ARF7 is very low, as can be seen from the faint band observed in the IP lane, despite 150ul of concentrated protein run. The same low level of SUMOylation was also observed for ARF19 (fig. 5.7). It is possible that these proteins are more highly SUMOylated in *Arabidopsis* root tissue compared to transient expression in leaves. This could be due to the spatiotemporal expression of ARFs and associated SUMOylation machinery.

DELLA proteins negatively regulate gibberellin (GA) signalling, resulting in reduced growth (Hussain & Peng, 2003). The binding of GA to its receptor (GID1) causes degradation of these proteins by the UPS (Eckardt, 2006), with recent work (Conti, et al., 2014) showing that SUMOylation of one of the DELLAs, RGA, halts this process. Recently, GA signalling has been shown to play an important role in lateral root formation through GA-Auxin cross-talk (Farquharson, 2010). Studies in transgenic Poplar have confirmed the inhibitory role of GA in lateral root development, suggesting that GA signalling is involved in root remodelling in response to stress (Goua, et al., 2010).

To investigate the role of DELLAs, a protein complex immunoprecipitation (CO-IP) with two DELLAs, GAI:HA and RGA:HA, and ARF19:GFP was performed (see, Methods 3.4.6). The transient expression data shows that RGA:HA and ARF19:GFP interact *in vivo* (fig. 5.8). The CO-IP data combined with the lateral root assay data (see, chapter 3.3) suggests a role for DELLA proteins in lateral root formation. It is currently unclear from the CO-IP data as to whether GAI:HA and ARF19:GFP interact due to dark smearing on the western blot.

FIGURE 5.5| PREDICTED SUMOYLATION SITES IN THE ACTIVATING ARFS

A.

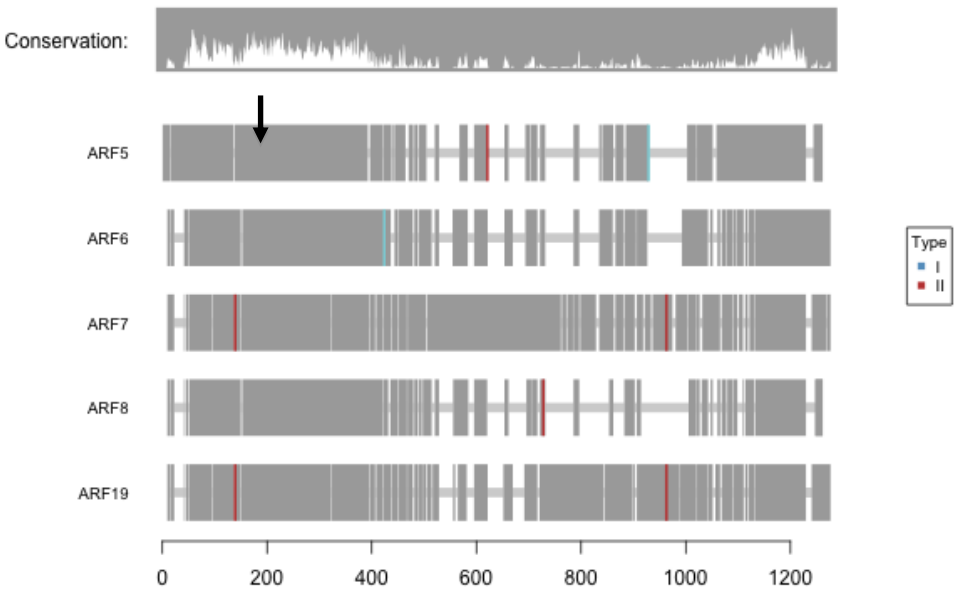

B.

Protein	Position	Type	Confidence	Sequence
ARF5	K665	I	99	GLKFDQ
ARF6	K390	I	99	GLKEDD
ARF5	K531	II	100	PAKPEN
ARF7	K104	II	96	VNKYDR
ARF7	K889	II	98	YSKSDM
ARF8	K561	II	97	FMKSDF
ARF19	K103	II	96	VNKYDR
ARF19	K800	II	100	YTKTES

A. *Schematic showing the highly predicted (85%+) SUMOylation sites in the ARF family of auxin-responsive transcription factors. Both ARF7 and ARF19 contain a SUMOylation site located within the DNA-binding region of the protein (indicated by arrowhead), which may play a vital role in SUMO-dependent regulation of the transcription of auxin responsive genes.*

B. *A table showing the location, type, percentage prediction and sequence of the predicted SUMO sites in the activating ARFs.*

FIGURE 5.6| ARF7:MYC IS SUMOYLATED IN TRANSIENT ASSAY

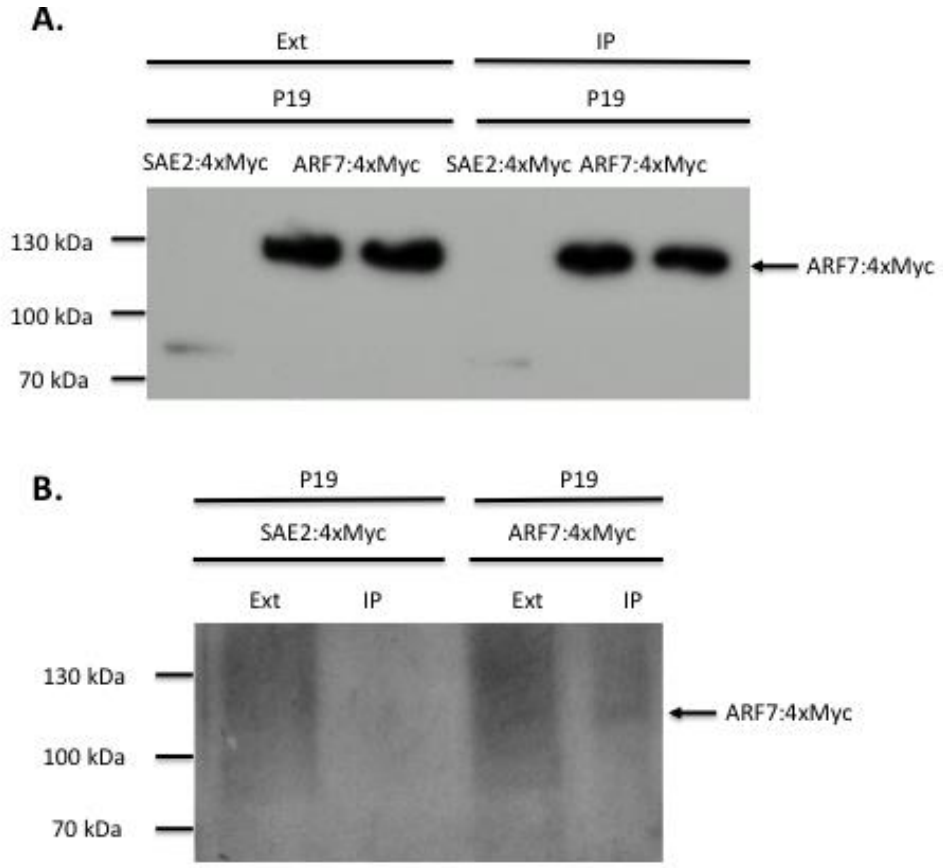

A. *Western blot showing α-c-MYC IP and α-c-MYC IB of recombinant ARF7:MYC plus a MYC-tagged control (SAE2) infiltrated with P19 suppressor protein in a 1:1 ratio. Bands can be seen in all lanes, showing expression and successful immunoprecipitation of ARF7:MYC and the MYC:SAE2 control. 25ul of extract and 10ul of IP was loaded.*

B. *Western blot showing α-c-MYC IP and α-SUMO IB of recombinant ARF7:MYC and MYC:SAE2 control. A faint band can be seen in the IP lane of ARF7:MYC, indicating SUMOylation of ARF7. 50ul of extract and 150ul of IP was loaded.*

FIGURE 5.7| ARF19:GFP IS SUMOYLATED IN TRANSIENT ASSAY

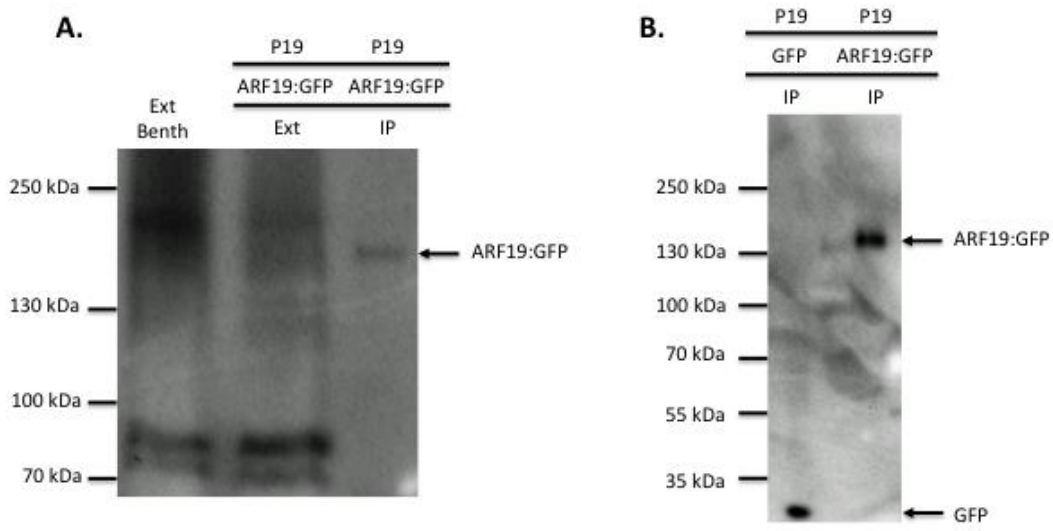

A. *Western blot showing α-GFP IP and α-SUMO IB of recombinant ARF19:GFP plus GFP-only control infiltrated with P19 suppressor protein in a 1:1 ratio. .A faint band can be seen in the IP lane of ARF19:GFP, indicating SUMOylation of ARF19. 50ul of extract and 150ul of IP was loaded.*

B. *Western blot showing α-GFP IP and α-GFP IB of recombinant ARF19:GFP and GFP-only control. . Bands can be seen in all lanes, showing expression and successful immunoprecipitation of ARF19:GFP and the GFP-only control. 10ul of IP was loaded.*

FIGURE 5.8| ARF19:GFP POTENTIALLY INTERACTS WITH GAI:HA AND RGA:HA

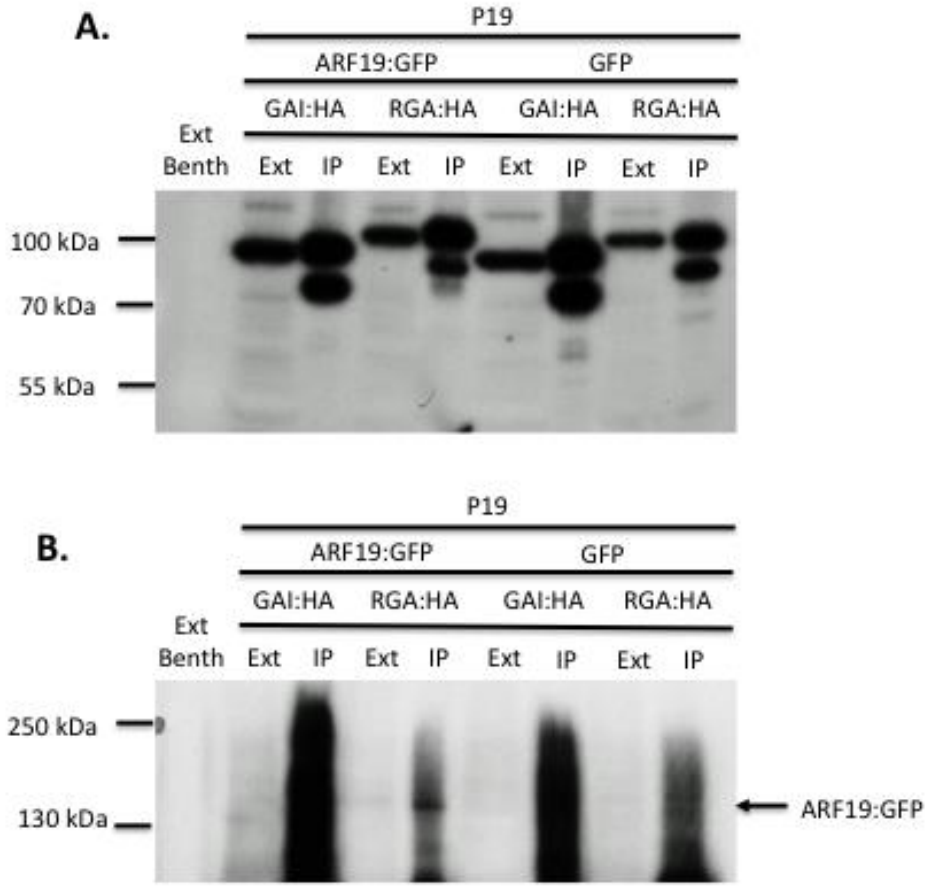

A. *Western blot showing α-HA IP and α-HA IB of recombinant DELLA proteins RGA:HA and GAI:HA infiltrated with either ARF19:GFP or GFP-only control and P19 suppressor protein in a 1:1:1 ratio. Bands can be seen in all lanes, showing expression and successful immunoprecipitation of RGA:HA and GAI:HA. 10ul of IP was loaded.*

B. *Western blot showing α-HA IP and α-GFP IB of recombinant DELLA proteins RGA:HA and GAI:HA to identify protein-protein interactions between RGA or GAI with ARF19:GFP. A band corresponding to ARF19:GFP can be seen in the IP lane of RGA:HA, indicating RGA-ARF19 interaction. No bad can be identified in the corresponding control lane. No bands can be identified in the GAI:HA IP lanes due to smearing. 50ul of extract and 30ul of IP was loaded.*

5.3 DR5:VENUS Signalling is Higher in the ots1 ots2 Background

In order to study the down-stream effects of SUMOylation on the auxin signalling machinery, plants containing the auxin-signalling marker, DR5::VENUS (Ulmasov, et al., 1997); Benková, et al., 2003), were crossed into the *ots1 ots2* mutant line (see, Methods 2.1.6). DR5::VENUS is a tool used to observe the effect of auxin-mediated transcription. It consists of a synthetic auxin-responsive promoter constructed of several repetitions of the auxin responsive element (AuxRE) motif, CCTTTTGTCTC (Mironova, et al., 2014). This promoter is used to drive the expression of the VENUS marker in an auxin-dependent fashion, allowing visualization of the auxin response *in vivo*.

Seeds from the siliques which developed from manually crossed flowers (DR5::VENUS male, *ots1 ots2* female), were collected and grown on soil under long day conditions. F1 hybrids for DR5::VENUS, *ots1* and *ots2* were determined by PCR of genomic DNA (see, Methods, 3.31 & 3.36). F1 hybrid seeds were then collected and grown on soil under long day conditions, with F2 plants homozygous for *ots1 ots2* and DR5::VENUS determined, again, by PCR (see, Appendix A.3). Seeds from the DR5::VENUS *ots1 ots2* triple mutant lines were collected and stored ready for further use.

In order to determine the effects of a hyper-SUMOylated environment upon auxin-mediated transcription, and therefore auxin signalling by proxy, 6-day-old seedlings containing the DR5::VENUS auxin reporter, either in the WT (Obtained from Malcolm Bennet, Nottingham University) or SUMO protease mutant (*ots1 ots2*) background, were subjected to treatment with 1uM IAA over a 24-hour period. At the 1 hour, 3 hour, 6 hour and 24 hour time points, the auxin-mediated transcriptional response of the WT and *ots1 ots2 Arabidopsis* lines was analysed using fluorescence microscopy.

Unsurprisingly, the levels of free VENUS observed in the auxin-treated *ots1 ots2* line seemed to be far higher than those observed in their WT counterpart (fig. 5.9). This indicates that increased levels of SUMO-conjugates within *Arabidopsis* may lead to in auxin signalling, and therefore sensitivity, further lending weight to the results observed in chapter 3; in a hyper-SUMOylated environment, auxin sensitivity is amplified. Very little VENUS was observed in both the treated and untreated WT controls. However, it is possible that this is due to silencing DR5 expression.

FIGURE 5.9| HIGHER LEVELS OF VENUS ARE OBSERVED AFTER AUXIN TREATMENT IN THE *OTS1 OTS2* BACKGROUND COMPARED TO WT

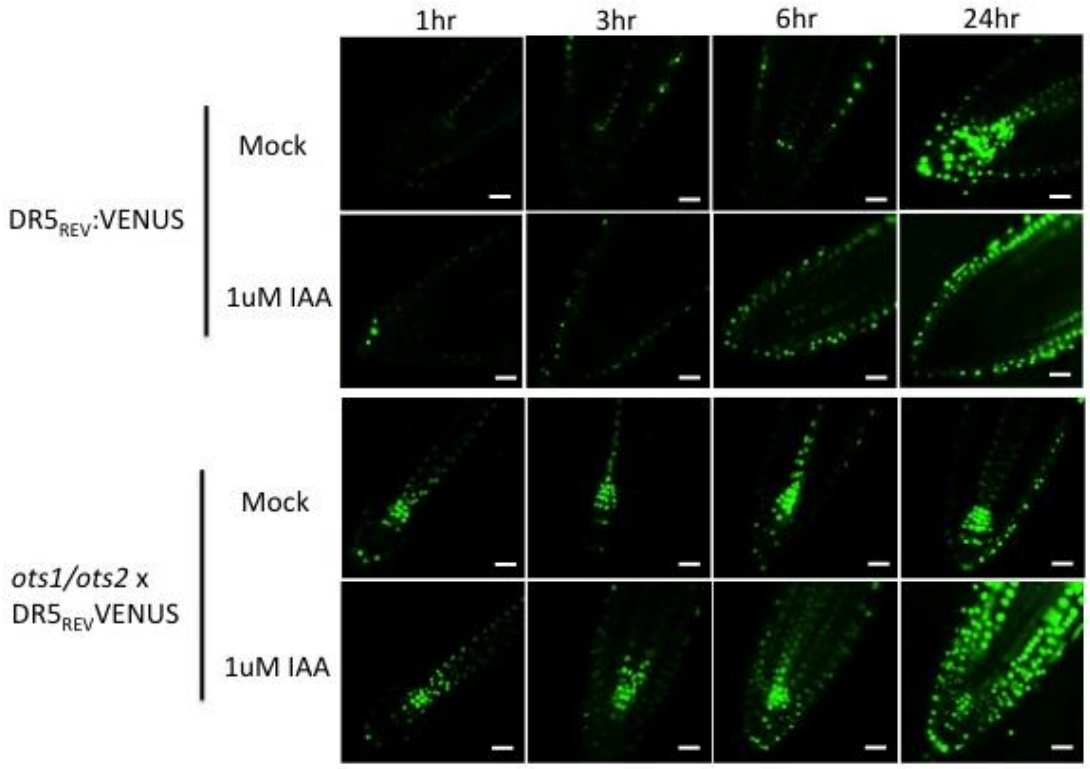

Roots of 7-day-old DR5::VENUS and DR5::VENUS x ots1 ots2 and seedlings at 60x magnification and excitation at λ488nm showing the difference in auxin transcriptional response upon exposure to IAA at selected time points. A higher transcriptional response is observed in the DR5::VENUS x ots1 ots2 line.

Seedlings were germinated on ½ MS plates with 0.8% phytoagar supplemented with 0.5% sucrose. The seedlings were germinated and grown under 24 hour light conditions for 7 days. The seedlings were then transferred to 20ml of liquid 1/2MS media, supplemented with 1uM IAA, and incubated under 24hr light conditions, with gentle shaking, for 1-24hrs. Scale bar = 20µm

5.4 Discussion

Sequence analysis of the AUX/IAA and ARF families of proteins via HyperSUMO revealed the presence of several potential SUMO binding sites within members of both families, lending credence to the hypothesis that several proteins involved in the auxin signalling cascade undergo SUMOylation.

In the first of these protein families, that of the AUX/IAA transcriptional repressors, several potential SUMO binding sites were identified (fig. 5.1). Indeed, only three of the 30 family members, IAA30/33/34, did not contain any predicted SUMO binding sites. Two potential SUMO binding sites, located towards the C-terminal end of the proteins, were conserved amongst over half of the AUX/IAA family. The high level of conservation of these sites amongst the AUX/IAAs merited further investigation, with several family members, particularly those involved in the growth and development of the lateral root primordia, selected for cloning.

However, despite the predictions of HyperSUMO with regards to SUMO binding, no SUMOylation was observed for the transiently expressed AUX/IAA proteins (fig. 5.3). Initially, it was thought that the lack of observed SUMOylation of the AUX/IAAs may have been due to the addition of SUMO inducing a reduction in protein stability. To test this theory, a non-degradable form of IAA28 was transiently expressed and probed for SUMO modification (fig. 5.4); no SUMOylation was observed for IAA28 in transient assay.

This is not to say, however, that no members of the AUX/IAA repressor protein family are SUMOylated. Though the family itself is large and fraught with functional redundancy between members, each of the AUX/IAAs do appear to play distinct roles within the plant. Indeed, though most members follow the same, four-domain structure, the different AUX/IAA proteins show variances in rate of turnover and spatiotemporal expression (Audran-Delalande, et al., 2012). It is possible that these differences also extend into the level of SUMO modification, perhaps with AUX/IAA proteins only undergoing SUMOylation under certain conditions or in certain tissues as part of a more complex network of regulation. Further work using *Arabidopsis* mutant lines expressing tagged AUX/IAA proteins under their own promoters would help tease out whether the AUX/IAAs are SUMOylated only in a spatiotemporal pattern or, indeed, not at all.

SUMO binding site analysis of the ARF family of transcription factors by HyperSUMO (fig. 5.5) indicated that several members of the activating ARF subfamily (ARF5/6/7/8/19) may undergo post-translational modification by SUMO. Of these ARFs, the two most promising candidates for SUMOylation were determined to be ARF7 and ARF19, both of which play an important role in the growth and development of the lateral root system in *Arabidopsis* (Okushima, et al., 2007). Two sites, one located at the N-terminus in the DNA binding region, and one at the C-terminus in the Q-rich region, were identified in ARF7 and ARF19.

Consequently, transient expression of both ARF7 and ARF19 was used to confirm the presence of covalently bound SUMO to the transcription factors (fig. 5.6 & 5.7). Unlike TIR1, little in the way of a band shift was observed for either protein when probed with α-SUMO1, indicating that relatively few SUMO moieties bind to the ARFs at any one time. Further work undertaken by Dr. Beatriz Orosa (Sadanandom lab, unpublished), has identified the location of main SUMO site for ARF7; mutation studies of ARF7 conducted by Dr. Orosa have shown that SUMOylation primarily occurs at the site located within the DNA binding region of ARF7. This leads to the hypothesis that SUMO is able to regulate the auxin responsive genes in a manner independent of auxin through alteration of the rate of ARF binding to gene promoter regions. Further work utilising a non-SUMOylatable form of ARF7 in a CHIP-seq assay (Donner, et al., 2009) would allow elucidation of the role SUMO plays in ARF transcription factor regulation.

Finally, the auxin-mediated transcriptional response of the *ots1 ots2* mutant line was investigated. The DR5::VENUS construct, a proxy for the transcriptional auxin response, was introduced into the *ots1 ots2* mutant line via crossing. Upon treatment of the DR5::VENUS *ots1 ots2* seedlings with the auxinic compound IAA, an increase in free VENUS was observed in comparison to WT, thereby indicating an increase in auxin-mediated transcription within the mutant line. The increase in free VENUS observed is consistent with the data presented in chapter 3 regarding the apparent increase in auxin response in a hyper-SUMOylated environment, such as that of the *ots1 ots2* mutant.

However, caution must be exercised when interpreting these results. It is possible, due to the relatively meagre auxin response seen in the WT, that the DR5::VENUS construct is undergoing silencing, thereby accounting for the observed difference in free VENUS between the WT and *ots1 ots2* seedlings. To confirm whether this is the case, additional experiments must be conducted; direct measurement of the transcript levels of auxin-responsive genes in response to IAA stimulus through qPCR would confirm the validity of the imaging results obtained.

5.5 Conclusion

In this chapter, another possible process through which the increased auxin sensitivity observed in the hyper-SUMOylated *Arabidopsis* SUMO protease mutant, *ots1 ots2*, (see, Chapter 3) is achieved has been shown.

The increase in auxin sensitivity observed in chapter 3 was further confirmed via the use of the auxin-mediated transcriptional response proxy DR5::VENUS; upon stimulation of the auxin signalling pathway by the auxin IAA, a dramatic increase in the transcriptional response is observed in the *ots1 ots2* background in comparison to WT.

Transient assay results in *N. benthamiana* indicate that two integral parts of the auxin signalling machinery, the auxin response factors ARF7 and ARF19, undergo SUMOylation *in planta* (see, fig. 5.6/5.7). It possible that the addition of SUMO moieties to the ARF transcription factors affect transduction of the auxin signal, potentially through changes in promoter binding, consequently resulting in increased auxin signalling within the plant. Experimental data obtained via a DR5::VENUS proxy regarding the level of auxin-mediated transcription within the *ots1 ots2* mutant line has indicated that auxin-induced transcription is increased in the mutant, consistent with the data obtained in chapter 3.

No SUMOylation of the auxin repressors, the AUX/IAAs, was observed under transient assay conditions.

6. Final Discussion

The results presented in chapters 3, 4 and 5 underline the possible significance of SUMOylation in auxin signalling. Previous research regarding the SUMO E3 ligases SIZ1 and HPY2 has inferred a connection between protein SUMOylation and auxin signalling through the observed alteration of auxin-mediated processes, such as cell proliferation in the root apical meristem (Huang, et al., 2009). Here, that connection has been further strengthened through phenotypic analysis of the SUMO protease double knock out mutant line, *ots1 ots2*, and the identification of several SUMOylated proteins involved in the auxin signalling cascade.

6.1 SUMO and the Regulation of Root Architecture

Results in chapter 3 indicated that *ots1 ots2* double mutants differ significantly in root architecture and the response to hormonal and environmental stimuli in comparison to WT. Under control conditions, the *ots1 ots2* mutant line displayed differences in lateral root production and in root hair growth and production (see, chapters 3.3 & 3.4). Upon the introduction of the mutant line to various external stimuli, such as the application of exogenous auxinic compounds or exposure to dramatic changes in water potential, further differences between the WT and the *ots1 ots2* line were observed; these included the dramatic reduction of the primary root, an increase in lateral root emergence and a highly positive hydrotropic response (see, chapters 3.2, 3.3 & 3.5). These differences were attributed to a number of different causes, such as increased auxin sensitivity and alterations to the primary root cap.

6.1.1 Auxin Signalling and Sensitivity

Results presented in chapter 3 indicated that SUMO plays an important role in the mediation of auxin signalling within *Arabidopsis*; the increase in SUMO conjugates accumulated within the *ots1 ots2* mutant line appeared to lead to a significant increase in sensitivity to the phytohormone auxin. The long root hairs produced by the mutant line were indicative of alterations in auxin homeostasis. Taken alongside the data generated regarding primary root length and lateral root emergence upon exposure to exogenous auxin stimulus, it was determined that a reduction in de-conjugation of SUMOylated proteins, and therefore an increase in the level of SUMO-conjugates present within the plant, had a significant influence on auxin signalling and its related responses.

Previous research regarding the two identified SUMO E3 ligases, SIZ1 and HPY2, by Catala, et al. (2007), Miura, et al. (2005; 2007), Ishida, et al. (2009) and Huang, et al. (2009) (see, Introduction, 1.2.3) has led to the hypothesis that SUMO is a key player in the regulation of the auxin response. SIZ1 and HPY2 are differentially expressed within the plant; with regards to roots, accumulation of SIZ1 is observed in both primary and lateral root tissue, whilst HPY2 is preferentially expressed in the tissues that form the root apical meristem. Knock out mutant lines of these genes display distinct auxin-related phenotypes (Catala, et al., 2007), therefore demonstrating that a reduction in SUMO-conjugates leads to an alteration the auxin response. This data is consistent with that reported in chapter 3, lending significant credence to the theory that SUMO plays a key role in auxin signalling.

However, this explanation may be somewhat simplistic. Though it is tempting to attribute all observed morphological changes of the *ots1 ots2* root architecture in comparison to WT to the sole influence of SUMO-mediated alterations in auxin homeostasis, it is important to take into consideration the considerable influence of hormone crosstalk. The idea that phytohormones act as independent modules regulating growth and stress responses in an antagonistic fashion, such as the classic auxin vs. cytokinin model, is a relatively outmoded one (Murphy, 2015). Indeed, the three classes of hormones primarily responsible for the regulation of plant growth, auxin, brassinosteroid and gibberellin, often work in a complementary fashion to regulate process such as cell elongation (Depuydt & Hardtke, 2011). Examples of this synergistic method of action can be seen in the regulation of the GA biosynthesis genes GA 3-oxidase and GA 20-oxidase by auxin (Reid, et al., 2011), the regulation of the DNA-binding activities of the transcription factors ARF6,

PIf4 and BZR1 by the DELLA growth repressor protein RGA (Oh, et al., 2014), and the regulation of the abundance of the PIN family of auxin efflux proteins via GA (Willige, et al., 2011).

The importance of SUMOylation has been implicated in many of the hormone pathways, such as those of auxin, gibberellic acid (GA), salicylic acid (SA), brassinosteroid (BR), jasmonic acid (JA), and abscisic acid (ABA) (Huang, et al., 2009; Nelis, et al., 2015; Bailey, et al., 2016; Khan, et al., 2014; Conti, et al., 2014). Recent research by Conti, et al. (2014), has shown that the growth supressing proteins RGA and GAI undergo SUMOylation *in planta*. The conjugation of SUMO to these repressors leads to their stabilisation, the result of which being the induction of growth inhibition in a manner independent of GA. As stated above, the interplay between the auxin and GA signalling pathways is complex, with many points of hormone crosstalk identified. Due to the global nature of SUMOylation, and the potential for cumulative effects of SUMOylation between the signalling pathways, it is therefore important that these factors are taken into consideration when assessing the role of SUMO in any one phytohormone signalling pathway.

6.1.2 The Primary Root Cap

Alongside the increase in auxin sensitivity observed for the *ots1 ots2* mutant, phenotypes relating to potential aberrations in the primary root cap were also identified for the mutant line. Results presented in chapter 3 indicated that an increase in SUMO-conjugate levels led to a decrease in the production of lateral root primordia under control conditions, as well as a significant increase in hydrotropic response upon exposure to a steep moisture gradient.

As previously stated, the *ots1 ots2* mutant line appeared to show an increased sensitivity to auxin. Upon the application of exogenous auxin stimulus to *ots1 ots2* seedlings, the number of emerged lateral roots increased, as expected. However, the average number of emerged lateral roots, even after auxin treatment, remained far below that of the WT. The increase in emerged lateral root number subsequent to auxin exposure suggested that the lateral root phenotype observed under control conditions was not due to a decrease in auxin sensitivity, as first thought, but instead due to irregularities in lateral root patterning. No increase in the number of arrested lateral root primordia was observed for the *ots1 ots2* mutant; indeed, the only difference seen between the

mutant and WT lines regarding the primordia was number alone, with the WT plants consistently producing more LR primordia of all stages in comparison to the *ots1 ots2* mutant. Taken together, this data led to the hypothesis that, though the *ots1 ots2* mutant was able to respond appropriately to auxin stimulus, it was unable to correctly prime the XPP cells that go on to form lateral root primordia, and therefore lateral roots.

SUMO-mediated aberrations in root cap signalling and/or perception were hypothesised to be the cause of the decrease in both lateral root primordia and emerged lateral roots in the *ots1 ots2* mutant under controlled conditions. This hypothesis is consistent with data from Xuan, et al. (2015), which identifies root cap derived IAA, and downstream activation of the kinase MKAR4, as the modulator of the auxin oscillations responsible for lateral root patterning and the priming of XPP cells. Additional data regarding the increase in hydrotropic response, a tropism in which the root cap plays an integral role (Cassab, et al., 2013), further implicated irregularities in the root cap as the source of the non-auxin mediated phenotypes observed for the mutant. It is clear that further research regarding root cap formation, sensing and signalling in the *ots1 ots2* mutant line is required in order to full understand the role SUMO plays in the establishment of the *Arabidopsis* root architecture.

6.2 SUMOylation in the Auxin Signalling Cascade

Results in chapters 4 and 5 indicated that several components of the auxin signalling cascade undergo SUMOylation. Though, as yet, it is unclear what role SUMOylation plays regarding the auxin signalling cascade, the potential significance of the modification of the proteins involved in the cascade by SUMO moieties will be discussed here.

6.2.1 SUMOylation of the Auxin Receptor TIR1

Transient expression of the auxin receptor TIR1 in *Nicotiana benthamiana* has shown that it undergoes modification by SUMO *in planta* (see, chapter 4). Subsequent conversion via mutation PCR of the lysine residues predicted to form the SUMO attachment sites to arginine residues, thereby maintaining binding site structure whilst removing the point of attachment, eliminated the conjugation of SUMO moieties to the TIR1 protein. The removal of these sites appeared to effect the stability of the TIR1 protein under transient assay conditions, leading to the hypothesis that SUMOylation of TIR1 is required to stabilise the receptor, thereby leading to an increase in auxin sensitivity through increased receptor signalling.

The postulated hypothesis is consistent with the data obtained in chapter 3. In the *ots1 ots2* mutant line, the levels of SUMO-conjugates increase due to the disruption of de-SUMOylation activity through the loss of SUMO proteases OTS1 and OTS2 (Conti, et al., 2014). Though it is not yet clear how SUMO and auxin interface, a good case can be made regarding the role of SUMOylated TIR1 in the establishment of the augmented auxin response observed in the *ots1 ots2* mutant line from the data presented here.

SUMO-mediated protein stabilisation has been demonstrated in previous research, not just in plants but also throughout all kingdoms. The stabilisation of target proteins via SUMO attachment with regards to cell cycle control (Schimmel, et al., 2014) and cancer development and progression (He, et al., 2015) is well documented in mammalian systems. Until relatively recently, research regarding the role of SUMOylation within the plant kingdom was decidedly lacking. To

date, relatively few papers have been published regarding the role of SUMOylation on the stability of the target protein.

However, recent research by Lin, et al. (2016) has set a precedent for the enhancement of phytohormone signalling through the SUMO-mediated stabilisation of a E3 ubiquitin ligase; through the use of loss-of-function *siz1* mutants, the role of SUMOylation in the stabilisation of the negative regulator of photomorphogenesis, CONSTITUATIVE PHOTOMORPHOGENIC 1 (COP1), was elucidated. Substitution of SUMO binding site residue K193 with arginine resulted in a reduction in the E3 ligase activity of COP1 through the destabilisation of the protein (Lin, et al., 2016). Similarly, in mammalian systems, the modification of ubiquitin E3 ligases, such as 53BP1 and BRCA-1, by SUMO has been shown to play an important role in double stranded DNA repair, possibly through SUMO-mediated induction of the E3 ligase activity (Wei & Lin, 2012). Taking into account the data obtained in chapter 3 and 4, it is therefore possible that TIR1 is regulated by SUMO in a similar fashion, therefore accounting for the increase in auxin sensitivity observed in the hyper-SUMOylated mutant line, *ots1 ots2*.

However, despite the attractiveness of the hypothesis outlined here, a great deal more research is required in order to determine its validity. Though SUMOylation of the TIR1 auxin receptor has been shown to occur under transient assay conditions, confirmation that this indeed occurs in *Arabidopsis* and is not an artefact of transient assay overexpression has yet to be demonstrated. The analysis of the generated transgenic *Arabidopsis* lines expressing the c-MYC:TIR1 and the c-MYC:TIR1^{3KR} in the auxin insensitive *tir1 afb2 afb3* background (see, chapter 4) should further elucidate the role of SUMO in auxin signalling, with regards to TIR1 stability and activity, therefore allowing the legitimacy of the hypothesis outlined above to be fully determined.

6.2.2 SUMO and the AUX/IAA Protein Family

Results in chapter 5 have indicated that, despite high confidence predictions regarding the presence of SUMO binding sites by the programme HyperSUMO, the AUX/IAA proteins IAA3 and IAA18 do not appear to undergo SUMOylation under transient expression conditions in *Nicotiana benthamiana*. The AUX/IAA family of transcriptional repressors are rapidly degraded in the

presence of auxin through ubiquitination by SCF^{TIR1} (Worley, et al., 2000). Taking this into account alongside the auxin-related phenotypes observed in the hyper-SUMOylated *ots1 ots2* mutant line (see, chapter 3), it was postulated that the addition of SUMO moieties to the AUX/IAA repressor proteins may lead to an increase in the rate of AUX/IAA turnover, therefore accounting for the lack of observed SUMOylation in the transient assay. The wealth of previous research regarding the interplay between SUMOylation and Ubiquitination lent credence to this idea, with many previous studies indicating that SUMO and Ub can work in a cooperative fashion in order to regulate protein stability (Liebelt & Vertegaal, 2016), such as in the regulation of Ub E3 ligase RNF4 targeting via SUMO in humans (Tatham, et al., 2008).

In order to test this hypothesis, a stabilised form of IAA28 was transiently expressed and its SUMOylation status determined; as with the previously investigated AUX/IAA proteins, no SUMOylation was observed for the stabilised IAA28 protein.

Whilst the transient assay data regarding the SUMOylation status of the AUX/IAA repressor proteins appears relatively clear, it is very likely that the answer to the question 'are the AUX/IAA family of transcriptional repressors SUMOylated?' is not a simple no. The AUX/IAA protein family is vast, comprising of 29 members, with each gene thought to differ somewhat in its physiological function (Muto, et al., 2007). Said members, though conforming to a highly conserved four-domain structure, vary widely in their sensitivity to auxin with regards to their auxin-mediated degradation (Shimizu-Mitao & Kakimoto, 2014) and in their pattern of expression (Audran-Delalande, et al., 2012). It is therefore not beyond the realms of possibility that SUMOylation status between the AUX/IAA family members also varies, possibly in a spatiotemporal fashion, resulting in the lack of SUMO modification observed under transient assay conditions. To truly determine the SUMOylation status of the AUX/IAA family members, a different approach, potentially involving the use of transgenic *Arabidopsis* lines, encompassing a wider array of AUX/IAA proteins must be undertaken.

6.2.3 SUMOylation of the ARF Protein Family Members, ARF7 and ARF19

Transient expression of the transcription factors ARF7 and ARF19 in *Nicotiana benthamiana* has shown that they undergo low-level modification by SUMO *in planta* (see, chapter 5). Further work undertaken by Dr. Beatriz Orosa (Sadanandom lab, unpublished), has subsequently confirmed the location of main SUMO biding site for ARF7. Work conducted by Dr. Orosa has shown that SUMOylation primarily occurs at a site located within the DNA binding region of ARF7. This leads to the hypothesis that SUMO is able to regulate the auxin responsive genes in a manner independent of auxin through alteration of the rate of ARF binding to gene promoter regions. Further work utilising a non-SUMOylatable form of ARF7 in a CHIP-seq assay (Donner, et al., 2009) would allow elucidation of the role SUMO plays in ARF transcription factor regulation.

6.3 Future Prospects

Alterations in gene expression, either through over-expression or gene knock-down/knock-out, provide exceptionally useful insights as to the roles said genes play at the whole organism level. Changes in gene expression can generate complex phenotypic traits within the organism; this is especially true for alterations in the regulation of global post-translational modifiers, like SUMO, and as such, a great deal of caution must be exercised during data interpretation. The need for such caution is apparent in the phenotypic data generated here, with an increase in SUMOylation levels resulting in a number of complex, and in some cases seemingly contradictory, phenotypes within the *Arabidopsis* root.

In order to tease out the underlying molecular processes responsible for the phenotypes displayed by the mutant lines, a more integrative global approach is required, such as whole transcriptome and proteasome studies. With the improvement of proteomic technologies, it has become clear that posttranslational modifications (PTMs) do not operate in isolation, but instead act as facilitators in the integration of many signalling pathways (Deribe, et al., 2010). Therefore, the necessity of study into PTMs and the role they play has never been of more importance, both in plant and animal research.

6.4 Knowledge Transfer

The model plant *Arabidopsis thaliana* has undergone extensive study since the 1980s, with almost 5000 papers describing research regarding this model plant system published in 2013 alone (Piquerez, et al., 2014). The use of *Arabidopsis* as a model plant has many benefits; though *Arabidopsis thaliana* has little in the way of direct significance when it comes to agriculture, widely considered a weed, the sheer wealth of data in terms of both genomic information and technical resources (eg. TAIR), alongside such biological benefits as a short life cycle (6 weeks germination to seed), prolific seed production, self-fertilization and the relative ease of floral dipping, makes *Arabidopsis* the organism of choice when it comes to plant research. It is, however, unclear as to how much of the research generated can be applied directly to the more economically and agriculturally relevant crop species, due to insufficient information regarding genetic synteny (Bevan & Walsh, 2004).

That said, the importance of knowledge transfer between model and economically relevant species cannot be understated. The intrinsic complexity of transcriptional regulation and the current lack of success regarding the more traditional up/down regulation of gene expression within crop plants is indicative of the necessity to re-think our current approach to the implementation of *Arabidopsis*-generated information within these species. With the advent of highly specific and elegant gene editing techniques, such as CRISPR (Song, et al., 2016), the ease of translation and subsequent implementation of research regarding SUMO-mediated signalling regulation within crop species is more achievable than ever before. Given the implications of SUMOylation demonstrated here in plant growth and development, continued research in this area with regards to economically important species will provide opportunities to help maintain, or indeed possibly improve, crop yields in less than ideal growing conditions.

A. Appendix

A.1 TIR1 and TIR1^{3KR} Sequence Alignment

```
TIR1    ATGCAGAAGCGAATAGCCTTGTCGTTTCCAGAAGAGGTACTAGAGCATGTGTTCTCGTTT
3KR     ATGCAGAAGCGAATAGCCTTGTCGTTTCCAGAAGAGGTACTAGAGCATGTGTTCTCGTTT
        ************************************************************

TIR1    ATTCAGCTGGATAAGGATAGGAACTCAGTCTCTCTGGTGTGCAAGTCATGGTACGAGATC
3KR     ATTCAGCTGGATAAGGATAGGAACTCAGTCTCTCTGGTGTGCAAGTCATGGTACGAGATC
        ************************************************************

TIR1    GAGCGGTGGTGCAGGAGGAAAGTCTTCATCGGGAACTGCTACGCCGTGAGTCCAGCGACG
3KR     GAGCGGTGGTGCAGGAGGAAAGTCTTCATCGGGAACTGCTACGCCGTGAGTCCAGCGACG
        ************************************************************

TIR1    GTGATTAGGAGGTTCCCGAAAGTGAGATCCGTGGAGCTTAAAGGAAAACCTCACTTTGCT
3KR     GTGATTAGGAGGTTCCCGAAAGTGAGATCCGTGGAGCTTAAAGGAAAACCTCACTTTGCT
        ************************************************************

TIR1    GACTTTAATTTGGTACCTGACGGATGGGGAGGTTACGTGTATCCATGGATTGAGGCCATG
3KR     GACTTTAATTTGGTACCTGACGGATGGGGAGGTTACGTGTATCCATGGATTGAGGCCATG
        ************************************************************

TIR1    TCTTCGTCTTACACGTGGCTTGAAGAGATAAGGCTGAAGAGGATGGTGGTCACCGACGAT
3KR     TCTTCGTCTTACACGTGGCTTGAAGAGATAAGGCTGAAGAGGATGGTGGTCACCGACGAT
        ************************************************************

TIR1    TGCTTGGAGCTCATAGCCAAGTCTTTTAAGAATTTTAAGGTTCTTGTGCTTTCTTCCTGC
3KR     TGCTTGGAGCTCATAGCCAAGTCTTTTAAGAATTTTAAGGTTCTTGTGCTTTCTTCCTGC
        ************************************************************

TIR1    GAAGGCTTCTCCACCGATGGTCTCGCTGCTATCGCTGCCACTTGCAGGAATCTGAAAGAG
3KR     GAAGGCTTCTCCACCGATGGTCTCGCTGCTATCGCTGCCACTTGCAGGAATCTGAAAGAG
        ************************************************************

TIR1    CTTGACTTACGAGAGAGTGATGTTGACGACGTTAGTGGCCACTGGCTTAGCCATTTCCCA
3KR     CTTGACTTACGAGAGAGTGATGTTGACGACGTTAGTGGCCACTGGCTTAGCCATTTCCCA
```

```
          ************************************************************

TIR1      GATACATACACTTCTTTGGTATCACTCAATATATCTTGCTTAGCATCTGAGGTCAGTTTC
3KR       GATACATACACTTCTTTGGTATCACTCAATATATCTTGCTTAGCATCTGAGGTCAGTTTC
          ************************************************************

TIR1      TCTGCTCTGGAAAGGCTGGTGACTAGGTGTCCCAATCTCAAGTCTCTCAAGCTTAACCGA
3KR       TCTGCTCTGGAAAGGCTGGTGACTAGGTGTCCCAATCTCAAGTCTCTCAAGCTTAACCGA
          ************************************************************

TIR1      GCTGTTCCACTTGAAAAATTGGCTACTTTACTTCAAAGAGCACCTCAATTGGAGGAATTG
3KR       GCTGTTCCACTTGAAAAATTGGCTACTTTACTTCAAAGAGCACCTCAATTGGAGGAATTG
          ************************************************************

TIR1      GGCACTGGTGGGTACACTGCAGAAGTGCGACCAGATGTTTACTCTGGTTTATCTGTAGCG
3KR       GGCACTGGTGGGTACACTGCAGAAGTGCGACCAGATGTTTACTCTGGTTTATCTGTAGCG
          ************************************************************

TIR1      CTCTCTGGGTGCAAGGAATTGAGGTGCTTATCTGGATTTTGGGATGCTGTTCCTGCCTAT
3KR       CTCTCTGGGTGCAAGGAATTGAGGTGCTTATCTGGATTTTGGGATGCTGTTCCTGCCTAT
          ************************************************************

TIR1      CTTCCAGCAGTTTATTCGGTTTGCAGTCGGCTTACAACTTTGAATCTGAGTTATGCAACA
3KR       CTTCCAGCAGTTTATTCGGTTTGCAGTCGGCTTACAACTTTGAATCTGAGTTATGCAACA
          ************************************************************

TIR1      GTCCAGAGCTATGATCTTGTCAAGCTTCTTTGTCAATGCCCTAAACTGCAGCGCCTCTGG
3KR       GTCCAGAGCTATGATCTTGTCAAGCTTCTTTGTCAATGCCCTAAACTGCAGCGCCTCTGG
          ************************************************************

TIR1      GTGCTTGACTACATCGAGGATGCTGGTCTTGAGGTGCTTGCTTCAACCTGCAAGGACCTA
3KR       GTGCTTGACTACATCGAGGATGCTGGTCTTGAGGTGCTTGCTTCAACCTGCAAGGACCTA
          ************************************************************

TIR1      CGCGAGCTGAGAGTGTTTCCGTCCGAGCCTTTTGTCATGGAACCAAATGTGGCATTGACG
3KR       CGCGAGCTGAGAGTGTTTCCGTCCGAGCCTTTTGTCATGGAACCAAATGTGGCATTGACG
          ************************************************************

TIR1      GAACAGGGGCTTGTCTCCGTCTCCATGGGCTGTCCAAAACTCGAGTCGGTTCTCTACTTC
3KR       GAACAGGGGCTTGTCTCCGTCTCCATGGGCTGTCCAAGACTCGAGTCGGTTCTCTACTTC
          ********************************** **********************

TIR1      TGCCGTCAAATGACCAATGCTGCATTGATAACCATTGCTAGGAACCGTCCCAACATGACT
3KR       TGCCGTCAAATGACCAATGCTGCATTGATAACCATTGCTAGGAACCGTCCCAACATGACT
          ************************************************************

TIR1      CGCTTCCGTTTGTGCATCATTGAGCCAAAAGCCCCAGACTATCTGACTCTAGAGCCACTG
3KR       CGCTTCCGTTTGTGCATCATTGAGCCAAAAGCCCCAGACTATCTGACTCTAGAGCCACTG
          ************************************************************

TIR1      GATATTGGATTTGGAGCCATAGTAGAGCACTGCAAGGATCTCCGTCGCCTCTCTCTATCT
3KR       GATATTGGATTTGGAGCCATAGTAGAGCACTGCAAGGATCTCCGTCGCCTCTCTCTATCT
          ************************************************************

TIR1      GGCCTCTTGACCGACAAGGTTTTTGAATACATTGGGACATATGCCAAGAAGATGGAAATG
3KR       GGCCTCTTGACCGACAAGGTTTTTGAATACATTGGGACATATGCCAAGAGGATGGAAATG
          ************************************************** **********
```

```
TIR1    CTCTCAGTGGCATTTGCAGGAGACAGTGACTTAGGCATGCATCATGTTTTGTCCGGGTGC
3KR     CTCTCAGTGGCATTTGCAGGAGACAGTGACTTAGGCATGCATCATGTTTTGTCCGGGTGC
        ************************************************************

TIR1    GATAGCTTGAGGAAACTAGAGATAAGGGACTGCCCGTTTGGAGACAAGGCGCTTTTGGCC
3KR     GATAGCTTGAGGAGACTAGAGATAAGGGACTGCCCGTTTGGAGACAAGGCGCTTTTGGCC
        ************* ************************************************

TIR1    AATGCTTCAAAGCTGGAGACAATGCGATCCCTTTGGATGTCTTCTTGTTCCGTGAGTTTT
3KR     AATGCTTCAAAGCTGGAGACAATGCGATCCCTTTGGATGTCTTCTTGTTCCGTGAGTTTT
        ************************************************************

TIR1    GGAGCCTGCAAGTTACTAGGACAGAAGATGCCAAAGCTGAATGTGGAAGTCATCGATGAA
3KR     GGAGCCTGCAAGTTACTAGGACAGAAGATGCCAAAGCTGAATGTGGAAGTCATCGATGAA
        ************************************************************

TIR1    CGGGGTGCACCGGACTCGAGACCAGAGAGCTGCCCTGTTGAGAGAGTCTTCATATACCGA
3KR     CGGGGTGCACCGGACTCGAGACCAGAGAGCTGCCCTGTTGAGAGAGTCTTCATATACCGA
        ************************************************************

TIR1    ACAGTGGCTGGTCCTCGATTTGACATGCCTGGCTTCGTCTGGAACATGGACCAAGACTCA
3KR     ACAGTGGCTGGTCCTCGATTTGACATGCCTGGCTTCGTCTGGAACATGGACCAAGACTCA
        ************************************************************

TIR1    ACAATGAGGTTTTCCAGGCAAATCATTACTACTAACGGATTATAA
3KR     ACAATGAGGTTTTCCAGGCAAATCATTACTACTAACGGATTATAA
        *********************************************
```

A.2 Primers

Primer	Sequence	Tm	Type
AttB1	ACA AGT TTG TAC AAA AAA GCA GGC T	58.1	Colony PCR
AttB2	ACC ACT TTG TAC AAG AAA GCT GGG T	61.3	Colony PCR
2OTS_TDNA	TGG TTC ACG TAG TGG GCC ATC G	65.8	Genotyping
OTS1_KO	CGA CAA GAA GTG GTT TAG ACC	59.5	Genotyping
OTS1_HOM	GTA ACG TAA CAC TTA TTA GAT GCC	60.3	Genotyping
OTS2_KO	GAC AGG GAT GCA TAT TTT GTG AAG	62	Genotyping
OTS2_HOM	TTA ATC TGT TTG GTT ACC CTT GCG G	64.1	Genotyping
VENUS_F	ACA AGC AGA AGA ACG GCA TC	60.4	Genotyping
VENUS_R	GAA CTC CAG CAG GAC CAT GT	60.1	Genotyping
TIR1_Detect_F	AGA TAA GGG ACT GCC CGT TT	59.9	Genotyping
TIR1_Detect_R	GAC CAG CCA CTG TTC GGT AT	60	Genotyping
TIR1_F	CAC CAT GCA GAA GCG AAT AGC CTT	59.1	Cloning
TIR1_R	TTA TAA TCC GTT AGT AGT AAT GAT TTG	54.7	Cloning
AFB1_F	CAC CAT GGG TCT CCG ATT CCC A	61.2	Cloning
AFB1_R	TTA CTT TAT GGC TAG ATG TGA AAC TCC	60.3	Cloning
AFB2_F	CAC CAT GAA TTA TTT CCC AGA TGA AGT AAT	57.7	Cloning
AFB2_R	TTA GAG AAT CCA CAC AAA TGG C	59.1	Cloning
AFB3_F	CAC CAT GAA TTA TTT CCC AGA CGA GGT	60.1	Cloning
AFB3_R	CTA AAG AAT CCT AAC ATA TGG TGG TG	59.3	Cloning
IAA2_F	CAC CAT GGC GTA CGA GAA AGT CAA C	66.5	Cloning
IAA2_R	TCA TAA GGA AGA GTC TAG AGC AGG A	58.7	Cloning
IAA3_F	CAC CAT GGA TGA GTT TGT TAA CCT CAA G	65.3	Cloning
IAA3_R	TCA TAC ACC ACA GCC TAA ACC TT	58.5	Cloning
IAA14_F	CAC CAT GAA CCT TAA GGA GAC GGA GC	67.5	Cloning
IAA14_R	TCA TGA TCT GTT CTT GAA CTT CTC C	59.6	Cloning
IAA18_F	CAC CAT GGA GGG TTA TTC AAG AAA CG	66.1	Cloning
IAA18_R	TCA TCT TCT CAT TTT CTC TTG CTT AC	58.2	Cloning
ASK1_F	CAC CAT GTC TGC GAA GAA GAT TGT GTT	67	Cloning
ASK1_R	TCA TTC AAA AGC CCA TTG GT	58.8	Cloning
CUL1_F	CAC CAT GGA GCG CAA GAC TAT TGA CT	67.1	Cloning
CUL1_R	CTA AGC CAA GTA CCT AAA CAT GTT AGG	58.7	Cloning
TIR1_K373R_F	CAT GGG CTG TCC AAG ACT CGA GTC GGT T	73	Mutation
TIR1_K373R_R	GAA CCG ACT CGA GTC TTG GAC AGC CCA T	73	Mutation
TIR1_K457R_F	GAC ATA TGC CAA GAG GAT GGA AAT GCT C	68.4	Mutation
TIR1_K457R_R	GAG AGC ATT TCC ATC CTC TTG GCA TAT GT	68.4	Mutation
TIR1_K485R_F	GCG ATA GCT TGA GGA GAC TAG AGA TAA G	61.3	Mutation
TIR1_K485R_R	CCC TTA TCT CTA GTC TCC TCA AGC TAT CG	61.3	Mutation
TIR1_Seq1	TTC GTC TTA CAC GTG GCT TG	60.2	Sequencing
TIR1_Seq2	GAG GTG CTT ATC TGG ATT TTG G	59.9	Sequencing
TIR1_Seq3	AGC CAA AAG CCC CAG ACT AT	60	Sequencing
AFB1_Seq1	CTT CTT GTG AAG GTT TCT CTA CTG ATG	59.7	Sequencing
AFB2_Seq1	TTT TCT AGA GGC TGC TCC TCA C	58.7	Sequencing
AFB3_Seq1	CTT TTT AGA GGT TGC TCC ACT CTG	59.4	Sequencing

A.3 Genotyping of the DR5::VENUS, *ots1 ots2* Cross (F2)

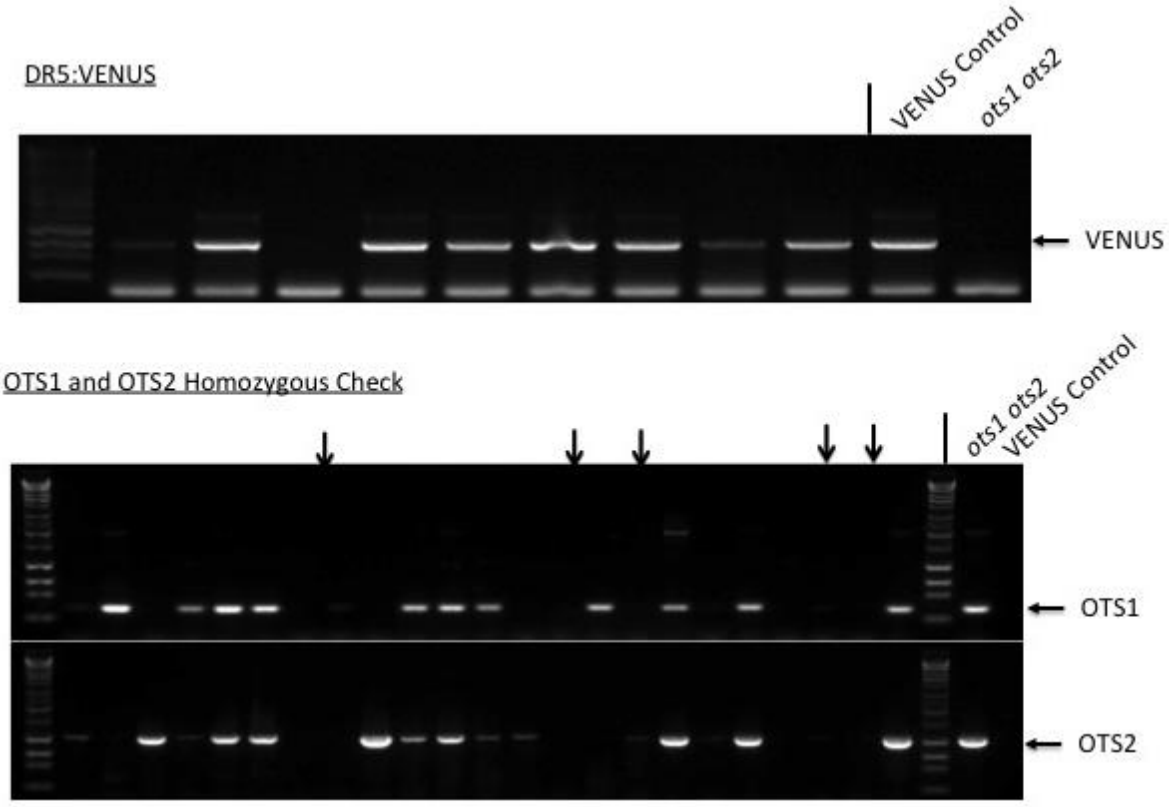

PCR products from the genomic DNA extracts from the F2 DR5::VENUS xots1 ots2 crosses, with DR5:VENUS and ots1 ots2 used as controls. Bands correspond to the VENUS gene (TOP) and OTS1 and OTS2 genes (bottom). OTS1 and -2 primers span the T-DNA insert region; the absence of bands in the OTS1 and -2 homozygous check correspond to the presence of the T-DNA insert.

Bibliography

Adamowski, M. & Friml, J., 2015. PIN-dependent auxin transport: action, regulation, and evolution. Plant Cell, 27(1), pp. 20-32.

Antoni, R., Dietrich, D., Bennett, M. J. & Rodriguez, P. L., 2016. Hydrotropism: Analysis of the Root Response to a Moisture Gradient. Methods Mol Biol, Volume 1398, pp. 3-9.

Audran-Delalande, C. et al., 2012. Genome-Wide Identification, Functional Analysis and Expression Profiling of the Aux/IAA Gene Family in Tomato. Plant Cell Physiol, 53(4), pp. 659-672.

Bailey, S., 2014. An investigation into the role of SUMO proteases OVERLY TOLERANT to SALT1 and -2 in salicylic acid mediated defense signalling in Arabidopsis thaliana:@ toward understanding the role of SUMOylation in SA signalling. (Unpublished PhD Thesis, University of Warwick).

Bailey, M. et al., 2016. Stability of small ubiquitin-like modifier (SUMO) proteases OVERLY TOLERANT TO SALT1 and -2 modulates salicylic acid signalling and SUMO1/2 conjugation in Arabidopsis thaliana. J Exp Bot, 67(1), pp. 353-363.

Barrett, A. J. & Rawlings, N. D., 2001. Evolutionary lines of cysteine peptidases. Biol Chem, 382(5), pp. 727-733.

Bates, T. R. & Lynch, J. P., 2000. Plant growth and phosphorus accumulation of wild type and two root hair mutants of Arabidopsis thaliana (Brassicaceae). Am J Bot, 87(7), pp. 958-963.

Bayer, P. et al., 1998. Structure determination of the small ubiquitin-related modifier SUMO-1. J Mol Biol, 280(2), pp. 275-286.

Beeckman, T., Burssens, S. & Inzé, D., 2001. The peri-cell-cycle in Arabidopsis. J Exp Bot, 52(Spec Issue), pp. 403-411.

Benková, E. et al., 2003. Local, efflux-dependent auxin gradients as a common module for plant organ formation. Cell, 115(5), pp. 591-602.

Bevan, M. & Walsh, S., 2004. Positioning Arabidopsis in Plant Biology. A Key Step Toward Unification of Plant Research. Plant Physiol, 135(2), pp. 602-606.

Booker, K. S., Schwarz, J., Garrett, M. B. & Jones, A. M., 2010. Glucose attenuation of auxin-mediated bimodality in lateral root formation is partly coupled by the heterotrimeric G protein complex. PLoS One, 5(9), p. e12833.

Bossis, G. & Melchior, F., 2006. Regulation of SUMOylation by reversible oxidation of SUMO conjugating enzymes. Mol Cell, 21(3), pp. 349-357.

Budhiraja, R. et al., 2009. Substrates related to chromatin and to RNA-dependent processes are modified by Arabidopsis SUMO isoforms that differ in a conserved residue with influence on desumoylation. Plant Physiol, 149(3), pp. 1529-1540.

Calderón Villalobos, L. I. et al., 2012. A combinatorial TIR1/AFB-Aux/IAA co-receptor system for differential sensing of auxin. Nat Chem Biol, 8(5), pp. 477-485.

Calderon-Villalobos, L. I., X, T., Zheng, N. & Estelle, M., 2010. Auxin perception-structural insights. Spring Harb Perspect Biol, Volume 2, p. 47–62.

Camilleri, C. & Jouanin, L., 1991. The TR-DNA region carrying the auxin synthesis genes of the Agrobacterium rhizogenes agropine-type plasmid pRiA4: nucleotide sequence analysis and introduction into tobacco plants. Mol Plant Microbe Interact, 4(2), pp. 155-162.

Capili, A. D. & Lima, C. D., 2007. Structure and analysis of a complex between SUMO and Ubc9 illustrates features of a conserved E2-Ubl interaction. J Mol Biol, 369(3), pp. 608-618.

Cardozo, T. & Pagano, M., 2004. The SCF ubiquitin ligase: insights into a molecular machine. Nat Rev Mol Cell Biol, 5(9), pp. 739-751.

Casimiro, I. et al., 2001. Auxin transport promotes Arabidopsis lateral root initiation. Plant Cell, 13(4), pp. 843-852.

Cassab, G. I., Eapen, D. & Campos, M. E., 2013. Root hydrotropism: an update. Am J Bot, 100(1), pp. 14-24.

Castaño-Miquel, L. et al., 2013. Diversification of SUMO-activating enzyme in Arabidopsis: implications in SUMO conjugation. Mol Plant, 6(5), pp. 1646-1660.

Catala, R. et al., 2007. The Arabidopsis E3 SUMO ligase SIZ1 regulates plant growth and drought responses. Plant Cell, 19(9), pp. 2952-2966.

Chandler, J. W., 2016. Auxin response factors. Plant Cell Environ, 39(5), pp. 1014-1028.

Chen, C. C. et al., 2011. Arabidopsis SUMO E3 ligase SIZ1 is involved in excess copper tolerance. Plant Physiol, 156(4), pp. 2225-2234.

Chen, R., Rosen, E. & Masson, P. H., 1999. Gravitropism in Higher Plants. Plant Physiol, 120(2), pp. 343-350.

Chosed, R., Mukherjee, S., Lois, L. M. & Orth, K., 2006. Evolution of a signalling system that incorporates both redundancy and diversity: Arabidopsis SUMOylation. Biochem J, 398(3), pp. 521-529.

Chosed, R. et al., 2007. Structural analysis of Xanthomonas XopD provides insights into substrate specificity of ubiquitin-like protein proteases. J Biol Chem, 282(9), pp. 6773-6782.

Clough, S. J. & Bent, A. F., 1998. Floral dip: a simplified method for Agrobacterium-mediated transformation of Arabidopsis thaliana. Plant J, 16(6), pp. 735-743.

Conti, L. et al., 2014. Small Ubiquitin-like Modifier protein SUMO enables plants to control growth independently of the phytohormone gibberellin. Dev Cell, 28(1), pp. 102-110.

Conti, L. et al., 2008. Small ubiquitin-like modifier proteases OVERLY TOLERANT TO SALT1 and -2 regulate salt stress responses in Arabidopsis. Plant Cell, 20(10), pp. 2894-2908.

Cooney, T. P. & Nonhebel, H. M., 1991. Biosynthesis of indole-3-acetic acid in tomato shoots: Measurement, mass-spectral identification and incorporation of (-2)H from (-2)H 2O into indole-3-acetic acid, D- and L-tryptophan, indole-3-pyruvate and tryptamine. Planta, 184(3), pp. 368-376.

Darwin, C. & Darwin, F., 1881. The power of movement in plants. London, England: Murray.

Davière, J. M. & Achard, P., 2013. Gibberellin signaling in plants. Development, 140(6), pp. 1147-1151.

De Smet, I. et al., 2007. Auxin-dependent regulation of lateral root positioning in the basal meristem of Arabidopsis. Development, 134(4), pp. 681-690.

Delano, W. L., 2002. The PyMOL molecular graphics system. Delano Scientific, San Carlos, CA, USA.

Den Herder, G., Van Isterdael, G., Beeckman, T. & De Smet, I., 2010. The roots of a new green revolution. Trends Plant Sci, 15(11), pp. 600-607.

Depuydt, S. & Hardtke, C. S., 2011. Hormone signalling crosstalk in plant growth regulation. Curr Biol, 21(9), pp. R365-373.

Deribe, Y. L., Pawson, T. & Dikic, I., 2010. Post-translational modifications in signal integration. Nat Struct Mol BioL, 17(6), pp. 666-672.

Deshaies, R. J., 1995. Make it or break it: the role of ubiquitin-dependent proteolysis in cellular regulation. Trends Cell Biol, 5(11), pp. 428-434.

Dharmasiri, N. et al., 2005. Plant development is regulated by a family of auxin receptor F box proteins. Dev Cell, 9(1), pp. 109-119.

Di Fiore, S. et al., 2002. Targeting tryptophan decarboxylase to selected subcellular compartments of tobacco plants affects enzyme stability and in vivo function and leads to a lesion-mimic phenotype. Plant Physiol, 129(3), pp. 1160-1169.

Dohmen, R. J., 2004. SUMO protein modification. Biochim Biophys Acta, 1695(1-3), pp. 113-131.

Dolan, L., 1996. Pattern in the root epidermis: an interplay of diffusible signals and cellular geometry. Ann Bot, Volume 77, p. 547–553.

Dolan, L., 1998. Pointing roots in the right direction: the role of auxin transport in response to gravity. Genes Dev, 12(14), pp. 2091-2095.

Donner, T., Sherr, I. & Scarpella, E., 2009. Regulation of preprocambial cell state acquisition by auxin signaling in Arabidopsis leaves.. Development, Volume 136, p. 3235–3246.

Dreher, K. A., Brown, J., Saw, R. E. & Callis, J., 2006. The Arabidopsis Aux/IAA protein family has diversified in degradation and auxin responsiveness. Plant Cell, 18(3), pp. 699-714.

Dubrovsky, J. G. et al., 2001. Auxin minimum defines a developmental window for lateral root initiation. New Phytol, 191(4), pp. 970-983.

Dubrovsky, J. G., Rost, T. L., Colón-Carmona, A. & Doerner, P., 2001. Early primordium morphogenesis during lateral root initiation in Arabidopsis thaliana. Planta, 214(1), pp. 30-36.

Eapen, D. et al., 2005. Hydrotropism: root growth responses to water. Trends Plant Sci, 10(1), pp. 44-50.

Earley, K. W. et al., 2006. Gateway-compatible vectors for plant functional genomics and proteomics. Plant J, 45(4), pp. 616-629.

Eckardt, N. A., 2006. Three Arabidopsis GID1 Genes Encode Gibberellin Receptors with Overlapping Functions. Plant Cell, 18(12), p. 3353.

Eliasson, L., Bertell, G. & Bolander, B., 1989. Inhibitory Action of Auxin on Root Elongation Not Mediated by Ethylene. Plant Physiol, 91(1), pp. 310-314.

Enserink, J. M., 2015. Sumo and the cellular stress response. Cell Div, Volume 10, p. 4.

Expósito-Rodríguez, M., Borges, A. A., Borges-Pérez, A. & Pérez, J. A., 2011. Gene structure and spatiotemporal expression profile of tomato genes encoding YUCCA-like flavin monooxygenases: the ToFZY gene family. Plant Physiol Biochem, 49(7), pp. 782-791.

Farquharson, K. L., 2010. Gibberellin-auxin crosstalk modulates lateral root formation. Plant Cell, 22(3), p. 540.

Fukaki, H., Okushima, Y. & Tasaka, M., 2007. Auxin-mediated lateral root formation in higher plants. Int Rev Cytol, Volume 256, pp. 111-137.

Galinat, W. C., 1959. The phytomer in relation to the floral homologies in the American Maydea. Bot Mus Leafl Harv Univ, Volume 19, pp. 1-32.

Gallavotti, A., 2013. The role of auxin in shaping shoot architecture. J Exp Bot, 64(9), pp. 2593-2608.

Ganguly, A. et al., 2010. Differential auxin-transporting activities of PIN-FORMED proteins in Arabidopsis root hair cells. Plant Physiol, 153(3), pp. 1046-1061.

Gareau, J. R. & Lima, C. D., 2010. The SUMO pathway: emerging mechanisms that shape specificity, conjugation and recognition. Nat Rev Mol Cell Biol, 11(12), pp. 861-871.

Gaudin, V., Camilleri, C. & Jouanin, L., 1993. Multiple regions of a divergent promoter control the expression of the Agrobacterium rhizogenes aux1 and aux2 plant oncogenes. Mol Gen Genet, 239(1-2), pp. 225-234.

Geldner, N. et al., 2001. Auxin transport inhibitors block PIN1 cycling and vesicle trafficking. Nature, Volume 413, pp. 425-428.

Gish, W. & States, D. J., 1993. Identification of protein coding regions by database similarity search. Nat Genet, 3(3), pp. 266-272.

Goda, H. et al., 2004. Comprehensive comparison of auxin-regulated and brassinosteroid-regulated genes in Arabidopsis. Plant Physiol, 134(4), pp. 1555-1573.

Goh, T. et al., 2012. Multiple AUX/IAA–ARF modules regulate lateral root formation: the role of Arabidopsis SHY2/IAA3-mediated auxin signalling. Philos Trans R Soc Lond B Biol Sci, 367(1595), p. 1461–1468.

Gonzali, S. et al., 2005. A turanose-insensitive mutant suggests a role for WOX5 in auxin homeostasis in Arabidopsis thaliana. Plant J, 44(4), pp. 633-645.

Goua, J. et al., 2010. Gibberellins Regulate Lateral Root Formation in Populus through Interactions with Auxin and Other Hormones. Plant Cell, 22(3), pp. 623-639.

Goyal, A., Szarzynska, B. & Fankhauser, C., 2013. Phototropism: at the crossroads of light-signaling pathways. Trends Plant Sci, 19(7), pp. 393-401.

Gray, W. M. et al., 2001. Auxin regulates SCF(TIR1)-dependent degradation of AUX/IAA proteins. Nature, 414(6861), pp. 271-276.

Gutjahr, C. et al., 2005. Cholodny-Went revisited: a role for jasmonate in gravitropism of rice coleoptiles. Planta, 222(4), pp. 575-585.

Hasenstein, K. H. & Rayle, D., 1984. Cell wall pH and auxin transport velocity. Plant Physiol, 76(1), pp. 65-67.

Hecker, C. M. et al., 2006. Specification of SUMO1- and SUMO2-interacting motifs. J Biol Chem, 281(23), pp. 16117-16127.

Hershko, A. & Ciechanover, A., 1998. The ubiquitin system. Annu Rev Biochem, Volume 67, pp. 425-479.

He, X. et al., 2015. Characterization of the loss of SUMO pathway function on cancer cells and tumor proliferation. PLoS One, 10(4), p. e0123882.

Hilbert, M. et al., 2012. Indole derivative production by the root endophyte Piriformospora indica is not required for growth promotion but for biotrophic colonization of barley roots. New Phytol, 196(2), pp. 520-534.

Huang, L. et al., 2009. The Arabidopsis SUMO E3 ligase AtMMS21, a homologue of NSE2/MMS21, regulates cell proliferation in the root. Plant J, 60(4), pp. 666-678.

Huang, W. C., Ko, T. P., Li, S. S. & Wang, A. H., 2004. Crystal structures of the human SUMO-2 protein at 1.6 A and 1.2 A resolution: implication on the functional differences of SUMO proteins. Eur J Biochem, 271(20), pp. 4114-4122.

Hull, A. K. & Celenza, J. L., 2000. Bacterial expression and purification of the Arabidopsis NADPH-cytochrome P450 reductase ATR2. Protein Expr Purif, 18(3), pp. 310-315.

Hussain, A. & Peng, J. R., 2003. DELLA proteins and GA signalling in Arabidopsis. J Plant Growth Regul, Volume 22, p. 134–140.

Ishida, T. et al., 2009. SUMO E3 ligase HIGH PLOIDY2 regulates endocycle onset and meristem maintenance in Arabidopsis. Plant Cell, 21(8), pp. 2284-2297.

Ishida, T., Yoshimura, M., Miura, K. & Sugimot, K., 2012. MMS21/HPY2 and SIZ1, Two Arabidopsis SUMO E3 Ligases, Have Distinct Functions in Development. PLoS One, 7(10), p. e46897.

Jaffe, M. J., Takahashi, H. & Biro, R. L., 1985. A pea mutant for the study of hydrotropism in roots. Science, 230(4724), pp. 445-447.

Johnson, E. S., 2004. Protein modification by SUMO. Annu Rev Biochem, Volume 73, pp. 355-382.

Kaltwasser, M., Wiegert, T. & Schumann, W., 2002. Construction and application of epitope- and green fluorescent protein-tagging integration vectors for Bacillus subtilis. Appl Environ Microbiol, 68(5), pp. 2624-2628.

Kaneyasu, T. et al., 2007. Auxin response, but not its polar transport, plays a role in hydrotropism of Arabidopsis roots. J Exp Bot, 58(5), pp. 1143-1150.

Khan, M. et al., 2014. Interplay between phosphorylation and SUMOylation events determines CESTA protein fate in brassinosteroid signalling. Nat Commun, Volume 5, p. 4687.

Kim, H, J., Lynch, J. P. & Brown, K. M., 2008. Ethylene insensitivity impedes a subset of responses to phosphorus deficiency in tomato and petunia. Plant Cell Environ, 31(12), pp. 1744-1755.

Kiss, J. Z., 2007. Where's the water? Hydrotropism in plants. Proc Natl Acad Sci U S A, 104(11), pp. 4247-42-48.

Krecek, P. et al., 2009. The PIN-FORMED (PIN) protein family of auxin transporters. Genome Biol, 10(12), p. 249.

Krizek, B. A., 2011. Auxin regulation of Arabidopsis flower development involves members of the AINTEGUMENTA-LIKE/PLETHORA (AIL/PLT) family. J Exp Bot, 62(10), pp. 3311-3319.

Kurepa, J. et al., 2003. The small ubiquitin-like modifier (SUMO) protein modification system in Arabidopsis. Accumulation of SUMO1 and -2 conjugates is increased by stress. J Biol Chem, 278(9), pp. 6862-6871.

Laskowski, M., 2013. Lateral root initiation is a probabilistic event whose frequency is set by fluctuating levels of auxin response. J Exp Bot, 64(9), pp. 2609-2617.

Lavenus, J. et al., 2013. Lateral root development in Arabidopsis: fifty shades of auxin. Trends Plant Sci, 18(8), pp. 450-458.

Lavenus, J. et al., 2013. Lateral root development in Arabidopsis: fifty shades of auxin. Trends Plant Sci, 18(8), pp. 450-458.

Lee, I. & Schindelin, H., 2008. Structural insights into E1-catalyzed ubiquitin activation and transfer to conjugating enzymes. Cell, 134(2), pp. 268-278.

Lee, R. D. & Cho, H. T., 2013. Auxin, the organizer of the hormonal/environmental signals for root hair growth. Front Plant Sci, Volume 4, p. 448.

Lemcke, K., Prinsen, E., van Onckelen, H. & Schmülling, T., 2000. The ORF8 gene product of Agrobacterium rhizogenes TL-DNA has tryptophan 2-monooxygenase activity. Molecular Plant-Microbe Interactions. Mol Plant Microbe Interact, 13(7), pp. 787-790.

Leyser, O., 2010. The power of auxin in plants. Plant Physiol, 154(2), pp. 501-505.

Leyser, O. & Fitter, A., 1998. Roots are branching out in patches. Trends Plant Sci, 3(6), pp. 203-204.

Liebelt, F. & Vertegaal, A. C. O., 2016. Ubiquitin-dependent and independent roles of SUMO in proteostasis. Am J Physiol Cell Physiol,, 311(2), pp. C284-C296.

Lin, X. L. et al., 2016. An Arabidopsis SUMO E3 Ligase, SIZ1, Negatively Regulates Photomorphogenesis by Promoting COP1 Activity. PLoS Genet, 12(4), p. e1006016.

Liscum, E. et al., 2014. Phototropism: growing towards an understanding of plant movement. Plant Cell, 26(1), pp. 38-55.

Li, S. J. & Hochstrasser, M., 2003. The Ulp1 SUMO isopeptidase: distinct domains required for viability, nuclear envelope localization, and substrate specificity. J Cell Biol, 160(7), pp. 1069-1081.

Li, Z. et al., 2013. Phosphate starvation of maize inhibits lateral root formation and alters gene expression in the lateral root primordium zone. BMC Plant Biol, Volume 12, pp. 89.

Lois, L. M. & Lima, C. D., 2005. Structures of the SUMO E1 provide mechanistic insights into SUMO activation and E2 recruitment to E1. EMBO J, 24(3), pp. 439-451.

Long, J. A., Ohno, C., Smith, Z. R. & Meyerowitz, E. M., 2006. TOPLESS regulates apical embryonic fate in Arabidopsis. Science, 312(5779), pp. 1520-1523.

Lucas, M. et al., 2008. An auxin transport-based model of root branching in Arabidopsis thaliana. PLoS One, 3(11), p. e3673.

Ludwig-Müller, J. & Hilgenberg, W., 1988. A plasma membrane-bound enzyme oxidizes L-tryptophan to indole-3-acetaldoxime. Physiol Plant, 74(2), pp. 240-250.

Mano, Y. & Nemoto, K., 2012. The pathway of auxin biosynthesis in plants. J Exp Bot, 63(8), pp. 2853-2872.

Mano, Y. et al., 2010. The AMI1 gene family: indole-3-acetamide hydrolase functions in auxin biosynthesis in plantS. J Exp Bot, 61(1), pp. 25-32.

Maraschin Fdos, S., Memelink, J. & Offringa, R., 2009. Auxin-induced, SCF(TIR1)-mediated poly-ubiquitination marks AUX/IAA proteins for degradation. Plant J, 59(1), pp. 100-109.

Marchant, A. et al., 2002. AUX1 Promotes Lateral Root Formation by Facilitating Indole-3-Acetic Acid Distribution between Sink and Source Tissues in the Arabidopsis Seedling. Plant Cell, 14(3), pp. 589-597.

Mashiguchi, K. et al., 2011. The main auxin biosynthesis pathway in Arabidopsis. Proc Natl Acad Sci U S A, 108(45), pp. 18512-18517.

Masucci, J. D. & Schiefelbein, J. W., 1996. Hormones act downstream of TTG and GL2 to promote root hair outgrowth during epidermis development in the Arabidopsis root. Plant Cell, 8(9), pp. 1505-1517.

Mikkelsen, M. D. et al., 2009. Controlled indole-3-acetaldoxime production through ethanol-induced expression of CYP79B2. Planta, 229(6), pp. 1209-1217.

Mikkelsen, M. D., Hansen, C. H., Wittstock, U. & Halkier, B. A., 2000. Cytochrome P450 CYP79B2 from Arabidopsis catalyzes the conversion of tryptophan to indole-3-acetaldoxime, a precursor of indole glucosinolates and indole-3-acetic acid. J Biol Chem, 275(43), pp. 33712-33717.

Millera, M. J., Barrett-Wilt, G. A., Hua, Z. & Vierstra, R. D., 2010. Proteomic analyses identify a diverse array of nuclear processes affected by small ubiquitin-like modifier conjugation in Arabidopsis. Proc Natl Acad Sci U S A, 107(38), p. 16512–16517.

Mironova, V. V., Omelyanchuk, N. A., Wiebe, D. S. & Levitsky, V. G., 2014. Computational analysis of auxin responsive elements in the Arabidopsis thaliana L. genome. BMC Genomics, 15(Suppl 12), p. S4.

Miura, K., Jin, J. B. & Hasegawa, P. M., 2007. Sumoylation, a post-translational regulatory process in plants. Curr Opin Plant Biol, 10(5), pp. 495-502.

Miura, K. et al., 2005. The Arabidopsis SUMO E3 ligase SIZ1 controls phosphate deficiency responses. Proc Natl Acad Sci U S A, 102(21), pp. 7760-7765.

Miura, K. et al., 2011. SIZ1 regulation of phosphate starvation-induced root architecture remodelling involves the control of auxin accumulation. Plant Physiol, 155(2), pp. 1000-1012.

Mockaitis, K. & Estelle, M., 2008. Auxin receptors and plant development: a new signaling paradigm. Annu Rev Cell Dev Biol, Volume 25, pp. 55-80.

Moreno-Risueno, M. A. et al., 2010. Oscillating gene expression determines competence for periodic Arabidopsis root branching. Science, 329(5997), pp. 1306-1311.

Muday, G. K., 2001. Auxins and tropisms. J Plant Growth Regul, Volume 3, pp. 226-243.

Murphy, A., 2015. Hormone crosstalk in plants. J Exp Bot, 66(16), pp. 4853-4854.

Muto, H., Watahiki, M. K. & Yamamoto, K. T., 2007. What Makes each Aux/IAA Gene Unique in its Gene Family, Expression Pattern or Properties of the Gene Product?. Plant Signal Behav, 2(5), pp. 390-392.

Nelis, S., 2014. An investigation into the role and mechanism of action of small ubiquitin-like modifier interacting motifs in Arabidopsis thaliana proteins (Unpublished PhD Thesis, University of Warwick).

Nelis, S., Conti, L., Zhang, C. & Sadanandom, A., 2015. A functional Small Ubiquitin-like Modifier (SUMO) interacting motif (SIM) in the gibberellin hormone receptor GID1 is conserved in cereal crops and disrupting this motif does not abolish hormone dependency of the DELLA-GID1 interaction. Plant Signal Behav, 10(2), p. e987528.

Nemoto, K. et al., 2009. Function of the aux and rol genes of the Ri plasmid in plant cell division in vitro. Plant Signal Behav, 4(12), pp. 1145-1147.

Niu, Y. F. et al., 2011. Responses of root architecture development to low phosphorus availability: a review. Ann Bot, 112(2), pp. 391-408.

Novatchkova, M. et al., 2012. Update on sumoylation: defining core components of the plant SUMO conjugation system by phylogenetic comparison. New Phytol, 195(1), pp. 23-31.

Offringa, I. A. et al., 1986. Complementation of Agrobacterium tumefaciens tumor-inducing aux mutants by genes from the TR-region of the Ri plasmid of Agrobacterium rhizogenes. Proc Natl Acad Sci U S A, 83(18), p. 6935–6939.

Oh, E. et al., 2014. Cell elongation is regulated through a central circuit of interacting transcription factors in the Arabidopsis hypocotyl. Elife, Volume 3, p. e03031.

Okushima, Y. et al., 2007. ARF7 and ARF19 regulate lateral root formation via direct activation of LBD/ASL genes in Arabidopsis. Plant Cell, 19(1), pp. 118-130.

Ortiz-Castro, R. et al., 2011. Transkingdom signaling based on bacterial cyclodipeptides with auxin activity in plants. Proc Natl Acad Sci U S A, 108(17), pp. 7253-7258.

Osmont, K. S., Sibout, R. & Hardtke, C. S., 2007. Hidden branches: developments in root system architecture. Annu Rev Plant Biol, Volume 58, pp. 93-113.

Overvoorde, P., Fukaki, H. & Beeckman, T., 2010. Auxin Control of Root Development. Cold Spring Harb Perspect Biol, 2(6), p. a001537.

Overvoorde, P. J. et al., 2005. Functional genomic analysis of the AUXIN/INDOLE-3-ACETIC ACID gene family members in Arabidopsis thaliana. Plant Cell, 17(12), pp. 3282-3300.

Ovid, Melville, A. D. & Kenney, E. J., 1998. Metamorphoses. Oxford, UK: Oxford University Press.

Parizot, B. et al., 2012. In silico analyses of pericycle cell populations reinforce their relation with associated vasculature in Arabidopsis. Philos Trans R Soc Lond B Biol Sci, 367(1595), pp. 1479-1488.

Park, B. S., Song, J. T. & Seo, H. S., 2011. Arabidopsis nitrate reductase activity is stimulated by the E3 SUMO ligase AtSIZ1. Nat Commun, Volume 2, p. 400.

Park, H. J. et al., 2011. SUMO and SUMOylation in Plants. Mol Cells, 32(4), pp. 305-316.

Parry, G. et al., 2009. Complex regulation of the TIR1/AFB family of auxin receptors. Proc Natl Acad Sci U S A, 106(52), pp. 22540-22545.

Pattison, R. J., Csukasi, F. & Catalá, C., 2014. Mechanisms regulating auxin action during fruit development. Physiol Plant, 151(1), pp. 62-72.

Pennazio, S., 2002. The discovery of the chemical nature of the plant hormone auxin. Riv Biol, 95(2), pp. 289-308.

Perdomo, J. et al., 2012. SUMOylation regulates the transcriptional repression activity of FOG-2 and its association with GATA-4. PLoS One, 7(11), p. e50637.

Péret, B. et al., 2009. Arabidopsis lateral root development: an emerging story. Trends Plant Sci, 14(7), pp. 399-408.

Perrot-Rechenmann, C., 2010. Cellular Responses to Auxin: Division versus Expansion. Cold Spring Harb Perspect Biol, 2(5), p. a001446.

Philippar, K. et al., 2004. Auxin activates KAT1 and KAT2, two K+-channel genes expressed in seedlings of Arabidopsis thaliana. Plant J, Volume 37, p. 815–827.

Philosoph-Hadas, S., Friedman, H. & Meir, S., 2005. Gravitropic bending and plant hormones. Vitam Horm, Volume 72, pp. 31-78.

Pickart, C. M., 2001. Mechanisms underlying ubiquitination. Annu Rev Biochem, Volume 70, pp. 503-533.

Piquerez, S. J. M., Harvey, S. E., Beynon, J. L. & Ntoukakis, V., 2014. Improving crop disease resistance: lessons from research on Arabidopsis and tomato. Front Plant Sci, Volume 5, p. 671.

Pitts, R. J., Cernac, A. & Estelle, M., 1998. Auxin and ethylene promote root hair elongation in Arabidopsis. Plant J, 16(5), pp. 553-560.

Pollmann, S., Düchting, P. & Weiler, E. W., 2009. Tryptophan-dependent indole-3-acetic acid biosynthesis by 'IAA-synthase' proceeds via indole-3-acetamide. Phytochemistry, 70(4), pp. 523-531.

Pollmann, S., Müller, A., Piotrowski, M. & Weiler, E. W., 2002. Occurrence and formation of indole-3-acetamide in Arabidopsis thaliana. Planta, 216(1), pp. 155-161.

Prigge, M. J. et al., 2016. The Arabidopsis Auxin Receptor F-Box Proteins AFB4 and AFB5 Are Required for Response to the Synthetic Auxin Picloram. G3 (Bethesda), 6(5), pp. 1383-1390.

Psakhye, I. & Jentsch, S., 2012. Protein Group Modification and Synergy in the SUMO Pathway as Exemplified in DNA Repair. Cell, 151(4), pp. 807 - 820.

Rahman, A. et al., 2007. Auxin, actin and growth of the Arabidopsis thaliana primary root.. Plant J, 50(3), pp. 514-528.

Rahman, A. et al., 2002. Auxin and ethylene response interactions during Arabidopsis root hair development dissected by auxin influx modulators. Plant Physiol, 130(4), pp. 1908-1917.

Reed, R., Brady, S. & Muday, G. K., 1989. Inhibition of Auxin Movement from the Shoot into the Root Inhibits Lateral Root Development in ArabidopsiS. Plant Physiol, 118(4), pp. 1369-1378.

Reid, J. B., Davidson, S. E. & Ross, J. J., 2011. Auxin acts independently of DELLA proteins in regulating gibberellin levels. Plant Signal Behav, 6(3), pp. 406-408.

Reinhold, L., Sachs, T. & Vislovska, L., 1972. Plant Growth Substances 1970. Berlin Heidelberg: Springer.

Sabatini, S. et al., 1999. An auxin-dependent distal organizer of pattern and polarity in the Arabidopsis root. Cell, 99(5), pp. 463-472.

Sabatini, S., Heidstra, R., Wildwater, M. & Scheres, B., 2003. SCARECROW is involved in positioning the stem cell niche in the Arabidopsis root meristem. Genes Dev, 17(3), pp. 354-358.

Sadanandom, A. et al., 2015. SUMOylation of phytochrome-B negatively regulates light-induced signaling in Arabidopsis thaliana. Proc Natl Acad Sci U S A, 112(35), pp. 11108-11113.

Saini, S., Sharma, I., Kaur, N. & Pati, P. K., 2013. Auxin: a master regulator in plant root development. Plant Cell Rep, 32(6), pp. 741-757.

Sampedro, J. & Cosgrove, D. J., 2005. The expansin superfamily. Genome Biol, 6(12), p. 242.

Saotome, M. et al., 1993. The identification of indole-3-acetic acid and indole-3-acetamide in the hypocotyls of Japanese cherry. Plant Cell Physiol, Volume 34, pp. 157-159.

Saracco, S. A., Miller, M. J., Kurepa, J. & Vierstra, R. D., 2007. Genetic analysis of SUMOylation in Arabidopsis: conjugation of SUMO1 and SUMO2 to nuclear proteins is essential. Plant Physiol, 145(1), pp. 119-134.

Scheres, B. & Laskowski, M., 2016. Root patterning: it takes two to tangle. J Exp Bot, 67(5), pp. 1201-1203.

Schimmel, J. et al., 2014. Uncovering SUMOylation dynamics during cell-cycle progression reveals FoxM1 as a key mitotic SUMO target protein. Mol Cell, 53(6), pp. 1053-1066.

Sheard, L. B. et al., 2010. Jasmonate perception by inositol-phosphate-potentiated COI1-JAZ co-receptor. Nature, 468(7322), pp. 400-405.

Shimizu-Mitao, Y. & Kakimoto, T., 2014. Auxin Sensitivities of All Arabidopsis Aux/IAAs for Degradation in the Presence of Every TIR1/AFB. Plant Cell Physiol, 55(8), pp. 1450-1459.

Shkolnik, D., Krieger, G., Nuriel, R. & Fromm, H., 2016. Hydrotropism: Root Bending Does Not Require Auxin Redistribution. Mol Plant. 2016 May 2;9(5):757-9, 9(5), pp. 757-759.

Sievers, F. et al., 2011. Fast, scalable generation of high-quality protein multiple sequence alignments using Clustal Omega. Mol Syst Biol, Volume 7, p. 539.

Somers, E. et al., 2005. Azospirillum brasilense produces the auxin-like phenylacetic acid by using the key enzyme for indole-3-acetic acid biosynthesis. Appl Environ Microbiol, 71(4), pp. 1803-1810.

Song, G. et al., 2016. CRISPR/Cas9: A powerful tool for crop genome editing. The Crop Journal, 4(2), pp. 75-82.

Songstad, D. D. et al., 1990. High levels of tryptamine accumulation in transgenic tobacco expressing tryptophan decarboxylase. Plant Physiol, 94(3), pp. 1410-1413.

Spiess, G. M. et al., 2014. Auxin Input Pathway Disruptions Are Mitigated by Changes in Auxin Biosynthetic Gene Expression in Arabidopsis. Plant Physiol, 165(3), pp. 1092-1104.

Srivastava, A. K., Zhang, C. & Sadanandom, A., 2016. Rice OVERLY TOLERANT TO SALT 1 (OTS1) SUMO protease is a positive regulator of seed germination and root development. Plant Signal Behav, 11(5), p. e1173301.

Stepanova, A. N. et al., 2008. TAA1-mediated auxin biosynthesis is essential for hormone crosstalk and plant development. Cell, 133(1), pp. 117-191.

Stepanova, A. N. et al., 2011. The Arabidopsis YUCCA1 flavin monooxygenase functions in the indole-3-pyruvic acid branch of auxin biosynthesis. Plant Cell, 23(11), pp. 3961-3973.

Sugawara, S. et al., 2009. Biochemical analyses of indole-3-acetaldoxime-dependent auxin biosynthesis in Arabidopsis. Proc Natl Acad Sci U S A. , 106(13), pp. 5430-5435.

Swarup, R. & Péret, B. 2012. AUX/LAX family of auxin influx carriers-an overview. Front Plant Sci, Volume 3, p. 225.

Takatsuka, H. & Umeda, M. 2014. Hormonal control of cell division and elongation along differentiation trajectories in roots. J Exp Bot, 65(10), pp. 2633-2643.

Tan, X. et al., 2007. Mechanism of auxin perception by the TIR1 ubiquitin ligase. Nature, 446(7136), pp. 640-645.

Tao, Y. et al., 2008. Rapid synthesis of auxin via a new tryptophan-dependent pathway is required for shade avoidance in plants. Cell, 133(1), pp. 164-176.

Tatham, M. H. et al., 2008. RNF4 is a poly-SUMO-specific E3 ubiquitin ligase required for arsenic-induced PML degradation. Nat Cell Biol, 10(5), pp. 538-546.

Thomashow, L. S., Reeves, S. & Thomashow, M. F., 1984. Crown gall oncogenesis: evidence that a T-DNA gene from the Agrobacterium Ti plasmid pTiA6 encodes an enzyme that catalyzes synthesis of indoleacetic acid. Proc Natl Acad Sci U S A, 81(16), pp. 5071-5075.

Tiffin, P. & Hahn, M. W., 2002. Coding sequence divergence between two closely related plant species: Arabidopsis thaliana and Brassica rapa ssp. pekinensis. J Mol Evol, 54(6), pp. 746-753.

Tivendale, N. D. & Cohen, J. D., 2015. Analytical History of Auxin. J Plant Growth Regul, 34(4), p. 708–722.

Uehara, T. et al., 2008. Domain II mutations in CRANE/IAA18 suppress lateral root formation and affect shoot development in Arabidopsis thaliana.. Plant Cell Physiol, 49(7), pp. 1025-1038.

Uggla, C., Moritz, T., Sandberg, G. & Sundberg, B., 1996. Auxin as a positional signal in pattern formation in plants. Proc Natl Acad Sci U S A, 93(17), pp. 9282-9286.

Ulmasov, T., Liu, Z. B., Hagen, G. & Guilfoyle, T. J., 1995. Composite structure of auxin response elements. Plant Cell, 7(10), pp. 1611-1623.

Ulmasov, T., Murfett, J., Hagen, G. & Guilfoyle, T. J., 1997. Aux/IAA proteins repress expression of reporter genes containing natural and highly active synthetic auxin response elements. Plant Cell, 9(11), pp. 1963-1971.

van Berkel, K., de Boer, R. J., Scheres, B. & ten Tusscher, K., 2013. Polar auxin transport: models and mechanisms. Development, 140(11), pp. 2253-2268.

Vertegaal, A. C., 2010. SUMO chains: polymeric signals. Biochem Soc Trans, 38(1), pp. 46-49.

Vethantham, V., Rao, N. & Manley, J. L., 2008. Sumoylation regulates multiple aspects of mammalian poly(A) polymerase function. Genes Dev, 22(4), pp. 499-511.

Vierstra, R. D., 2009. The ubiquitin-26S proteasome system at the nexus of plant biology. Nat Rev Mol Cell Biol, 10(6), pp. 385-397.

Walsh, C. K. & Sadanandom, A., 2014. Ubiquitin chain topology in plant cell signaling: a new facet to an evergreen story. Front Plant Sci, Volume 5, p. 122.

Weigel, D. & Glazebrook, J., 2006. Setting up Arabidopsis crosses. CSH Protoc, Volume 5, p. prot4623.

Weigel, D. & Jürgens, G., 2002. Stem cells that make stems. Nature, 415(6873), pp. 751-754.

Wei, W. & Lin, H., 2012. The key role of ubiquitination and sumoylation in signaling and cancer: a research topic. Front Oncol, Volume 2, p. 187.

Went, F. & Thimann, K., 1937. Phytohormones. New York: Macmillan.

Whippo, C. W. & Hangarter, R. P., 2004. Phytochrome modulation of blue-light phototropism. Plant Cell Environ, Volume 27, p. 1223–1228.

Willemsen, V. et al., 2003. Cell polarity and PIN protein positioning in Arabidopsis require STEROL METHYLTRANSFERASE1 function. Plant Cell, 15(3), pp. 612-625.

Willige, B. C. et al., 2011. Gibberellin regulates PIN-FORMED abundance and is required for auxin transport-dependent growth and development in Arabidopsis thaliana. Plant Cell, 23(6), pp. 2184-2195.

Won, C. et al., 2011. Conversion of tryptophan to indole-3-acetic acid by TRYPTOPHAN AMINOTRANSFERASES OF ARABIDOPSIS and YUCCAs in Arabidopsis. Proc Natl Acad Sci U S A, 108(45), pp. 18518-18523.

Worley, C. K. et al., 2000. Degradation of Aux/IAA proteins is essential for normal auxin signalling. Plant J, 21(6), pp. 553-562.

Xuan, W. et al., 2015. Root Cap-Derived Auxin Pre-patterns the Longitudinal Axis of the Arabidopsis Root. Curr Biol, 25(10), pp. 1381-1388.

Xu, P. & Yang, C., 2013. Emerging role of SUMOylation in plant development. Plant Signal Behav, 8(7), p. e24727.

Yamamoto, Y. et al., 2007. Auxin biosynthesis by the YUCCA genes in rice. Plant Physiol, 143(3), pp. 1362-1371.

Yamasaki, K. et al., 2004. A novel zinc-binding motif revealed by solution structures of DNA-binding domains of Arabidopsis SBP-family transcription factors. J Mol Biol, 337(1), pp. 49-63.

Yoo, C. Y. et al., 2006. SIZ1 small ubiquitin-like modifier E3 ligase facilitates basal thermotolerance in Arabidopsis independent of salicylic acid. Plant Physiol, 142(4), pp. 1548-1558.

Yu, H. et al., 2015. Untethering the TIR1 auxin receptor from the SCF complex increases its stability and inhibits auxin response. Nat Plants, 1(3), p. 14030.

Zazímalová, E. et al., 2010. Auxin transporters--why so many?. Cold Spring Harb Perspect Biol, 2(3), p. a001552.

Zhang, S., Qi, Y. & Yang, C., 2010. Arabidopsis SUMO E3 ligase AtMMS21 regulates root meristem development. Plant Signal Behav, 5(1), pp. 53-55.

Zhao, Y. et al., 2001. A role for flavin monooxygenase-like enzymes in auxin biosynthesis. Science, 291(5502), pp. 306-309.

Zhao, Y. et al., 2002. Trp-dependent auxin biosynthesis in Arabidopsis: involvement of cytochrome P450s CYP79B2 and CYP79B3. Genes Dev, 16(23), pp. 3100-3112.